DISSERTATION

Visual detection of a cryptic predator by its prey fish

PhD candidate: Matteo Santon

Visual detection of a cryptic predator by its prey fish

DISSERTATION

der Mathematisch-Naturwissenschaftlichen Fakultät
der Eberhard-Karls Universität Tübingen
zur Erlangung des Grades eines
Doktors der Naturwissenschaften
(Dr. rer. nat.)

vorgelegt von
MATTEO SANTON
aus Vicenza, Italien

TÜBINGEN
2019

Tag der mündlichen Qualifikation:	18.02.2019
Dekan:	Prof. Dr. Wolfgang Rosenstiel
1. Berichterstatter:	Prof. Dr. Nico Michiels
2. Berichterstatter:	Prof. Dr. Katharina Foerster

Table of Contents

Summary

Animal interactions based on visual signals have been one of the oldest and most interesting research topics for early naturalists and biologists, that led to a better understanding of animal behaviour and its evolutionary implications. This study underlines the importance of considering the perspective of the species of interests when investigating visual communication in prey-predator interactions. Indeed, inaccurate conclusions are often made when we interpret animal behaviour basing ourselves on human vision, which outperforms that of most animals. Built on this premise, this dissertation focuses on the visual interaction between a small marine fish, the yellow black-faced triplefin, and one of its common cryptic predators, the black scorpionfish. The research approach first aims at better understanding the visual perspective of a triplefin when facing its predator (chapter 1 and 2), and then behaviourally and theoretically tests a new form of active sensing in the context of this prey-predator interaction (chapter 3).

The first chapter describes the contrast sensitivity function of triplefins, later combined with other known visual features to estimate the amount of information that this species can visually perceive from natural scenes where predators might be concealed.

The second chapter investigates how triplefins perceive the eye of a scorpionfish, and focuses on the unusual daytime eyeshine featured by this predator. This study describes, quantifies the phenomenon and tests its potential role for pupil camouflage in the context of visual inspection by triplefins under different light scenarios.

The last chapter finally introduces and tests “diurnal active photolocation”, a new mechanism of active sensing that redirects ambient light (rather than emitting sound waves or electric fields) to detect reflective targets. By combining behavioural experiments with theoretical visual modelling, this final study provides first evidence for the functionality of diurnal active photolocation in triplefins by means of light redirected from their iris. This process supplements regular vision by increasing the chances of detection of a cryptic predator by exploiting its daytime eyeshine, and may have strong implications for the evolution of fish eyes.

Papers included in the thesis

1. **Santon, M., Münch, T. A. & Michiels, N. K. (2019).** The contrast sensitivity function of a small cryptobenthic marine fish. Journal of Vision *19*(2).

2. **Santon, M., Bitton, P-P., Harant, U.K., and Michiels, N.K. (2018).** Daytime eyeshine contributes to pupil camouflage in a cryptobenthic marine fish. Scientific Reports *8*, 7368.

3. **Santon, M., Bitton, P-P., Dehm, J., Fritsch, R., Harant, U.K., Anthes, N. & Michiels, N.K. (2019).** Active sensing with light improves predator detection in a diurnal fish (under review).

Papers not included in the thesis

4. **Locatello L., Mazzoldi C., Santon M., Sparaciari S., Rasotto M.B. (2016).** Unexpected female preference for smaller males in the marbled goby *Pomatoschistus marmoratus*. Journal of Fish Biology. *89*(3):1845-50.

5. **Locatello L., Santon M., Mazzoldi C., Rasotto M.B. (2017).** The marbled goby, *Pomatoschistus marmoratus*, as a promising species for experimental evolution studies. Organisms Diversity & Evolution. *17*(3):709-16.

6. **Harant, U.K., Santon, M., P-P Bitton., Wehrberger, F., Griessler, T., Meadows M. G., Champ C.M. & Michiels N.K. (2018).** Do the fluorescent red eyes of the marine fish *Tripterygion delaisi* stand out? In situ and in vivo measurements at two depths. Ecology and Evolution *8*(9): 4685-4694.

7. **Bitton P-P., Yun Christmann S.A., Santon M., Harant U.K., Michiels N.K. (2018).** Visual modelling validates prey detection by means of diurnal active photolocation in a small cryptobenthic fish (in review for Scientific Reports).

Introduction

Investigating the dynamics of inter- and intraspecific species interactions has been one of the oldest and most prolific topics of research in evolutionary biology. This subject has been challenging the minds of great evolutionary biologists like Alfred Russel Wallace and Charles Darwin, and eventually led to the formulation of the theory of evolution by natural selection [2]. In particular, among the different animal interactions, the ones based on visual signals (e.g. complex mating rituals, stunning colourations) attracted the attention of early naturalists and biologist.

Animal interactions based on visual signals

It is inarguable that a good pair of eyes provides great evolutionary advantages: the visual sensory system generates immediate and detailed information about objects of interests beyond compare. For this reason, a growing amount of literature focuses on species interactions based on vision. Yet, some of these studies investigated visual signals without considering the perspective of focal species, but rather basing themselves on human vision, which outperforms that of most animals [3, 4].

Evolution has generated many different eye designs in nature: from camera-type eyes, to compound eyes and eyes that use mirrors. This diversity led to strong differences in visual abilities among animals, which should not be ignored when investigating visual signals. Despite the eye type, there are other features that are important to understand how species see their surroundings. Among them, spectral sensitivity and spatial resolution are certainly fundamental. The first determines the perceived colour of an object, where its hue depends on the light radiated from it and on the absorption spectra of the retina's photoreceptors [5]. Most animals are colour sensitive, and their vision can be based from two to 12 different colour channels (Figure 1). Their variation in number and in position across wavelength of the absorption peaks generates great differences in colour perception abilities.

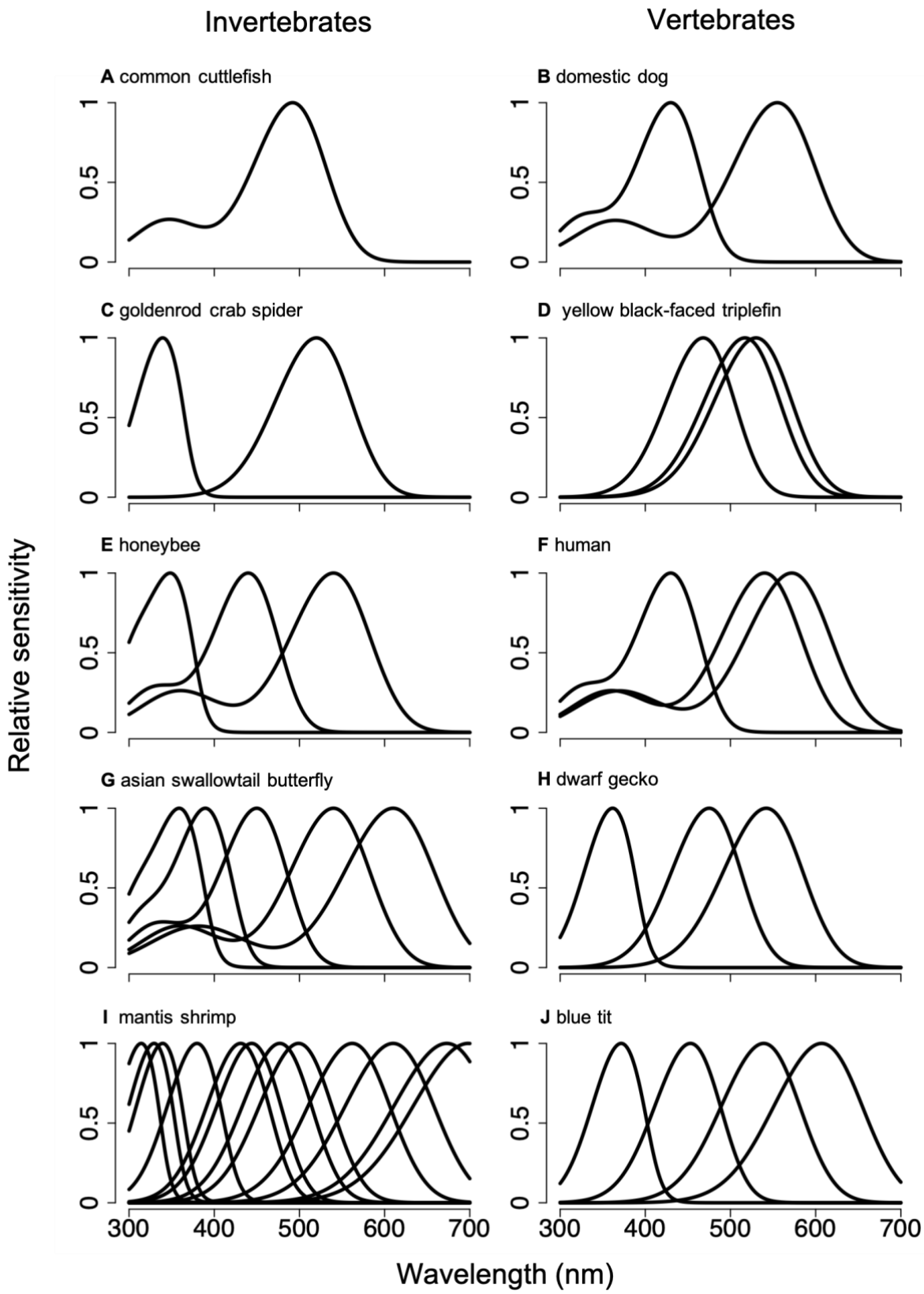

Figure 1. Spectral sensitivity is very diverse in the animal kingdom. Relative sensitivity of a selection of animals as a function of wavelength (nm). A. Common cuttlefish (*Sepia officinalis*). B. Domestic dog (*Canis familiaris*). C. Goldenrod crab spider (*Misumena vatia*). D. Yellow black-faced triplefin (*Tripterygion delaisi*). E. Western honeybee (*Apis mellifera*). F. Human (*Homo sapiens*). G. Asian swallowtail butterfly (*Papilio xuthus*). H. Dwarf gecko

(*Gonatodes albogularis*). I. Mantis shrimp (*Neogonodactyus oerstedii*). J. Blue tit (*Paris caeruleus*). A, B and H estimated from sensitivity of visual pigments alone, without correcting for ocular media or other filters. Curves based on peaks of sensitivity according to Govardovskii, et al. [6] and normalised by dividing each curve by its maximum value. Sensitivities data from Thoen, et al. [7], Marshall and Oberwinkler [8], Hart and Vorobyev [9], Ellingson, et al. [10], Defrize, et al. [11], Bitton, et al. [12], Menzel and Blakers [13], Arikawa, et al. [14], Schnapf, et al. [15], Mäthger, et al. [16], Neitz, et al. [17]. Graph compiled by Matteo Santon using all the references cited.

The second is defined as the ability to resolve static spatial details in a given scene [3]. This visual feature is dependent on the sampling frequency of the retina, defined as $v_s = f / (2s)$, where f is the focal length of the eye (directly proportional to its dimensions) and s the separation distance between two photoreceptors in the retina [4]. Animals show great diversity in their spatial resolution, varying from poor resolution of e.g. flatworms to the elite resolution of eagles (Figure 2).

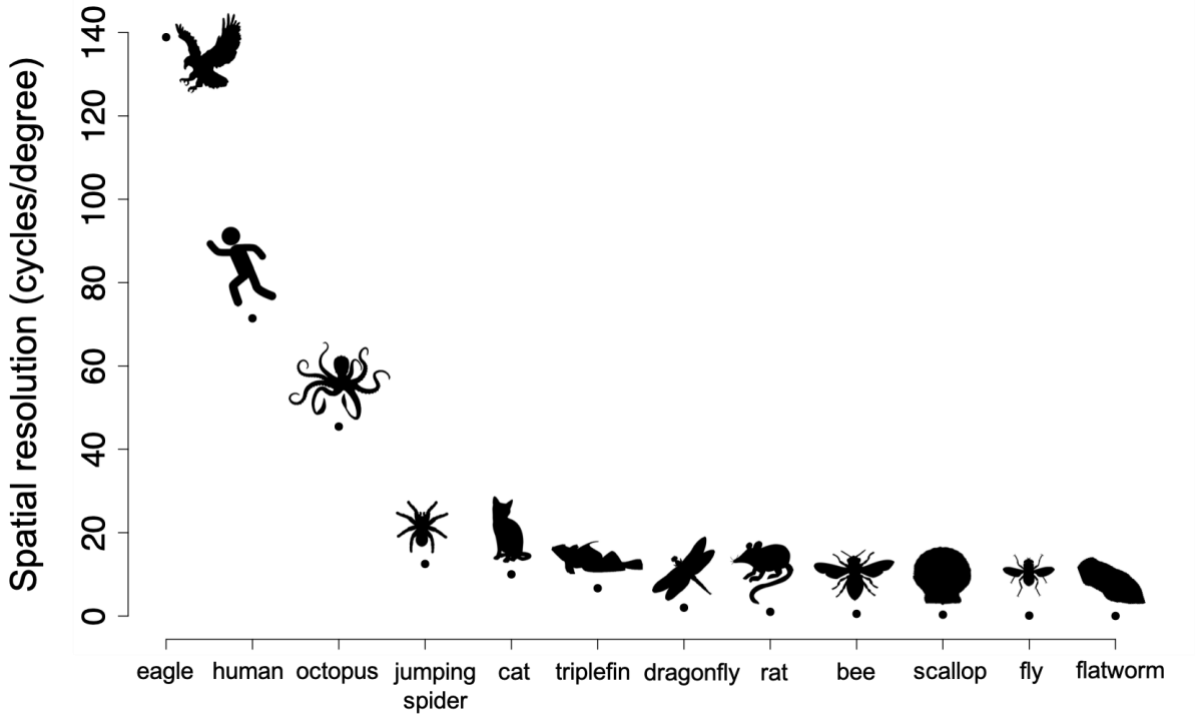

Figure 2. Spatial resolution is very diverse in the animal kingdom. Spatial resolution of a selection of animals expressed as sampling frequency of the retina (cycles/degree). In descending resolution order the listed species are: wedge-tailed eagle (*Aquila audax*), modern human (*Homo sapiens*), common octopus (*Octopus vulgaris*), jumping spider (*Portia sp.*), domestic cat (*Felix catus*), yellow black-faced triplefin (*Tripterygion delaisi*), hawker dragonfly (*Aeschna sp.*), hooded rat (*Rattus norvegicus domestica*), worker western honeybee (*Apis mellifera*), scallop (*Pecten sp.*), common fruit fly (*Drosophila melanogaster*), flatworm (*Planaria torva*). Resolution data from Reymond [18], Land [19], Land [20], Charman [21] and Fritsch, et al. [22]. Graph compiled by Matteo Santon using all the references cited.

By combining these two visual features with the contrast perception threshold at the optimally resolvable sampling frequency (around 2 % for most organisms in optimal light conditions, according to Douglas and Djamgoz [23]), it is possible to estimate the amount of information that a specific visual system perceives from a given scene. For example, Figure 3 shows the image of a dandelion as perceived by humans or bees considering their spectral sensitivity and spatial resolution. In contrast to humans, bees perceive this flower as dichromatic (i.e. featuring two hues) because they are sensitive to UV light. This contrasting colour pattern might help them to locate a dandelion, thus compensating for their relatively poor resolution that doesn't allow them to resolve the flower even from short (on a human scale) distances.

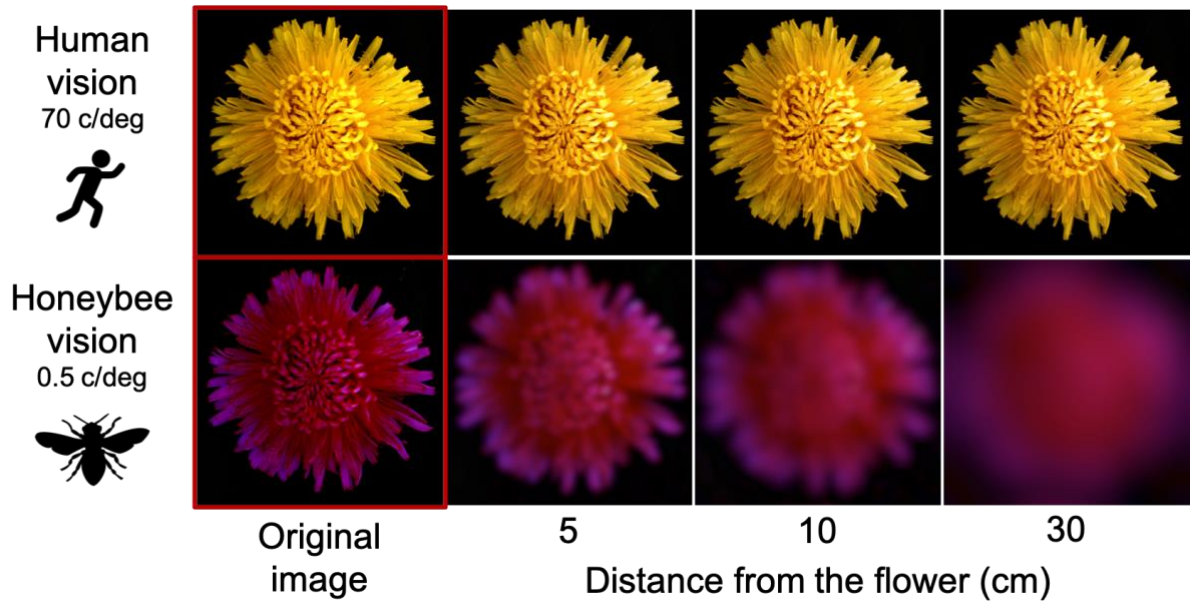

Figure 3. The perception of a dandelion differs between human and bee vision. Human's spatial resolution (top row) allows to resolve spatial details from a greater distance than bee's resolution (bottom row). However, bee's colour vision perceives the flower as dichromatic, whereas human's as monochromatic. Each image (originals excluded) displays the spatial information of the scene adjusted by distance and spatial resolution. Original images are only corrected for human's and bee's colour vision. The size of the flower is around 5.5 cm. Original colour corrected images generated using the MicaToolbox for ImageJ [24]. Images corrected for spatial resolution are generated using the R package Acuity View [25]. Photo credit: Matteo Santon.

Considering the visual features of the species of interest is therefore fundamental when investigating animal interactions based on visual signals. Not doing so could result in making inaccurate or wrong conclusions that overlook the real information content of a scene or that are based on our own sensory system.

Active sensing in the animal kingdom

When the environment is unsuitable for vision (e.g. in the dark or in murky waters), some animals evolved active sensing. In the context of this study, this process is defined as the ability of species to enhance their sensory system by emitting or redirecting energy in the surroundings and perceiving its reflections from objects nearby. A well-known form of such active sensing is echolocation by emitting sound waves e.g. by bats or dolphins. Other forms involve electric fields, touch or the hydrodynamic properties of water (e.g. weak electric fish) [26].
In contrast to sound and electric fields, the use of light for active sensing is considered to be rare. Some deep sea and nocturnal fishes possess a chemiluminescent light organ close to their pupils (Figure 4A), proposed to induce detectable reflections (eyeshine) in the pupils of predators, prey and conspecifics [27, 28]. In such target species eyeshine should be retroreflective: light that enters their pupils is returned to the source in a narrow angle (e.g. a cat's eye). As a consequence, retroreflective eyeshine can only be induced and detected by species featuring a light source close to their eyes.

This form of active sensing using light has been termed ***active photolocation*.** This process is defined as the induction and detection of reflections in targets by means of ocular radiance emitted by the observer [29].

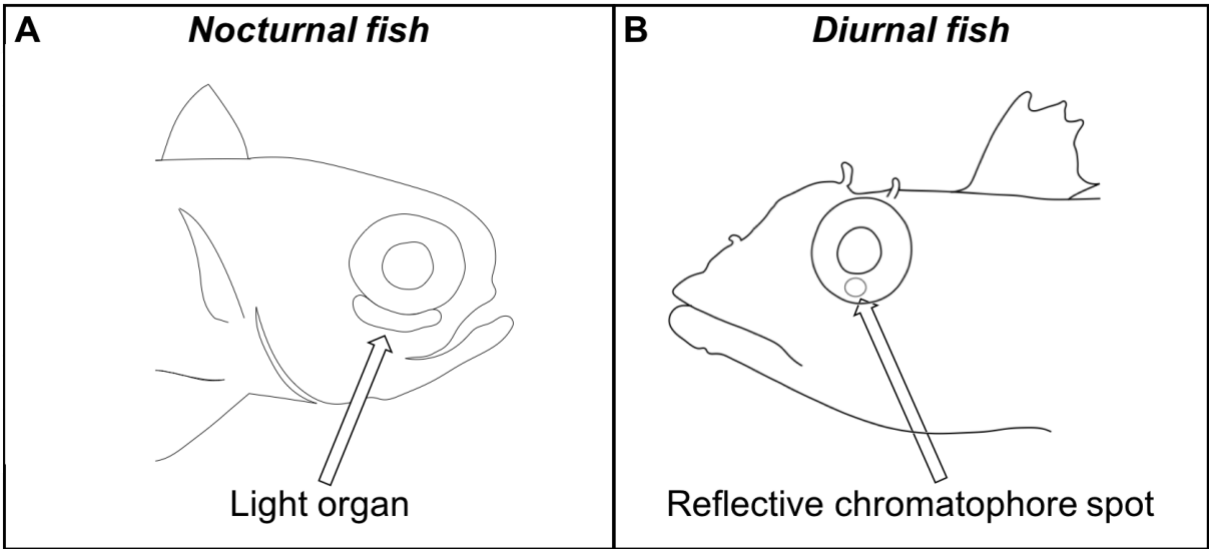

Figure 4. Nocturnal and diurnal fish feature similar strategies to emit light from nearby their pupils. A. Nocturnal chemiluminiscent fish feature a light organ just below their iris (e.g. *Photoblepharon palpebratus*). B. Diurnal fish can feature a reflective chromatophore spot on the iris (e.g. *Tripterygion delaisi*). Scheme credit: Nico Michiels and Matteo Santon.

Diurnal active photolocation

Although this is well-established for chemiluminescent fishes [30], it has never been considered whether diurnal fishes might use active photolocation to supplement regular vision. Rather than using chemiluminescent light organs, many diurnal fishes could achieve this by redirect ambient light with their irides [29]. This close vicinity between the light source (reflective iris or structure on it) and the detector's eye is reminiscent of the position of the light organ in nocturnal fishes (Figure 4B) [27, 28, 31-34]. This analogy suggests that diurnal fish could redirect light from their iris to similarly enhance detection of organisms nearby.

In fishes, eyes are considered key features for recognition of predators, prey or conspecifics [35, 36]. Not surprisingly, specific adaptations to camouflage the eyes are widespread among marine organisms (Figure 5) [37-39].

For this reason, the detection of well-camouflaged organisms such as transparent invertebrate prey or cryptic predators might challenge fish visual detection abilities even during daytime. The induction and perception of eyeshine using active photolocation could therefore help to reveal overlooked eyes in the surroundings, increasing the chances of detection of cryptic organisms.

Figure 5. Selection of adaptations to conceal the eye. A. Common lionfish (*Pterois miles*) features an eye mask, where a vertical stripe through the eye disrupts the circular shape of

the eye. B. Crocodile flathead (*Cymbacephalus beauforti*) features skin flaps, where the pupil is partly covered by an irregular extension of the cryptic iris. C. Black scorpionfish (*Scorpaena porcus*) features daytime eyeshine, where an unusually bright pupil reduces the contrast again the surrounding tissue (chapter 2). D. Broadclub cuttlefish (*Sepia latimanus*) features a modified horizontal slit-pupil, considered to improve vision but also to disrupt the circular shape of the eye. Bottom right subpanels show an enlarged view of the eyes. Photo credit: Matteo Santon.

Yellow black-faced triplefin – *Tripterygion delaisi*

The yellow black-faced triplefin*Tripterygion delaisi* (Fam. Tripterygiidae) is a small (4–5 cm) NE-Atlantic and Mediterranean micro-predatory species found on rocky substrates from 5 to 30 m depth (Figure 6A) [40]. Except from breeding males that display a yellow body with a black hood, individuals are highly cryptic and mainly feed on small invertebrates.

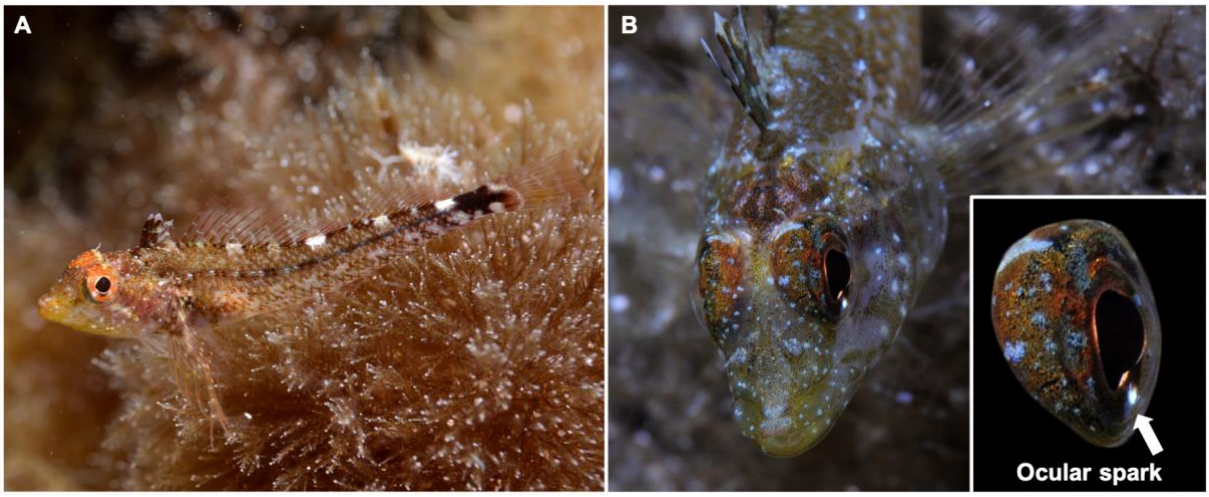

Figure 6. The yellow black-faced triplefin in its natural environment. A. Full body picture of *Tripterygion delaisi* at 3 m depth. B. *T. delaisi* showing a blue ocular spark at 8 m depth. Bottom right subpanel shows an enlarged view of the eyeball generating the spark. Photo credit: Matteo Santon.

This is an ideal species to investigate visual detection abilities because most of its fundamental visual features, such as spectral sensitivities [12] and spatial resolution [22] have been already described (see Figure 1 and Figure 2). This fish also features a behaviourally-controlled form of ocular radiance termed “ocular spark”: a bright point of light focused on the iris below the pupil (Figure 6B) [29]. This effect is generated by the spherical lens which protrudes from the pupil of the fish, allowing downwelling light to be focused on the iris below. This mechanism of light redirection from the iris makes this species a promising case to test active photolocation in diurnal fishes. In triplefins,

ocular sparks can be either red or blue depending on whether light is focused on a red part of the iris, or on a bluish chromatophore spot. A behavioural experiment showed that ocular sparks increase in frequency when prey is offered to triplefins [29]. The same experiment also shows that blue ocular sparks increase against a red background and vice versa. This may allow triplefins to generate stronger chromatic contrasts between a target´s reflection and its background [29]. However, this hypothesis has not been confirmed by later visual modelling, which suggests that only achromatic contrast play a significant role for prey detection [41]. If small diurnal fish could detect prey using active photolocation, they may also use it to locate their predators.

Black scorpionfish – *Scorpaena porcus*

The black scorpionfish *Scorpaena porcus* (Fam. Scorpaenidae) is a cryptobenthic sit-and-wait predator (12–20 cm) from coastal marine hard substrates and seagrass habitats in the NE-Atlantic and Mediterranean Sea (Figure 7A) [40].

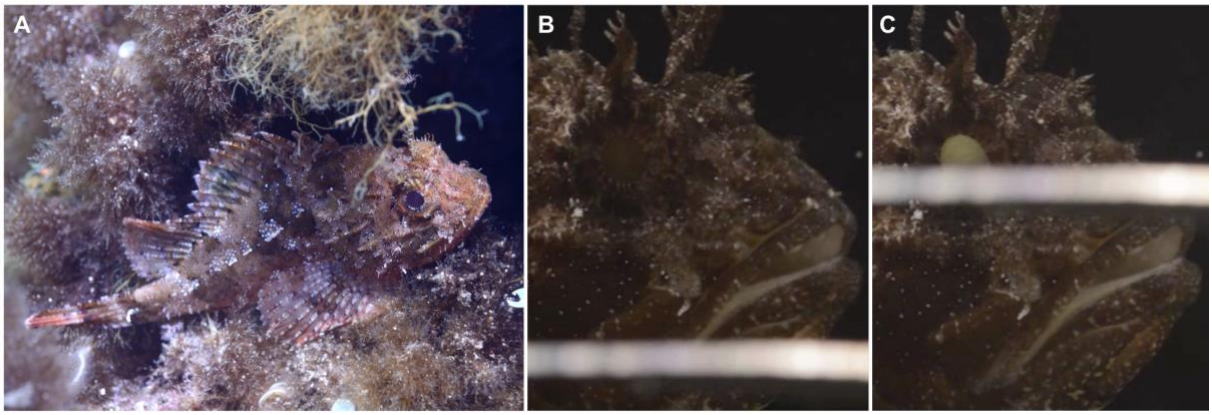

Figure 7. The black scorpionfish. A. *Scorpaena porcus* in its natural environment at 7 m depth. This species shows retroreflective eyeshine when illuminated coaxially, even with a weak diffuse reflector like a narrow strip of white paper (compare B and C). Photo credit: Matteo Santon.

Small benthic fish, such as triplefins, are often a component of its diet [42]. This scorpionfish possesses large eyes, a reflective *stratum argenteum* and partially translucent retinal pigment epithelium that allows for the generation of daytime reflected eyeshine (Figure 7B/C) [43, 44]. This species represents an ideal target to test if diurnal active photolocation can enhance detection of cryptic predators by exploiting their daytime reflected eyeshine.

Objectives and structure

This PhD project investigated the visual detection by triplefins of their cryptic scorpionfish predator. The research approach combines behavioural experiments, spectroradiometry and visual modelling. The overall structure of this dissertation takes the form of three chapters, where the first two provide fundamental data to conduct the final study (third chapter). In particular, the first chapter measures a visual feature that is fundamental to estimate how triplefins visually perceive their predator in the natural environment. The second chapter quantifies a special adaptation of the scorpionfish eyes, describing how it can enhance pupil concealment from the perspective of triplefins. These first two studies provide insights on the triplefins' visual perception of scorpionfish, highlighting potential key traits for predator detection in fish (e.g. eyes). Based on the knowledge acquired with the first two chapters, the last study provides first evidence for the functionality of diurnal active sensing using light in triplefins to enhance the chances of detection of their cryptic scorpionfish predator.

Short summary of the study included in this dissertation:

1. The first chapter aims at determining the contrast sensitivity threshold at the optimally resolvable sampling frequency in the triplefins. Combining this visual feature with spectral sensitivity and foveal spatial resolution allows to estimate the information that this species can visually perceive from a natural scene where a scorpionfish predator is concealed.

2. The second chapter investigates how triplefins perceive the eye of a black scorpionfish. It focuses on quantifying the reflective and transmissive eye properties that explain the unusual daytime eyeshine featured by this predator, and models its functionality as a strategy to camouflage the pupil.

3. The third chapter investigates if triplefin can redirect light from their irides to actively detect eyeshine in the black scorpionfish. This final chapter combines three behavioural experiments with theoretical visual modelling that include parameters determined in the previous two chapters.

Contrast sensitivity function of *T. delaisi*

(in collaboration with Prof. Thomas Münch, from the Centre of Integrative Neuroscience, department of Retinal Circuits and Optogenetics)

Related publication

Santon, M., Münch, T. A. & Michiels, N. K. (2018). The contrast sensitivity function of a small cryptobenthic marine fish. *Journal of Vision* (in press).

Extended summary

This study determines the contrast sensitivity threshold of triplefins by measuring its contrast sensitivity function (CSF) [45, 46], which describes contrast sensitivity as a function of spatial frequency. The latter is defined as the number of achromatic vertical bright and dark stripe pairs per degree of visual angle. This CSF was estimated by exploiting the optokinetic reflex, that consists of rotational eye movements to improve global image stabilisation against relative motion of the environment. This involuntary response is considered to depend on peripheral vision in animals featuring a fovea [3, 23]. In this study, such reflex was induced by placing the animal in the centre of a horizontally rotating drum displaying greyscale vertical striped patterns defined by combinations of spatial frequency (cycles per degree) and contrast (Michelson) calculated as $(L_1-L_2)/(L_1+L_2)$, where L_1 and L_2 are the photon radiances of the bright and dark stripes.

The maximum value obtained for the contrast sensitivity was 125 (inverse of 0.8% Michelson contrast), indicating an optimal spatial frequency of 0.375 cycle/degree (Figure 8).

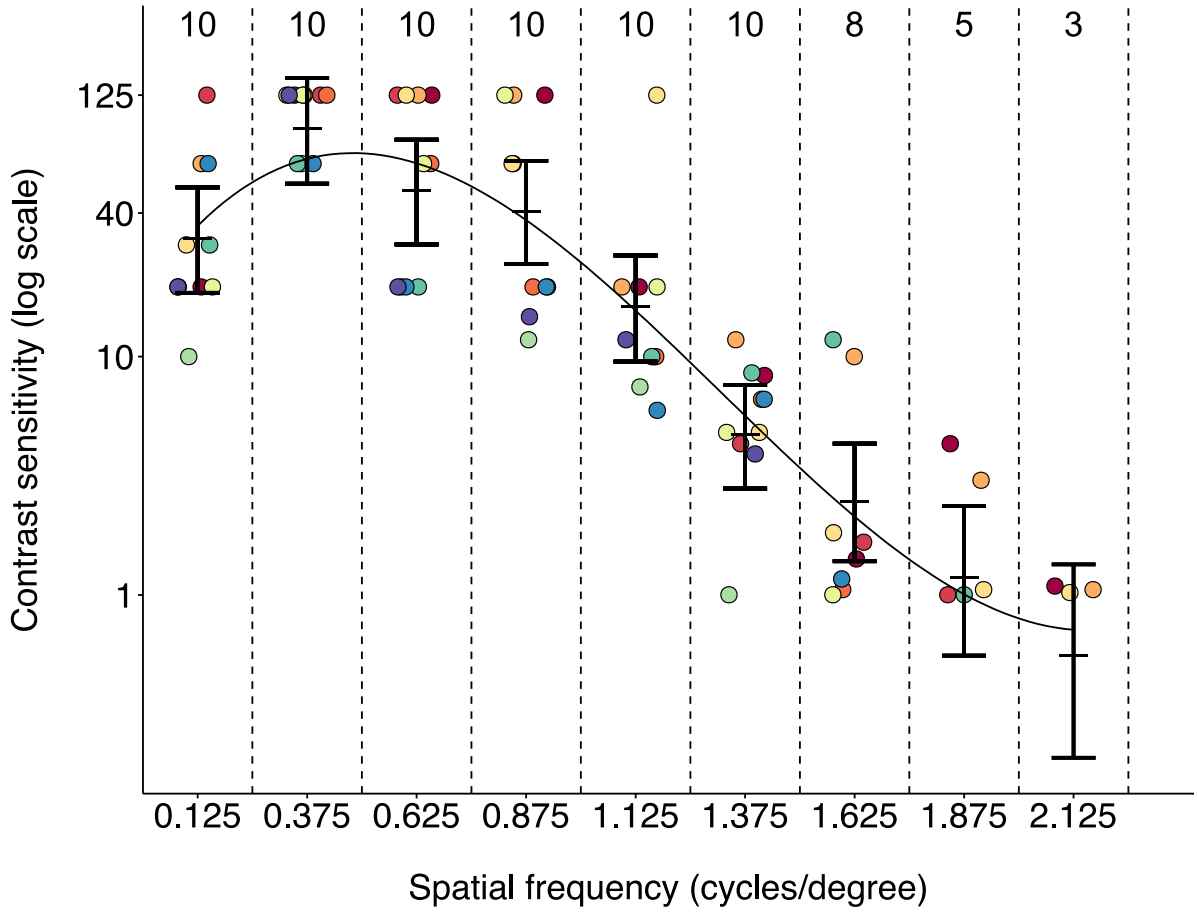

Figure 8. Contrast sensitivity function (CSF) of *Tripterygion delaisi*. Contrast sensitivity, expressed as the reciprocal of the Michelson contrast, as a function of spatial frequency. The optimal sensitivity was around 0.375 cycles/degree, where 7 out of 10 fish showed the maximum sensitivity of 125, which corresponds to a 0.8% Michelson contrast. Contrast sensitivity is plotted on a log-scale. Numbers at the top indicate individuals' number (n = 10) responding to each spatial frequency. None of the individuals responded to the spatial frequency of 2.375 (not shown). Each colour represents a different individual (jittered for clarity). Error bars display the model-predicted group means ± 95 % Credible Intervals. The black curve shows the relationship between contrast sensitivity and spatial frequency on a continuous scale.

This contrast sensitivity threshold was similar to other fish species (sensitivity up to 111) [23, 47-49], but excellent if compared to other animals (e.g. birds, up to 20) [50-52]. Marine fish may benefit from excellent contrast sensitivity because underwater contrasts are degraded by light scatter by suspended particles in the water [23].

The CSF also allowed to identify the maximum spatial resolution at 2.125 cycles/degree. This value suggests a rather coarse peripheral spatial resolution (if compared to the fovea), that matches the estimates derived from the resolution of the

peripheral retinal ganglion cell density [22]. We concluded that the optokinetic reflex seems to be adapted to process low spatial frequency information from stimuli in the peripheral visual field. Our results suggest that triplefins could use peripheral vision for resolving the outline of big predators (e.g. groupers, Fam. Serranidae), while simultaneously using foveal vision to find invertebrate micro-prey or for intraspecific communication.

Combining the contrast sensitivity threshold measured in this study with the spectral sensitivity and foveal spatial resolution of triplefins finally allows to estimate how this small marine fish sees its scorpionfish predator in a natural scene (Figure 9). From such estimates, it is for example possible to suggest that eyes are a key feature for scorpionfish detection.

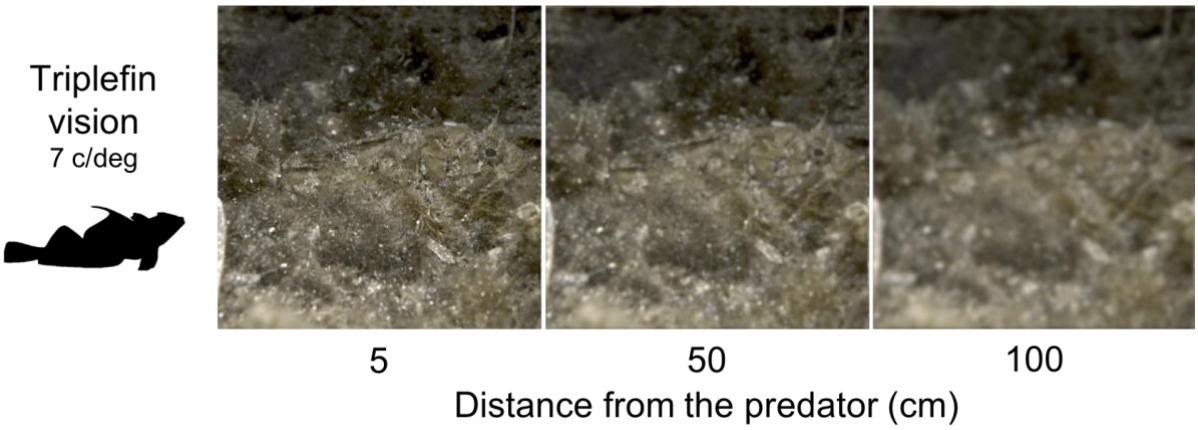

Figure 9. A triplefins' view of the black scorpionfish. Triplefins are theoretically able to roughly resolve some key details (e.g. circular dark pupil) of their predator up to 100 cm. Each image displays the spatial information of the scene adjusted by distance and spatial resolution. All images are corrected for triplefins' colour vision. The size of the scorpionfish is assumed to be 16 cm. Colour corrected images generated using the MicaToolbox for ImageJ [24]. Images corrected for spatial resolution generated using the R package Acuity View [25]. Photo credit: Matteo Santon.

Limitations

The study is based on the optokinetic reflex, used to behaviourally estimate visual features of the peripheral retina. This approach likely underestimates spatial resolution or contrast sensitivity in animals that possess a fovea (such as triplefins). To obtain behavioural assessments of the foveal contrast sensitivity function, other experimental approaches based on tracking of small visual targets rather than wide-field stimuli are required. Most of these methods rely on training individuals to distinguish horizontally from vertically striped stimuli of different sizes and contrasts [53-55]. However, if training is not feasible, an alternative method could expose animals to small shapes that move against a uniform or complex background. If such visual target elicits tracking, no training would be required. This approach could be particularly promising for small species that naturally track micro-prey against complex backgrounds when foraging.

Daytime eyeshine in *S. porcus*

Related publication

Santon, M., Bitton, P.P., Harant, U.K., and Michiels, N.K. (2018). Daytime eyeshine contributes to pupil camouflage in a cryptobenthic marine fish. Scientific Reports *8*, 7368.

Extended summary

The black scorpionfish eyes feature an ocular reflector (s*tratum argenteum*) that generates daytime eyeshine. This is opposite to most fish, that instead occlude their reflectors during the day and keep it exposed at night [56, 57]. For this reason, ocular reflectors are commonly considered to enhance eye sensitivity in dim light [57]. In the black scorpionfish, this inverted occlusive mechanism results in daytime eyeshine (Figure 7C), suggested to enhance pupil camouflage by reducing the contrast between the otherwise black pupil and the surrounding tissue [44].

In this study, we show that daytime eyeshine in this species is the result of two mechanisms: the already known *Stratum Argenteum Reflected* (SAR) eyeshine and the *Pigment Epithelium Transmitted* (PET) eyeshine, a previously undescribed mechanism for this species. SAR eyeshine is generated when light passes through the photoreceptor layer and the translucent choroid, reaches the *stratum argenteum,* and is then reflected out of the pupil [58]. PET eyeshine is instead generated when light that penetrates the dorsal part of the eye is transmitted through the sclera, choroid and retinal pigment epithelium and then leaves through the pupil [58].

We measured the relative contribution of SAR and PET eyeshine to pupil brightness and showed how these two parameters can be used to reliably predict eyeshine in the field. We then implemented visual models for different natural light scenarios that were relevant for the prey-predator interaction between scorpionfish and triplefin and where the contribution of SAR and PET eyeshine to total daytime eyeshine differs. The models estimated pupil brightness of the scorpionfish in relation to that of the surrounding iris and skin patches as perceived by the diurnal fish triplefin. Under

all tested scenarios, the perceived achromatic contrast of a scorpionfish pupil with either PET or SAR eyeshine against its iris was substantially smaller when compared to a pupil without any eyeshine. Furthermore, the contrast between a scorpionfish pupil against the iris was always within the range of the achromatic contrasts between the skin patches found near the iris (Figure 10). These results support the eye-concealment hypothesis.

A similar mechanism to conceal a dark pupil has been described for pelagic stomatopod larvae that use a photonic structure external to the optical pathway to reflect ambient light and match the appearance of the pupil with the background [39]. Since in the black scorpionfish the ocular reflector is located in the optical pathway of light, we cannot exclude a visual purpose. Eyeshine in the black scorpionfish might therefore have a dual function: concealing the pupil throughout all day, while improving sensitivity in dim light only. Yet, the occlusion of the ocular reflector at night suggests that the visual function might be secondary to camouflage. We concluded that daytime eyeshine in the black scorpionfish has evolved as a compromise between camouflage and vision.

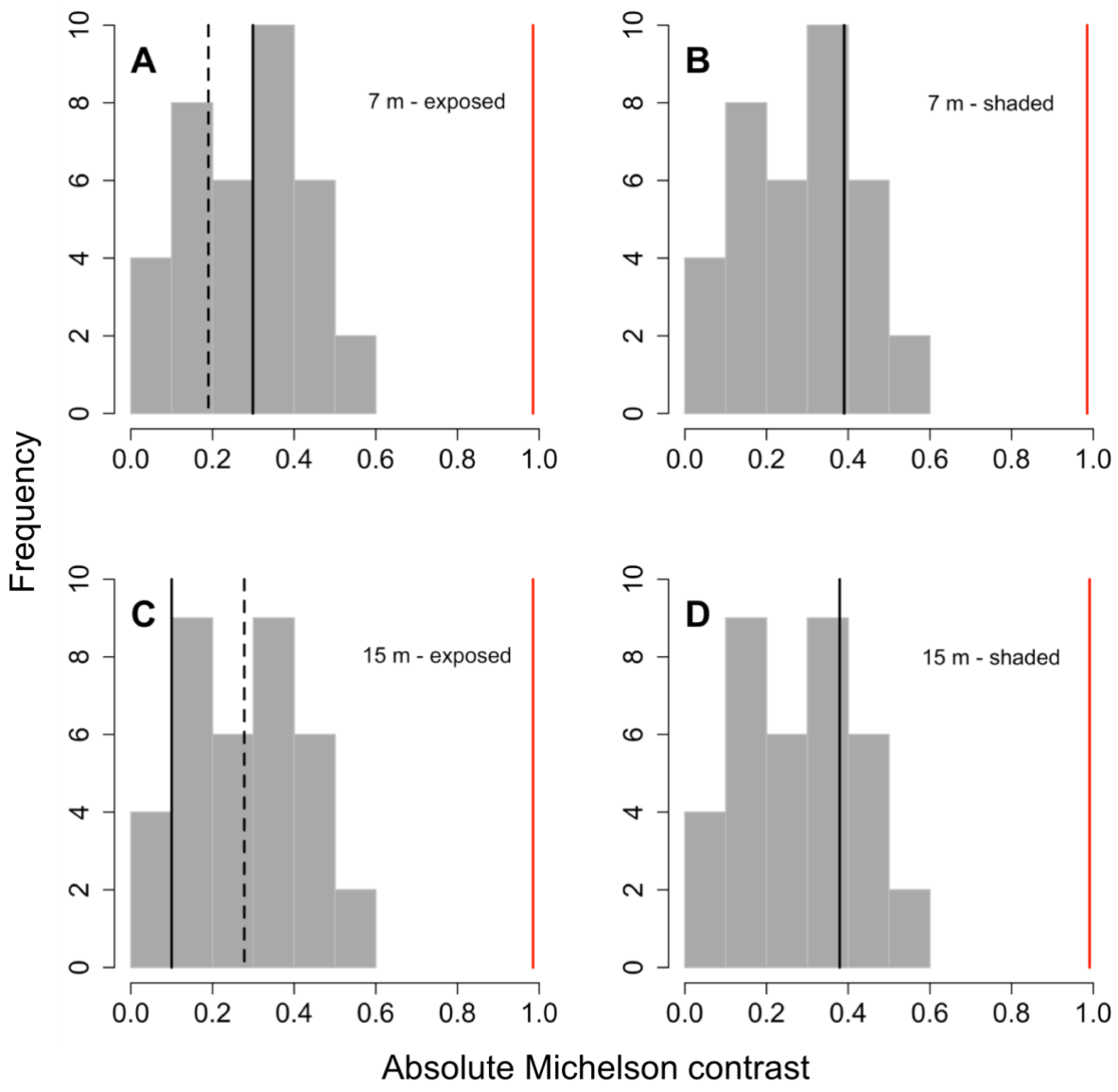

Figure 10. Predicted absolute achromatic contrast of the pupil with and without eyeshine against the iris of *S. porcus* compared to the contrast among body patches as perceived by triplefins. The achromatic contrast between a scorpionfish pupil with eyeshine and its iris (black lines) always fell within the distribution of the achromatic contrasts between skin patches. This was not the case when eyeshine was prevented (red lines). Black lines indicate contrast values between the scorpionfish pupil and the iris when *T. delaisi* is shaded (dashed) or exposed (solid) for four *S. porcus* scenarios: **(A)** exposed and (**B**) shaded at 7 m depth, **(C)** exposed and **(D)** shaded at 15 m depth. Red lines indicate contrast values between a pupil without eyeshine and the iris when *T. delaisi* is shaded (dashed) or exposed (solid) for the same four *S. porcus* scenarios (note that in scenario A and C two lines overlap).

Limitations

This study assumes that eyes are the key element of detection of cryptic scorpionfish by triplefins. However, there's much more than just eyes in this predator. To get a more comprehensive picture, it would be interesting to analyse how scorpionfish is visually perceived by triplefins under natural field conditions against different backgrounds. Calibrated image analysis could be one of the best approaches to tackle this question [24, 59] (e.g. Figure 9). By taking several calibrated pictures of scorpionfish in the field and statistically evaluating how well it is camouflaged (e.g. by using disruptive camouflage estimates), it should be possible to identify the most salient traits that are likely to give away its outline to triplefins at difference sighting distances.

Testing diurnal active photolocation

Related publication

Santon, M., Bitton, P-P., Dehm, J., Fritsch, R., Harant, U. K., Anthes, N. & Michiels, N. K. (2018). Active sensing with light improves predator detection in a diurnal fish (under review).

Extended summary

By combining data and observations collected in the first two chapters, this final study investigates whether a triplefin's blue ocular spark can be sufficient to induce a perceptible retroreflective eyeshine in the eye of a black scorpionfish.

We first tested this hypothesis behaviourally by blocking the ability of triplefins to redirect light with opaque plastic mini-hats (Figure 11). Two controls allowed the formation of ocular sparks: unhatted sham control and clear-hatted (Figure 11A-B). In the opaque-hatted treatment, ocular sparks formation was instead prevented by casting a shadow over the eyes of the fish (Figure 11C).

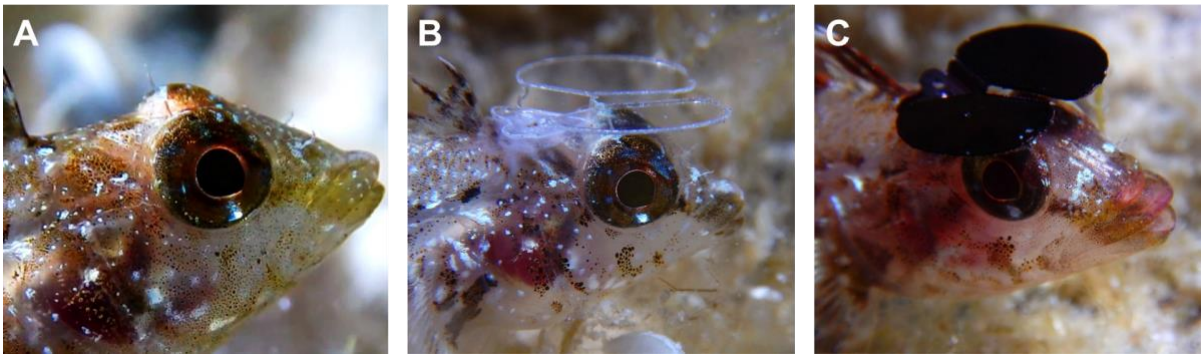

Figure 11. Mini-hats used to manipulate the production of ocular sparks in triplefins. A. Unhatted sham control treatment. B. Clear-hatted control treatment. C. Opaque-hatted shaded treatment. Only triplefins wearing a shading hat were not able to generate ocular sparks (compare A and B with C). Photo credit: A: Nico Michiels, B and C: Matteo Santon.

Triplets of manipulated triplefins were then released in large tanks with sandy substrate and visually exposed to either a scorpionfish or a stone placed in the shade behind a windowpane. We expected triplefins to be attracted to the display compartment as they

prefer hard shady substrates over the shade-free sand. However, we also expected triplefins to be careful at approaching the predator scorpionfish. We predicted that this combination of attraction and deterrence would result in shorter "safe distances" kept by shaded triplefins from scorpionfish compared to the controls. No such effect was expected for the stone stimulus. We tested such paradigm independently in a laboratory and in a field experiment, recording the distance fish kept from the display compartment over 2 days. Stimuli were always present in the tank, yet alternately visible one day each. In the field experiment, fish were placed in translucent plexiglass tanks placed at 15 m depth on a sandy patch following two main orientations, north and south.

In both experiments, triplefins kept greater mean distance from the predator compared to the stone independently of the hat treatment (Figure 12 & Figure 13). A comparison of the distance of the pooled controls relative to the shaded fish showed the same stimulus effect, but additionally included a hat treatment effect. Shaded fish moved significantly closer to the predator than the controls. This effect was absent when the stone was shown. While such results were neat in the laboratory experiment (Figure 12), the field experiment showed the same result only in tanks oriented north (Figure 13).

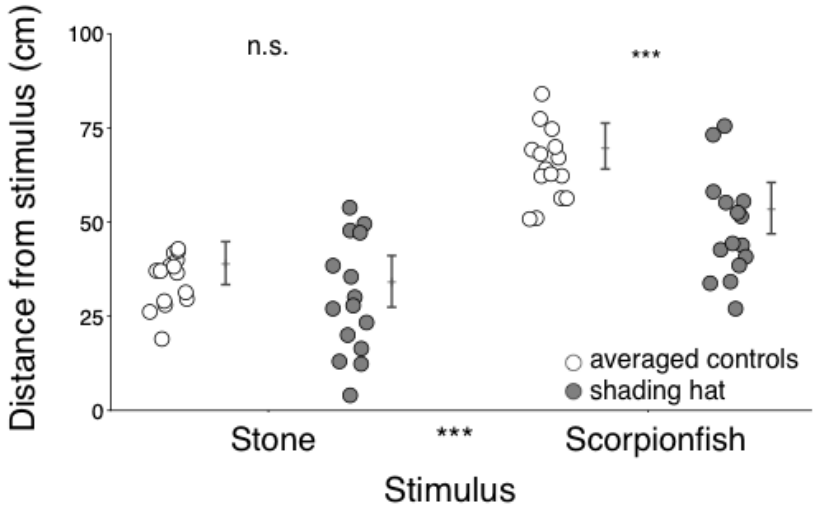

Figure 12. Laboratory experiment. Average distance from the stimulus compartment as a function of stimulus type (stone or scorpionfish) and hat treatment (controls or shading hat). Relative to the controls, shaded individuals stayed significantly closer to the scorpionfish. Symbols = average of 5 measurements per triplet; *n* = 15 triplets; error bars: model-predicted group means ± 95 % credible intervals; *** = $p < 0.001$, n.s. = $p > 0.05$. Note that statistical comparisons between treatments rested on the connected measures within triplets, making group means and error bars imprecise indicators of the statistical significance of paired measures.

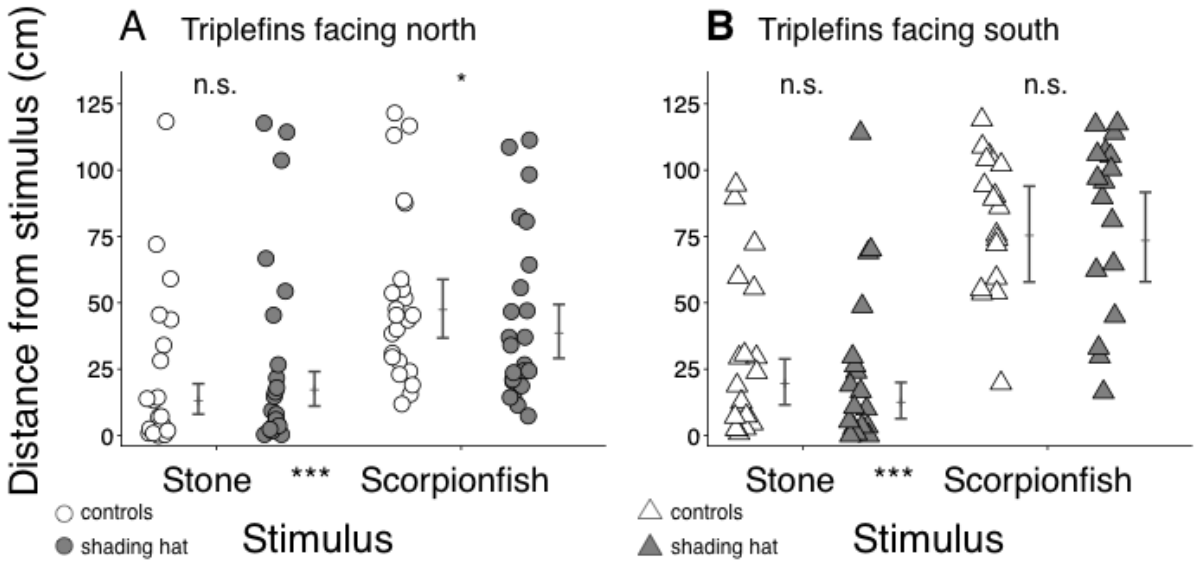

Figure 13. Field experiment at 15 m depth. Distance from stimulus as a function of stimulus type (stone or scorpionfish), hat treatment (controls or shading hat), and orientation (north or south). A. In north-facing triplefins, shaded fish stayed closer to a scorpionfish than the controls (*n* = 24 triplets). B. In south-facing triplefins, such effect was absent (*n* = 19 triplets). Symbols: average of 3 measurements per individual; error bars: model-predicted means ± 95 % credible intervals. * = $p < 0.05$, n.s. = $p > 0.05$. Note that statistical comparisons between treatments rested on the connected measures within triplets, making group means and error bars imprecise indicators of the statistical significance of paired measures.

In these first two experiments we tested the average response of triplefins over a long time period (2 days), ignoring immediate fish responses. For this reason, we conducted a follow up field experiment at 10 m depth, were we tested hatted individuals (only clear vs shaded) individually and observed how close they approached a scorpionfish immediately after release, and then monitored their distance from the predator for the next 90-100 minutes.

Immediately after the release in the middle of the tank, most fish rushed in front of the display compartment, many to less than 5 cm from the windowpane behind which the scorpionfish was displayed (Figure 14). Shaded fish kept shorter distances from the scorpionfish than clear-hatted controls already one minute after the release (Figure 14). Across time, both treatments moved away from the predator, resulting in shaded fish coming back to the middle of the tank about 20 minutes later than controls. Both treatments reached similar distances after about 50 minutes.

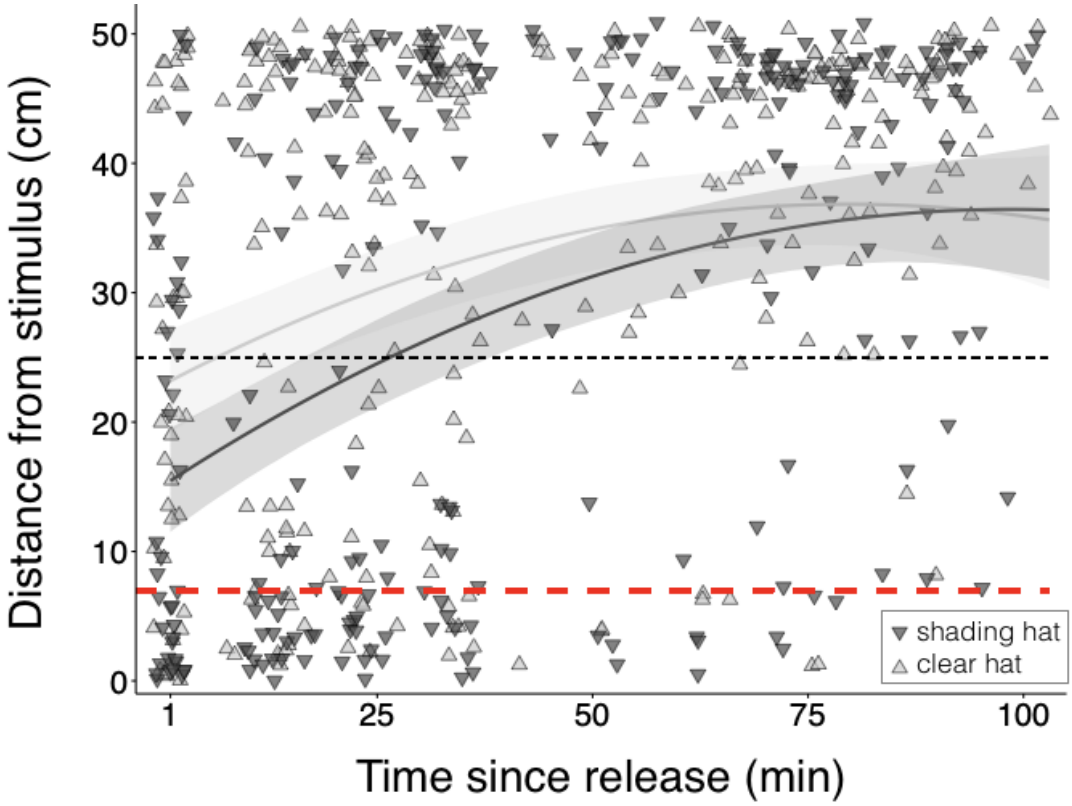

Figure 14. Field experiment at 10 m depth. Distance kept from a scorpionfish as a function of time and hat treatment (shading hat or clear hat). The first measurement took place about one minute after releasing a single triplefin in the middle of a 50 cm long tank (*n* = 80). The curved lines indicate the average distance across time of shaded (dark gray) and clear-hatted (light grey) triplefins with 95% credible intervals (shaded areas). Each triplefin was observed at 7 time points. Black dashed line: point of release (25 cm). Red dashed line: average detection distance (7 cm) at which diurnal active photolocation allows a triplefin to induce and perceive scorpionfish eyeshine, according to visual modelling (Figure 15). Symbols were slightly jittered to reveal overlapping observations in the graph.

Although these experiments tested the effects of triplefins' ocular sparks, they did not directly show whether the observed results were caused by an ability to generate eyeshine in the eye of the scorpionfish. Using visual modelling, we therefore tested whether the light emitted by a blue ocular spark is sufficient to increase the brightness of a nearby shaded scorpionfish's pupil above triplefins' perception threshold. Our results show that triplefin can induce and perceive such eyeshine over biologically relevant short distances (7 cm) (Figure 15), well matching the distances observed in the second field experiment (Figure 14).

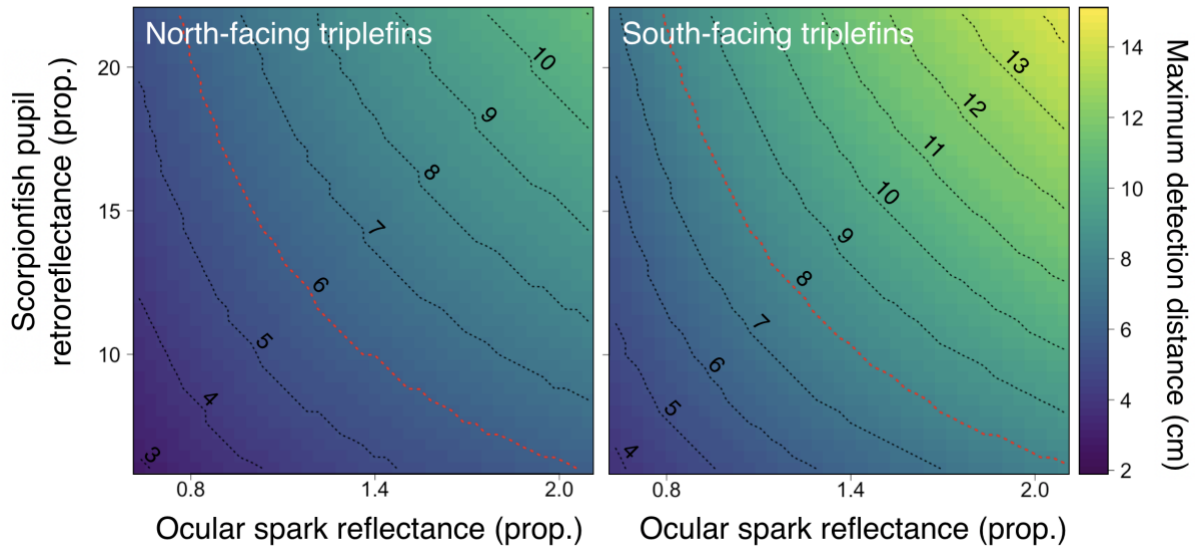

Figure 15. Theoretical triplefin's detection distance of a blue ocular spark reflected by a scorpionfish's pupil. Visual modelling outputs show maximum detection distance (colour) of scorpionfish's eyeshine induced by a triplefin's blue ocular spark at 10 m depth. The outcome is shown as a function of ocular spark reflectance, scorpionfish pupil retroreflectance, orientation and distance. Values were obtained from calculating the Michelson contrast between a pupil with and without eyeshine based on triplefins' cone-catches for each millimetre between 1 and 15 cm, and identifying the maximum distance at which the contrast was equal to or exceeded the achromatic contrast threshold of *T. delaisi* (chapter 1).

By combining the results of the three behavioural experiments and of the visual models, this chapter concludes that triplefins can use their blue ocular sparks to increase the chances to detect an overlooked cryptic predator by exploiting its retroreflective eyeshine over short distances. This new active sensing mechanism has the potential to become an important aspect of the sensory biology of marine fish in the context of prey-predator visual interactions.

Limitations

In the first field experiment the tanks were placed at 15 m depth on a sandy substrate, causing loads of behavioural noise generated by other fish species swimming around the tanks (e.g. Serranidae). A major improvement consisted in using tanks that float above the substrate (Figure 16). Such setup was developed during the years 2017-2018 and already used for the second field experiment at 10 m depth.

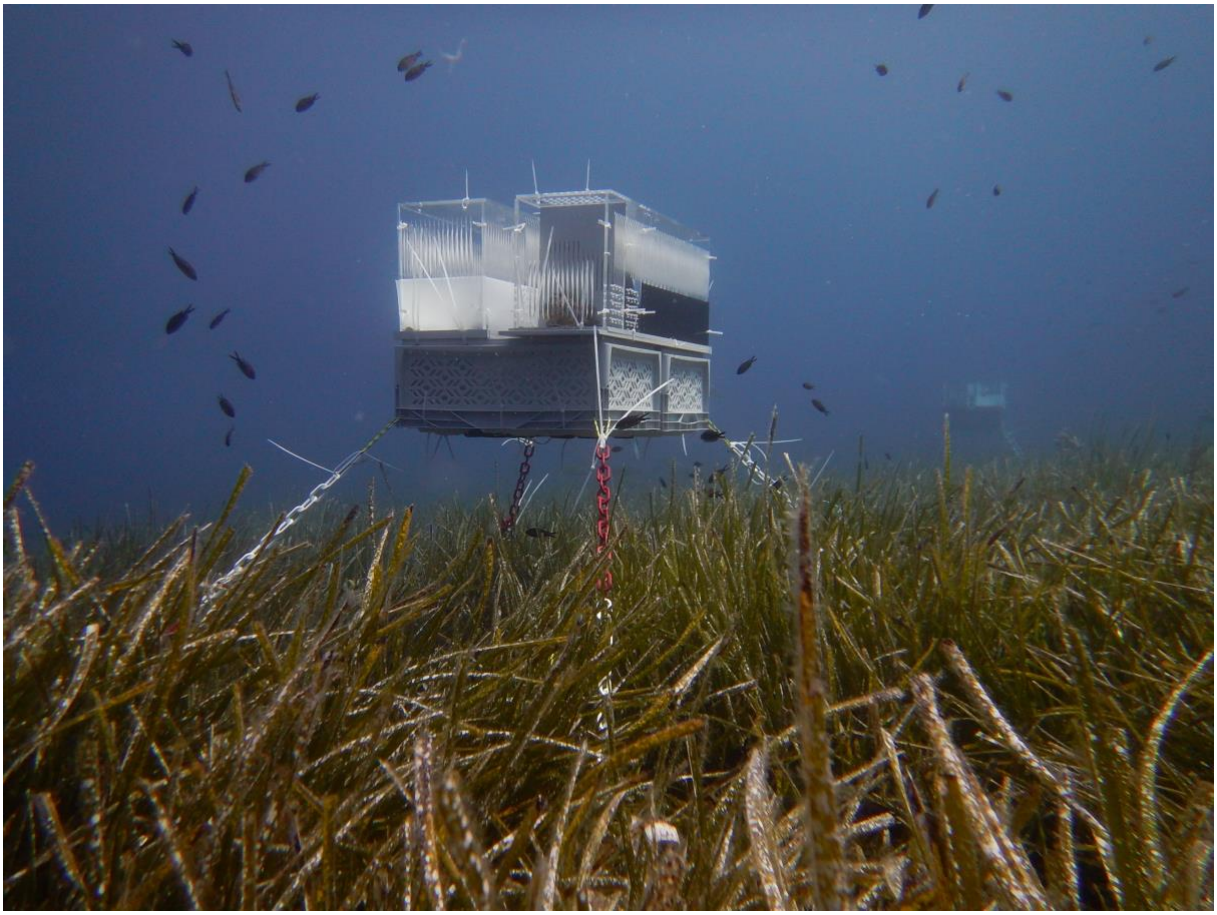

Figure 16. Experimental setup to run prey-predator behavioural experiment at 10 m depth. Plastic chains are used to connect iron rods screwed into the substrate to a float containing air-filled cannisters. Two experimental tanks were attached to the float. Photo credit: Nico Michiels.

Conclusions

The aim of this study was to investigate the visual detection by triplefins of their cryptic scorpionfish predator. This was achieved by first better understanding how a scorpionfish is visually perceived by a triplefin, and then by testing for the use of diurnal active photolocation by triplefins to increase the chances of detection of their cryptic predator. The combined findings of the three chapters provide first evidence for the functionality of diurnal active photolocation in marine fish.

This active sensing mechanism increases the chances of detection of an overlooked cryptic predator, but it is not meant to replace regular vision, nor to be a failproof safeguard. Spotting an unnoticed threat at the last moment is likely to increase the probability of survival since scorpionfish strike over short distances only [60, 61]. For this reason, this behavioural trait could be strongly favoured by natural selection.

The properties exemplified here for one triplefin and one scorpionfish species are not unique: mechanisms that redirect downwelling light are widespread and diverse across diurnal fish families [29, 62], as are retroreflective eyes in cryptic, diurnal predators [1]. Other cryptobenthic, micro-predatory species with a similar lifestyle and behaviour to triplefins may be promising candidates for diurnal active pholocation. Blennies (Fam. Blenniidae), gobies (Fam. Gobiidae) or dragonets (Fam. Callionymidae) in particular seem to face similar conditions and challenges, and their cryptobenthic predators such as scorpionfishes (Fam. Scorpaenidae), toadfishes (Fam. Batrachoididae), and stonefishes (Fam. Synanceiidae) feature daytime retroreflective eyeshine.

Future directions

The interpretation of the results of the behavioural experiments on diurnal active photolocation assumes that the observed effects are caused by the retroreflective properties of the target's eyes. Even if it is hard to imagine which other factors could generate such results, specific experiments that manipulate the reflectivity of the eyes of the target are still missing. To achieve that, scorpionfish with or without reflective eyes could be used as visual stimuli. However, since it is problematic to manipulate the reflectivity of the eyes of a live scorpionfish in a long-lasting non-invasive way, 3D printed models of this predator with interchangeable eyes could replace the live specimens. The next logical step would be the use of artificial eyes only, retroreflective or not, perhaps embedded in a natural scene. Using such stimuli, large-scale field behavioural experiments (that use the setup described in Figure 16) could compare the responses of manipulated triplets of triplefins (wearing hats) facing a target with or without retroreflective properties. Video cameras could be used to record the experimental runs, allowing to observe behavioural responses as well as distances kept from the stimuli across time. The expectation would be that fish wearing a shading hat move closer to the target with retroreflective properties compared to control hatted fish. Yet, when facing a target without retroreflective properties, such effect should be absent.

A second topic for future work is investigating other fish species and contexts in which diurnal active photolocation may supplement regular vision by increasing the chances of detection of cryptic predators. For example, structurally complex and diverse environments such as coral reefs host several small micro-predatory species showing different types of ocular radiance (e.g. ocular sparks), as well as many species of cryptobenthic predators featuring daytime retroreflective eyeshine.

Contributors

Matteo Santon: planned and conducted almost all the experiments, managed, analysed the data and contributed as first author to the three publications listed in this dissertation.

Nico K. Michiels: supervised all the experiments, helped with field work, conceptualised the research idea of the third chapter, provided great scientific input whenever needed, contributed to all manuscripts.

Pierre-Paul Bitton: conceptualised the visual models, provided great scientific input whenever needed, contributed to the second and third chapter.

Nils Anthes: provided statistical advice, provided great scientific input whenever needed, contributed to the third chapter.

Ulrike Harant: contributed with great effort and dedication to the field data collection of the second and third chapter.

Thomas A. Münch: collaborated in the second chapter by providing the setup and great scientific input whenever needed.

Jascha Dehm: conducted the lab experiment of the third chapter.

Roland Fritsch: developed the fish hatting technique used in the third chapter and provided great scientific input whenever needed.

Martin J. How: second official supervisor of the PhD candidate. Provided great scientific input whenever needed.

References

1. **Santon, M., Bitton, P-P., Harant, U.K., and Michiels, N.K. (2018).** Daytime eyeshine contributes to pupil camouflage in a cryptobenthic marine fish. Scientific Reports *8*, 7368.
2. **Darwin, C. (1859).** On the origin of species by means of natural selection; or, the preservation of favoured races in the struggle for life. (London: Murray).
3. **Caves, E.M., Brandley, N.C., and Johnsen, S. (2018).** Visual acuity and the evolution of signals. Trends in Ecology and Evolution *33*, 358-372.
4. **Land, M.F., and Nilsson, D.E. (2012).** Animal Eyes, Second Edition, (Oxford University Press).
5. **Cronin, T.W., Johnsen, S., Marshall, N.J., and Warrant, E.J. (2014).** Visual Ecology. (Princeton University Press).
6. **Govardovskii, V.I., Fyhrquist, N., Reuter, T., Kuzmin, D.G., and Donner, K. (2000).** In search of the visual pigment template. Visual Neuroscience *17*, 509-528.
7. **Thoen, H.H., Chiou, T.-H., and Marshall, N.J. (2017).** Intracellular recordings of spectral sensitivities in stomatopods: a comparison across species. Integrative and Comparative Biology *57*, 1117-1129.
8. **Marshall, J., and Oberwinkler, J. (1999).** The colourful world of the mantis shrimp. Nature *401*, 873.
9. **Hart, N.S., and Vorobyev, M. (2005).** Modelling oil droplet absorption spectra and spectral sensitivities of bird cone photoreceptors. Journal of Comparative Physiology A *191*, 381-392.
10. **Ellingson, J.M., Fleishman, L.J., and Loew, E.R. (1995).** Visual pigments and spectral sensitivity of the diurnal gecko *Gonatodes albogularis*. Journal of Comparative Physiology A *177*, 559-567.
11. **Defrize, J., Lazzari, C.R., Warrant, E.J., and Casas, J. (2011).** Spectral sensitivity of a colour changing spider. Journal of Insect Physiology *57*, 508-513.
12. **Bitton, P-P., Harant, U.K., Fritsch, R., Champ, C.M., Temple, S.E., and Michiels, N.K. (2017).** Red fluorescence of the triplefin *Tripterygion delaisi* is

increasingly visible against background light with increasing depth. Royal Society Open Science *4*.

13. **Menzel, R., and Blakers, M. (1976).** Colour receptors in the bee eye — Morphology and spectral sensitivity. Journal of Comparative Physiology *108*, 11-13.
14. **Arikawa, K., Inokuma, K., and Eguchi, E. (1987).** Pentachromatic visual system in a butterfly. Naturwissenschaften *74*, 297-298.
15. **Schnapf, J.L., Kraft, T.W., and Baylor, D.A. (1987).** Spectral sensitivity of human cone photoreceptors. Nature *325*, 439.
16. **Mäthger, L.M., Barbosa, A., Miner, S., and Hanlon, R.T. (2006).** Color blindness and contrast perception in cuttlefish (*Sepia officinalis*) determined by a visual sensorimotor assay. Vision Research *46*, 1746-1753.
17. **Neitz, J., Geist, T., and Jacobs, G.H. (1989).** Color vision in the dog. Visual Neuroscience *3*, 119-125.
18. **Reymond, L. (1985).** Spatial visual acuity of the eagle *Aquila audax*: a behavioural, optical and anatomical investigation. Vision research *25*, 1477-1491.
19. **Land, M.F. (1981).** Optics and vision in invertebrates. In Handbook of sensory physiology (ed. Autrum, H.), Volume Vol. VII/6B. (Berlin: Springer), pp. 471-592.
20. **Land, M.F. (1985).** The morphology and optics of spider eyes. In Neurobiology of arachnids (ed. Barth, F.G.). (Berlin: Springer), pp. 53-78.
21. **Charman, W.N. (1991).** The vertebrate dioptric apparatus. In Vision and visual dysfunction, Volume Vol. 2. (Basingstoke: Macmillan), pp. 82-117.
22. **Fritsch, R., Collin, S.P., and Michiels, N.K. (2017).** Anatomical analysis of the retinal specializations to a crypto-benthic, micro-predatory lifestyle in the Mediterranean triplefin blenny *Tripterygion delaisi*. Frontiers in Neuroanatomy *11*.
23. **Douglas, R., and Djamgoz, M. (2012).** The visual system of fish. (Springer Netherlands).
24. **Troscianko, J., and Stevens, M. (2015).** Image calibration and analysis toolbox – a free software suite for objectively measuring reflectance, colour and pattern. Methods in Ecology and Evolution *6*, 1320-1331.

25. **Caves, E.M., and Johnsen, S. (2018).** AcuityView: An R package for portraying the effects of visual acuity on scenes observed by an animal. Methods in Ecology and Evolution *9*, 793-797.
26. **Nelson, M.E., and MacIver, M.A. (2006).** Sensory acquisition in active sensing systems. Journal of Comparative Physiology A: Neuroethology, Sensory, Neural, and Behavioral Physiology *192*, 573-586.
27. **Howland, H.C., Murphy, C.J., and McCosker, J.E. (1992).** Detection of eyeshine by flashlight fishes of the family Anomalopidae. Vision Research *32*, 765-769.
28. **Hellinger, J., Jägers, P., Donner, M., Sutt, F., Mark, M.D., Senen, B., Tollrian, R., and Herlitze, S. (2017).** The flashlight fish *Anomalops katoptron* uses biolumescent light to detect prey in the dark. Plos One *12*, e0170489.
29. **Michiels, N.K., Seeburger, V.C., Kalb, N., Meadows, M.G., Anthes, N., Mailli, A.A., and Jack, C.B. (2018).** Controlled iris radiance in a diurnal fish looking at prey. Royal Society Open Science *5*.
30. **Howland, H.C., Murphy, C.J., and McCosker, J.E. (1992).** Detection of eyeshine by flashlight fishes of the family Anomalopidae. Vision Research *32*, 765-769.
31. **Douglas, R.H., Partridge, J.C., Dulai, K.S., Hunt, D.M., Mullineaux, C.W., and Hynninen, P.H. (1999).** Enhanced retinal longwave sensitivity using a chlorophyll-derived photosensitiser in *Malacosteus niger*, a deep-sea dragon fish with far red bioluminescence. Vision Research *39*, 2817-2832.
32. **Douglas, R.H., Mullineaux, C.W., and Partridge, J.C. (2000).** Long-wave sensitivity in deep-sea stomiid dragonfish with far-red bioluminescence: evidence for a dietary origin of the chlorophyll-derived retinal photosensitizer of *Malacosteus niger*. Philosophical Transactions of the Royal Society of London Series B-Biological Sciences *355*, 1269-1272.
33. **Sutton, T.T., and Hopkins, T.L. (1996).** Trophic ecology of the stomiid (Pisces: Stomiidae) fish assemblage of the eastern Gulf of Mexico: strategies, selectivity and impact of a top mesopelagic predator group. Marine Biology *127*, 179-192.
34. **Sutton, T.T. (2005).** Trophic ecology of the deep-sea fish *Malacosteus niger* (Pisces: Stomiidae): An enigmatic feeding ecology to facilitate a unique visual system? Deep Sea Research Part I: Oceanographic Research Papers *52*, 2065-2076.

35. **Kjernsmo, K., Grönholm, M., and Merilaita, S. (2016).** Adaptive constellations of protective marks: eyespots, eye stripes and diversion of attacks by fish. Animal Behaviour *111*, 189-195.
36. **Satoh, S., Tanaka, H., and Kohda, M. (2016).** Facial recognition in a discus fish (Cichlidae): Experimental approach using digital models. Plos One *11*, e0154543.
37. **Cott, H.B. (1940).** Adaptive coloration in animals. (London, UK: Methuen & Co. Ltd.).
38. **Lythgoe, J.N. (1975).** The structure and function of iridescent corneas in teleost fishes. Proceedings of the Royal Society of London. Series B. Biological Sciences *188*, 437-457.
39. **Feller, K.D., and Cronin, T.W. (2014).** Hiding opaque eyes in transparent organisms: a potential role for larval eyeshine in stomatopod crustaceans. Journal of Experimental Biology *217*, 3263-3273.
40. **Louisy, P. (2015).** Europe and Mediterranean marine fish identification guide. (Ulmer).
41. **Bitton, P-P., Yun Christmann, S.A., Santon, M., Harant, U.K., and Michiels, N.K. (2018).** Visual modelling validates prey detection by means of diurnal active photolocation in a small cryptobenthic fish (in review for Scientific Reports).
42. **Compaire, J.C., Casademont, P., Cabrera, R., Gómez-Cama, C., and Soriguer, M.C. (2017).** Feeding of *Scorpaena porcus* (Scorpaenidae) in intertidal rock pools in the Gulf of Cadiz (NE Atlantic). Journal of the Marine Biological Association of the United Kingdom, 1-9.
43. **Best, A.C.G., and Nicol, J.A.C. (1980).** Eyeshine in fishes. A review of ocular reflectors. Canadian Journal of Zoology *58*, 945-956.
44. **Nicol, J.A.C. (1980).** Studies on the eyes of toadfishes *Opsanus*. Structure and reflectivity of the stratum argenteum. Canadian Journal of Zoology *58*, 114-121.
45. **De Valois, R.L., and De Valois, K.K. (1990).** Spatial Vision. (Oxford University Press).
46. **Uhlrich, D.J., Essock, E.A., and Lehmkuhle, S. (1981).** Cross-species correspondence of spatial contrast sensitivity functions. Behavioural Brain Research *2*, 291-299.

47. **Bilotta, J., and Powers, M.K. (1991).** Spatial contrast sensitivity of goldfish: mean luminance, temporal frequency and a new psychophysical technique. Vision Research *31*, 577-585.
48. **Northmore, D.P.M., Oh, D.J., and Celenza, M.A. (2007).** Acuity and contrast sensitivity of the bluegill sunfish and how they change during optic nerve regeneration. Visual Neuroscience *24*, 319-331.
49. **Northmore, D.P.M., and Dvorak, C.A. (1979).** Contrast sensitivity and acuity of the goldfish. Vision Research *19*, 255-261.
50. **Ghim, M.M., and Hodos, W. (2006).** Spatial contrast sensitivity of birds. Journal of Comparative Physiology A *192*, 523-534.
51. **Harmening, W.M., Nikolay, P., Orlowski, J., and Wagner, H. (2009).** Spatial contrast sensitivity and grating acuity of barn owls. Journal of Vision *9*, 13-13.
52. **Lind, O., and Kelber, A. (2011).** The spatial tuning of achromatic and chromatic vision in budgerigars. Journal of Vision *11*, 2-2.
53. **Champ, C., Wallis, G., Vorobyev, M., Siebeck, U., and Marshall, J. (2014).** Visual acuity in a species of coral reef fish: *Rhinecanthus aculeatus*. Brain, behavior and evolution *83*, 31-42.
54. **Nakamura, E.L. (1968).** Visual acuity of two tunas, *Katsuwonus pelamis* and *Euthynnus affinis*. Copeia, 41-49.
55. **Yamanouchi, T. (1956).** The visual acuity of the coral fish *Microcanthus strigatus* (Cuvier & Valenciennes). Publication Seto Marine Biology Laboratory *5*, 133–156.
56. **Denton, E.J., and Nicol, J.A.C. (1964).** The chorioidal tapeta of some cartilaginous fishes (Chondrichthyes). Journal of the Marine Biological Association of the United Kingdom *44*, 219-258.
57. **Ollivier, F.J., Samuelson, D.A., Brooks, D.E., Lewis, P.A., Kallberg, M.E., and Komaromy, A.M. (2004).** Comparative morphology of the tapetum lucidum (among selected species). Veterinary ophthalmology *7*, 11-22.
58. **Fritsch, R., Ullmann, J.F.P., Bitton, P-P., Collin, S.P., and Michiels, N.K. (2017).** Optic-nerve-transmitted eyeshine, a new type of light emission from fish eyes. Frontiers of Zoology *14*, 14.
59. **Troscianko, J., Skelhorn, J., and Stevens, M. (2017).** Quantifying camouflage: how to predict detectability from appearance. BMC Evolutionary Biology *17*, 7.

60. **Montgomery, J.C., and Hamilton, A.R. (1997).** Sensory contributions to nocturnal prey capture in the dwarf scorpion fish (*Scorpaena papillosus*). Marine and Freshwater Behaviour and Physiology.
61. **Harmelin-Vivien, M.L., Kaim-Malka, R.A., Ledoyer, M., and Jacob-Abraham, S.S. (1989).** Food partitioning among scorpaenid fishes in Mediterranean seagrass beds. Journal of Fish Biology *34*, 715-734.
62. **Anthes, N., Theobald, J., Gerlach, T., Meadows, M.G., and Michiels, N.K. (2016).** Diversity and ecological correlates of red fluorescence in marine fishes. Frontiers in Ecology and Evolution *4*.

Appendix

The contrast sensitivity function of a small cryptobenthic marine fish

Matteo Santon
Animal Evolutionary Ecology, Institute of Evolution and Ecology, Department of Biology, Faculty of Science, University of Tübingen, Tübingen, Germany

Thomas A. Münch
Retinal Circuits and Optogenetics, Institute for Ophthalmic Research, Department of Ophthalmology, and Centre for Integrative Neuroscience, University of Tübingen, Tübingen, Germany

Nico K. Michiels
Animal Evolutionary Ecology, Institute of Evolution and Ecology, Department of Biology, Faculty of Science, University of Tübingen, Tübingen, Germany

Spatial resolution is a key property of eyes when it comes to understanding how animals' visual signals are perceived. This property can be robustly estimated by measuring the contrast sensitivity as a function of different spatial frequencies, defined as the number of achromatic vertical bright and dark stripe pairs within one degree of visual angle. This contrast sensitivity function (CSF) has been estimated for different animal groups, but data on fish are limited to two free-swimming, freshwater species (i.e., goldfish and bluegill sunfish). In this study, we describe the CSF of a small marine cryptobenthic fish (*Tripterygion delaisi*) using an optokinetic reflex approach. *Tripterygion delaisi* features a contrast sensitivity that is as excellent as other fish species, up to 125 (reciprocal of Michelson contrast) at the optimal spatial frequency of 0.375 c/°. The maximum spatial resolution is instead relatively coarse, around 2.125 c/°. By comparing our results with acuity values derived from anatomical estimates of ganglion cells' density, we conclude that the optokinetic reflex seems to be adapted to process low spatial frequency information from stimuli in the peripheral visual field and show that small marine fish can feature excellent contrast sensitivity at optimal spatial frequency.

Introduction

Vision shows such a diversity in anatomy, physiology, and performance across animal species that we cannot make predictions on the functionality of animals' visual signals based on our own human perception (Bennett, Cuthill, & Norris, 1994; Caves, Brandley, & Johnsen, 2018; Land & Nilsson, 2012). An important start to the investigation of such signals is to measure species-specific visual properties such as spectral sensitivity and spatial resolution (Caves, Frank, & Johnsen, 2016; Olsson, Lind, Kelber, & Simmons, 2017). Such properties are traditionally estimated anatomically, but they should also be assessed behaviorally (Kelber, Vorobyev, & Osorio, 2003): whereas anatomy provides estimates of the theoretical upper limit of vision, behavioral tests should match reality more closely (Caves et al., 2018).

Spatial resolution (Land & Nilsson, 2012) plays a critical role in defining the active space (i.e., the maximum perception distance) of a visual signal (Caves et al., 2018; Caves et al., 2016). Because this property is affected by the contrast of the signal, spatial resolution is better estimated with a contrast sensitivity function (CSF; De Valois & De Valois, 1990; Uhlrich, Essock, & Lehmkuhle, 1981). This approach is more comprehensive than measuring maximum spatial resolution only (Lind & Kelber, 2011), as it expresses contrast sensitivity as a function of spatial frequency (number of vertical bright and dark stripe pairs within one degree of visual angle).

The CSF has been behaviorally estimated for at least two insects (Chakravarthi, Baird, Dacke, & Kelber, 2016; Srinivasan & Lehrer, 1988), seven birds (Harmening, Nikolay, Orlowski, & Wagner, 2009; Hirsch, 1982; Hodos, Ghim, Potocki, Fields, & Storm, 2002; Jarvis, Abeyesinghe, McMahon, & Wathes, 2009; Lind & Kelber, 2011; Lind, Sunesson, Mitkus, & Kelber,

Citation: Santon, M., Münch, T. A., & Michiels, N. K. (2019). The contrast sensitivity function of a small cryptobenthic marine fish. *Journal of Vision*, *19*(2):1, 1–10, https://doi.org/10.1167/19.2.1.

https://doi.org/10.1167/19.2.1 Received August 1, 2018; published February 1, 2019 ISSN 1534-7362

2012; Reymond & Wolfe, 1981), and 13 mammals (Birch & Jacobs, 1979; Bisti & Maffei, 1974; De Valois, Morgan, & Snodderly, 1974; Hanke, Scholtyssek, Hanke, & Dehnhardt, 2011; Jacobs, 1977; Jacobs, Birch, & Blakeslee, 1982; Jacobs, Blakeslee, McCourt, & Tootell, 1980; Langston, Casagrande, & Fox, 1986; Merigan, 1976; Petry, Fox, & Casagrande, 1984). Data on fish are limited to two free-swimming, freshwater species (i.e., goldfish and bluegill sunfish; Bilotta & Powers, 1991; Northmore & Dvorak, 1979; Northmore, Oh, & Celenza, 2007). Although marine fish are a common subject of visual ecology studies, according to our knowledge a CSF has not been determined for any of them.

Here, we describe the CSF of a small marine cryptobenthic (i.e., bottom-living and camouflaged) fish, the triplefin *Tripterygion delaisi*, that lives in complex coastal hard-bottom environments where interactions with other species are frequent (e.g., prey or predators) and therefore good contrast sensitivity and spatial resolution can be expected to be advantageous.

We used an optokinetic reflex approach, which is traditionally elicited by placing an animal in the center of a rotating drum featuring a vertical grating. The optokinetic reflex consists of rotational eye movements to improve stabilization against relative motion of the environment rather than visual tracking of an individual object. It is therefore assumed to primarily depend on peripheral vision in animals that feature a fovea (Caves et al., 2018; Douglas & Djamgoz, 2012). The spatial resolution estimate obtained for *T. delaisi* from the CSF coincides well with previous anatomy-based resolution estimates of the peripheral retina (Fritsch, Collin, & Michiels, 2017), and the extremely fine contrast sensitivity measured is comparable to two freshwater fish species (Bilotta & Powers, 1991; Douglas & Djamgoz, 2012; Northmore & Dvorak, 1979; Northmore et al., 2007).

Materials and methods

Model species

The triplefin *Tripterygion delaisi* is a small (4–5 cm) northeast Atlantic and Mediterranean cryptobenthic fish, common in rocky coastal areas between 5 m to below 20 m depth (De Jonge & Videler, 1989; Domingues, Almada, Santos, Brito, & Bernardi, 2007). Preferred prey are small crustaceans (Zander & Hagemann, 1989), which are caught with sudden strikes over distances between 1–3 cm (unpublished data). During the breeding season (March through May), individuals show a sex color dimorphism: males develop black heads and a bright yellow body; females maintain the partially translucent coloration with red irides featured by individuals of both sexes throughout the rest of the year (Bitton et al., 2017). We collected individuals close to the Station de Recherches Sous-marines et Océanographiques (STARESO) near Calvi, Corsica (France). Sampling took place under the general sampling permit of the station. *Tripterygion delaisi* is a non-threatened, non-protected, non-commercial, common species.

Fish collection and housing

Animals were transported individually in plastic fish breathing bags™ (Kordon, Hayward, CA) filled with 250 ml purified seawater. At the University of Tübingen, fish were kept in individual tanks ($L \times W \times H = 24 \times 35 \times 39$ cm^3) illuminated by weak, diffuse blue light. Coral sand covered the bottom, and a rock was provided as shelter. All aquaria were interconnected to a flow-through filtering and UV-sterilization system (23°C, salinity 35‰, pH 8.2, 12 h light/dark cycle). Water quality was checked on a weekly basis. Fish were fed with a mixture of Tetramin (Hauptfutter für alle Zierfische; Tetra GmbH, Melle, Germany) and Mysis (Einzelfuttermittel; Aki Frost GmbH, Ganderkesee, Germany) every day. Animal husbandry was carried out in accordance with German animal welfare legislation. Because the individuals were not experimentally manipulated, a formal permit was not required for this study (as confirmed by the Animal Care Officer at the Biology Department of the University of Tübingen).

Optokinetic virtual arena

To characterize the contrast sensitivity function we observed individuals ($N = 10$) in the center of an "optokinetic drum" (Benkner, Mutter, Ecke, & Münch, 2013) while exposed to horizontally rotating grayscale vertical striped patterns defined by combinations of spatial frequency (cycles per degree) and contrast (Michelson) calculated as $(L_1 - L_2)/(L_1 + L_2)$, where L_1 and L_2 are the photon radiances of the bright and dark stripes. As is true for many benthic teleosts (Fritsches & Marshall, 2002), triplefins show independent eye movement (Michiels et al., 2018). Their optokinetic reflex consists of tracking behavior (at least one eye or the body following the rotation direction of the pattern), often mixed with opposing saccades (sudden eye movement in the opposite direction of the pattern movement; Supplementary Movie S1).

The virtual arena (OptoDrum software; Striatech UG, Tübingen, Germany; L × W × H: 53 × 53 × 30

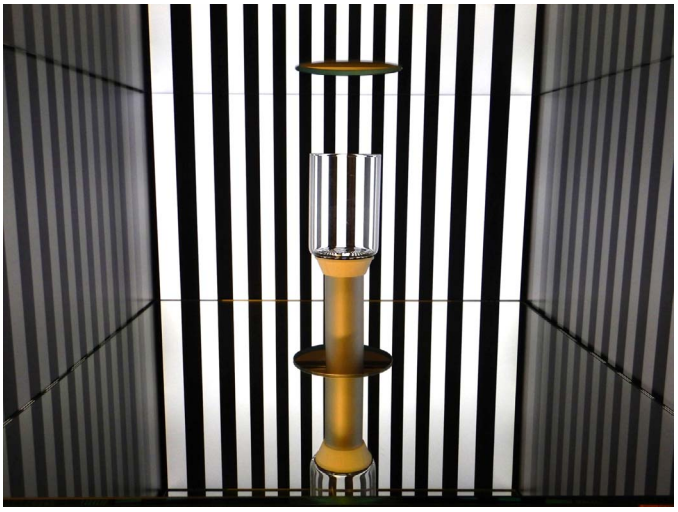

Figure 1. Virtual arena inside the optokinetic drum. Individual fish were placed in a central transparent glass cylinder positioned on an elevated circular platform. The four screens surrounding the fish displayed the grating pattern. Mirrors on the bottom and top of the setup assured the grating to be visible in a radial pattern (not visible from the camera perspective shown here). Photo credit: Matteo Santon.

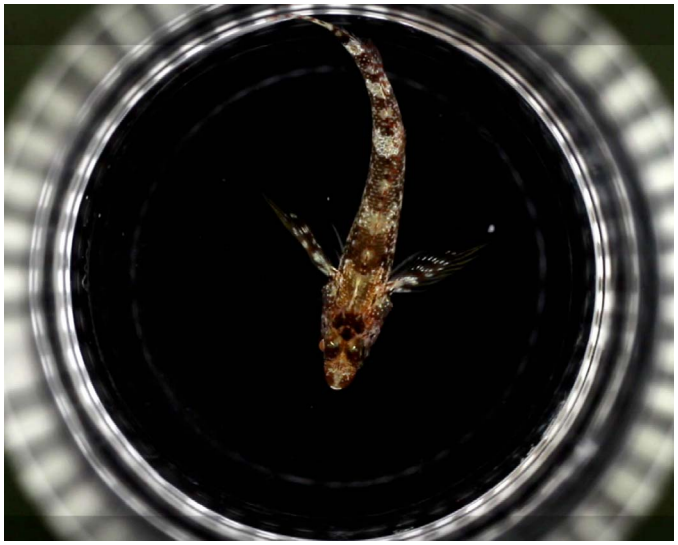

Figure 2. Top view of the optokinetic drum virtual arena. A fish in the center of a glass cylinder experiences the moving grating pattern on the screens as a rotating cylinder. Photo credit: Matteo Santon.

cm^3) consisted of four 23.8 in. LCD monitors (EIZO EV2450) set to DICOM presentation mode. Individuals were placed in a transparent glass cylinder (D × H: 6.5 × 10 cm^2) with a black bottom, filled with home tank water and positioned on an elevated circular platform (Figure 1). The bottom and the top of the arena consisted of two mirrors to ensure that the fish would see the pattern even if looking up or down (Figure 1). Circular holes in the mirrors (D = 10 cm) were used for inserting the platform, and to position a Canon EOS 7D (Canon Inc., Tokyo, Japan) with a 100 mm macro lens above the setup to record the fish. The width of the horizontally moving vertical stripes on the screens was electronically widened toward the corners to maintain the same angular resolution from the center of the setup. For the fish in the setup, this generates the optical illusion of being in the center of a cylindrical drum (Figure 2). Overall brightness in the setup was kept constant across all stimuli at the value obtained when all four screens were set at 50% homogeneous gray. Michelson contrasts between the stripes ranged from of 0.8% to 99.7%. These values represent the smallest and largest contrasts the setup could generate. The total photon radiance (integrated from 380 to 780 nm) of a polytetrafluoroethylene (PTFE) white reflectance standard (Lake Photonics, Uhldingen-Mühlhofe, Germany) placed flat on the platform surrounded by uniform 50% gray screens was measured from above using a calibrated SpectraScan PR 670 spectroradiometer (Photo Research, Syracuse, NY) and was 1.13 × 10^{17} photons s^{-1} sr^{-1} m^{-2} nm^{-1}, similar to the total radiance measured in a comparable way in the shade around 20 m depth in the field where this species occurs (Harant et al., 2018). The OptoDrum software (Striatech) allows the free adjustment of the perceived width (spatial frequency), contrast, rotation direction (left or right) and angular speed of the striped pattern.

Behavioral tests

We acclimated fish with uniform 50% gray screens for 5 min. Every test consisted of several sessions (quantity depending on the fish performance), in which a fish was recorded while looking at a rotating grating. Each fish ($N = 10$) was tested once. Following preliminary tests, we kept the rotation at the speed of 4°/s, which was optimal for this species in this experimental setup. We randomized the order in which different spatial frequencies were displayed and alternated the rotation direction between sessions. As a transition to the next stimulus, a uniform 50% gray display was shown for 10 to 20 s. We live-evaluated and recorded a fish's response to spatial frequencies from 0.125 c/° to the individual perception threshold in steps of 0.250 c/°. Within each spatial frequency step, we gradually reduced the contrast of the stripes starting from the maximum of 99.7% down to the contrast value at which the fish did not show a response anymore. To minimize the number of sessions and therefore reduce potential stress generation in the fish, the descending contrast steps displayed were slightly

different for each individual in accordance with previous fish responses at the different spatial frequencies tested. The contrast sensitivity limit at any given spatial frequency was determined as the weakest contrast still eliciting a response. As a control, we recorded the response to 50% gray uniform screens for three minutes. All videos were zoomed in to such an extent that only the snout and eyes of the fish were visible, but not the stimulus (Supplementary Movie S1). Run duration was decided by the experimenter based on the live image and ranged from 1 min (if a fish showed immediate, unequivocal reflexes) to maximum 3 min (when a fish showed weak or no reaction). Fish that showed tracking behavior at least once or several saccadic reflexes during the entire live run were considered to have perceived the stimulus. To confirm these live assessments, a second observer naïve to the experiment evaluated the recordings in random order. The second observer assessed if the fish was showing an optokinetic reflex, and also in which direction. To minimize false positives, a fish was considered "non-responding" when reflex-like behavior was detected but its direction was not in accordance with the rotation direction of the grating. Also, to further reduce the risk of false positives, only the sessions in which the first observer (live assessment) and the second observer (unbiased assessment) noted a response were counted as positives.

Data analysis

Behavioral data were analyzed using generalized linear mixed effects models (gamma distribution, link = log) with the glmmTMB package (Brooks et al., 2017) for R v. 3.4.3 (R Core Team, 2017). We used contrast sensitivity as response variable, the main predictor spatial frequency and rotation direction as factorial fixed components, and individual ID as random component. We performed backward model selection using the Akaike information criterion (AIC) to identify the best fitting model with the smallest number of covariates (Zuur, Ieno, Walker, Saveliev, & Smith, 2009). We only report the final reduced model and its overall goodness-of-fit (conditional R^2; i.e., the proportion of variation explained by the model considering fixed and random factors [Nakagawa & Schielzeth, 2010]). Model assumptions were validated by plotting residuals versus fitted values and each covariate present in the full, non-reduced model. We used Wald *z*-tests to assess the significance of fixed effects. Multiple comparisons of contrast sensitivity among different spatial frequencies were computed by using 95% credible intervals (CrIs), a Bayesian analogue of confidence intervals (Bolker et al., 2009). For the response variable contrast sensitivity, we

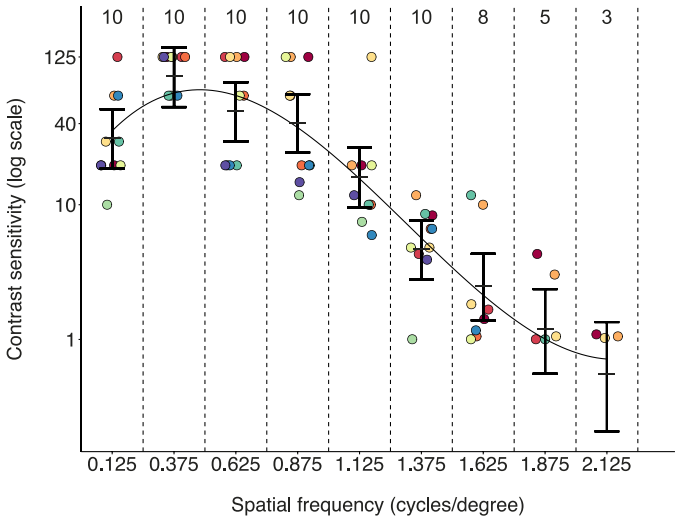

Figure 3. Contrast sensitivity function (CSF) of *Tripterygion delaisi*. Contrast sensitivity, expressed as the reciprocal of the Michelson contrast, as a function of spatial frequency. The optimal sensitivity was around 0.375 c/°, where seven out of 10 fish showed the maximum sensitivity of 125, which corresponds to a 0.8% Michelson contrast. Contrast sensitivity is plotted on a log-scale. Numbers at the top indicate the number of individuals ($N = 10$) responding to each spatial frequency. None of the individuals responded to the spatial frequency of 2.375 (not shown). Each color of the points represents a different individual (jittered for clarity). Error bars display the model-predicted group means ± 95% credible intervals. The black curve shows the relationship between contrast sensitivity and spatial frequency on a continuous scale (see Materials and methods section for details).

computed model-predicted means and the associated 95% CrIs from 10,000 simulations of the model, using the simulate function of the R package stats. If the mean sensitivity at one spatial frequency falls outside the credible interval of another frequency, the difference between the two groups is significant.

To visualize the relationship between contrast sensitivity and spatial frequency on a continuous scale, we also generated an analogue model that used spatial frequency as a continuous predictor and that included a quadratic and a cubic term to compensate for non-linear patterns (tested using the *gam* function of the R package mgcv (Wood, 2006)). This model was only used to generate the smoothing curve in Figure 3.

All data were processed using R v. 3.4.3 (R Core Team, 2017). Means are shown ± standard deviation unless specified otherwise. Contrast sensitivity values are shown as the reciprocal of the Michelson contrasts values. Raw data to perform the analyses are provided in the Appendix (Table A1).

Results

We obtained the contrast sensitivity function of *T. delaisi* from 10 individuals by observing the smallest contrast that elicited the optokinetic reflex, in response to a vertical stripe pattern rotating around the fish horizontally at a speed of 4 °/s. We measured such contrast sensitivity threshold at 10 different spatial frequencies of the stripe pattern, ranging from 0.125 c/° to 2.375 c/° in equal steps of 0.250 c/°. The results are displayed as colored dots in Figure 3, where each individual is identified by a unique color. We analyzed these data by fitting a generalized linear mixed effects model (see Materials and methods for details). Model validation did not show any violation of the model assumptions. The direction of rotation of the drum was dropped during model selection. The final model only contained spatial frequency as fixed factor (generalized linear mixed effects model: R^2_{cond}: 0.86, spatial frequency: $p < 0.0001$). At the highest stimulus contrast (99.7% Michelson contrast, equal to a contrast sensitivity of 1), the high frequency cutoff was at 2.125 c/° (Figure 3), where three fish out of 10 still showed optokinetic reflexes. None of the fish responded to the stimulus at 2.375 c/° (not shown in Figure 3). On average, fish showed a high spatial frequency cutoff of 1.8 ± 0.3 c/°. The optimal spatial frequency eliciting an optokinetic reflex was at 0.375 c/°, with seven out of 10 fish still showing responses to a Michelson contrast as low as 0.8%, equal to a contrast sensitivity of 125 (Figure 3). At this spatial frequency, the model estimated an average contrast sensitivity around 90.33 (95% credible interval from 53.1 to 147.6; Figure 3). At the lowest experimental spatial frequency (0.125 c/°), contrast sensitivity significantly dropped to the model-estimated mean value of 31.4 (95% credible interval from 18.5 to 51.2; Figure 3). The characteristic optokinetic eye movements were also never observed with a uniform 50% gray screen control.

Discussion

The shape of the contrast sensitivity function of *T. delaisi* is consistent with the one found in most species, a classic inverted U-profile (Figure 3; Uhlrich et al., 1981) and shows a maximum contrast sensitivity of 125 (0.8% Michelson contrast, lowest testable contrast) at a spatial frequency of 0.375 c/°. This maximum contrast sensitivity value is comparable to what is known from freshwater free-swimming fish species (sensitivity up to 111; Bilotta & Powers, 1991; Douglas & Djamgoz, 2012; Northmore & Dvorak, 1979; Northmore et al., 2007), and higher than in most of birds tested so far (sensitivity up to 20; Ghim & Hodos, 2006; Harmening et al., 2009; Lind & Kelber, 2011). For fish, high contrast sensitivity may help to maximize contrast perception in aquatic environments, where contrasts are usually strongly degraded because of light scatter by suspended particles (Douglas & Djamgoz, 2012).

At higher spatial frequencies, sensitivity drops until it reaches a cutoff at 2.125 c/°. This relatively coarse spatial resolution limit suggests an adaptation of the optokinetic reflex to process low spatial frequency information from stimuli in the peripheral visual field. This statement is further supported by the fact that underwater light fields tend to act as a high spatial-frequency cutoff filter, where the light scattered by suspended particles blurs the edges of objects at distance (Douglas & Djamgoz, 2012).

The decrease of sensitivity at low spatial frequency probably represents the center-surround receptive field properties of the retinal neurons perceiving the moving environment.

A recent description of the retinal distribution of photoreceptors and ganglion cells in *T. delaisi* (Fritsch et al., 2017) estimated that its spatial resolution lies between 6.7 to 9 c/° for the fovea, and 2.4 c/° for the peripheral retina. This fits well with the spatial resolution estimated behaviorally in this study (2.125 c/°), assuming that the optokinetic reflex is based on peripheral vision. This close match suggests that the anatomical foveal acuity estimates of the same study (Fritsch et al., 2017) might also be close to reality.

It has been already suggested that spatial resolution measures based on the optokinetic reflex in animals featuring a fovea underestimate their maximum acuity (Caves et al., 2018). To obtain a behavioral assessment of foveal spatial resolution, a different approach is required. One possibility is to induce animals to track small visual targets rather than wide-field stimuli. This can be achieved for example by training species to distinguish vertically from horizontally striped targets (Champ, Wallis, Vorobyev, Siebeck, & Marshall, 2014; Nakamura, 1968; Yamanouchi, 1956) or a specific black shape from a uniform gray background (Champ et al., 2014).

Considering the ecology of *T. delaisi*, the anatomically estimated spatial resolution of 6.7 c/° (fovea) or 2.4 c/° (periphery) makes a significant difference. At a distance of 20 cm, peripheral vision would roughly allow the resolution of conspecifics, while foveal vision would reach the same limit at four times that distance (Figure 4). However, the resolving power of peripheral vision would still be sufficient to detect the outline of predators (which are about four times larger than *T. delaisi*) up to 80 cm (Figure 4), a distance that still allows for fast fleeing responses. This suggests that foveal vision could function to search for small prey when foraging or for intraspecific interactions, while

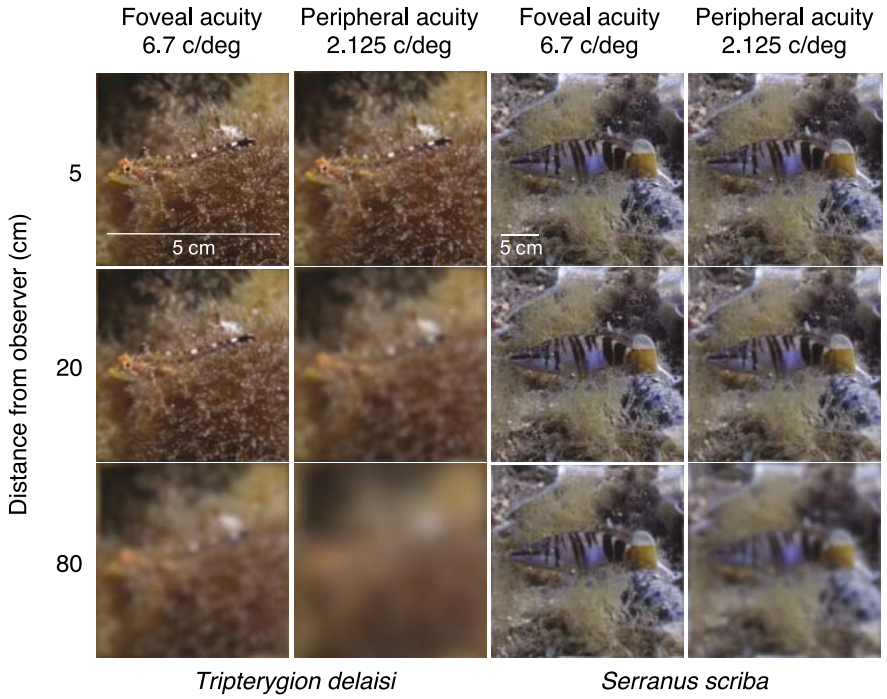

Figure 4. A *Tripterygion delaisi*'s view of a conspecific and of a predator. Foveal acuity (first column) allows resolution of conspecifics (*T. delaisi*) at a greater distance than peripheral acuity (second column), while both acuities allow to resolve the outline of a potential predator (*Serranus scriba*) up to 80 cm (third and fourth column). Each image shows the spatial information content of the scene, adjusted for spatial resolution and distance. We also assume that the total length of *T. delaisi* in the picture is 5 cm, and the length of *S. scriba* is 20 cm. All manipulated images have been generated using the R package AcuityView (Caves & Johnsen, 2018). Photo credits: Matteo Santon.

peripheral vision could at least allow the perception of bigger predators.

In conclusion, this study shows that the optokinetic reflex can be reliably used to estimate the spatial resolution of the peripheral retina and that this small marine cryptobenthic fish features excellent contrast sensitivity of up to 125. These estimates are important in planning future behavioral experiments and to inform visual models based on the vision of small marine benthic fishes.

Keywords: contrast sensitivity function, spatial resolution, optokinetic reflex, vision, marine fish, Tripterygion

Acknowledgments

The authors warmly thank Valentina Richter for the evaluation of the recordings, Oeli Oelkrug for fish maintenance at the University of Tübingen, and Gregor Schulte for invaluable IT assistance. We further thank Dr. Pierre-Paul Bitton, Dr. Nils Anthes, and Dr. Martin J. How for fruitful suggestions or discussions.

MS conceptualized the study, performed data collection, and analyzed the data. TAM provided the setup and the OptoDrum software. MS drafted the manuscript. All authors discussed the data, edited, and finalized the manuscript.

The project was funded by the by the German Science Foundation Koselleck grant (Mi482/13-1) and the Volkswagen Foundation (Az. 89148 and Az. 91816) awarded to NKM. Development of the OptoDrum device was supported by funds from the University of Tübingen (Innovation Grant). TAM received support from the Kerstan foundation.

Commercial relationships: none. Although TAM is co-owner of Striatech UG, who is the manufacturer of the optokinetic arena used for this study, all data collection and analysis was performed by MS.
Corresponding author: Matteo Santon.
Email: matteo.santon@uni-tuebingen.de.
Address: Animal Evolutionary Ecology, Institute of Evolution and Ecology, Department of Biology, Faculty of Science, University of Tübingen, Tübingen, Germany.

References

Benkner, B., Mutter, M., Ecke, G., & Münch, T. A. (2013). Characterizing visual performance in mice: An objective and automated system based on the optokinetic reflex. *Behavioral Neuroscience*, *127*(5), 788–796.

Bennett, A. T. D., Cuthill, I. C., & Norris, K. J. (1994). Sexual selection and the mismeasure of color. *The American Naturalist*, *144*(5), 848–860.

Bilotta, J., & Powers, M. K. (1991). Spatial contrast sensitivity of goldfish: Mean luminance, temporal frequency, and a new psychophysical technique. *Vision Research*, *31*(3), 577–585, https://doi.org/10.1016/0042-6989(91)90108-H.

Birch, D., & Jacobs, G. H. (1979). Spatial contrast sensitivity in albino and pigmented rats. *Vision Research*, *19*(8), 933–937, https://doi.org/10.1016/0042-6989(79)90029-4.

Bisti, S., & Maffei, L. (1974). Behavioural contrast sensitivity of the cat in various visual meridians. *The Journal of Physiology*, *241*(1), 201–210, https://doi.org/10.1113/jphysiol.1974.sp010649.

Bitton, P.-P., Harant, U. K., Fritsch, R., Champ, C. M., Temple, S. E., & Michiels, N. K. (2017). Red fluorescence of the triplefin *Tripterygion delaisi* is increasingly visible against background light with increasing depth. *Royal Society Open Science*, *4*(3): 161009, https://doi.org/10.1098/rsos.161009.

Bolker, B. M., Brooks, M. E., Clark, C. J., Geange, S. W., Poulsen, J. R., Stevens, M. H. H., & White, J.-S. S. (2009). Generalized linear mixed models: A practical guide for ecology and evolution. *Trends in Ecology & Evolution*, *24*(3), 127–135, https://dx.doi.org/10.1016/j.tree.2008.10.008.

Brooks, M. E., Kristensen, K., van Benthem, K. J., Magnusson, A., Berg, C. W., Nielsen, A., … Bolker, B. M. (2017). glmmTMB balances speed and flexibility among packages for zero-inflated generalized linear mixed modeling. *The R Journal*, *9*(2), 378–400.

Caves, E. M., Brandley, N. C., & Johnsen, S. (2018). Visual acuity and the evolution of signals. *Trends in Ecology & Evolution*, *33*(5), 358–372, https://doi.org/10.1016/j.tree.2018.03.001.

Caves, E. M., Frank, T. M., & Johnsen, S. (2016). Spectral sensitivity, spatial resolution and temporal resolution and their implications for conspecific signalling in cleaner shrimp. *The Journal of Experimental Biology*, *219*(4), 597–608, https://doi.org/10.1242/jeb.122275.

Caves, E. M., & Johnsen, S. (2018). AcuityView: An R package for portraying the effects of visual acuity on scenes observed by an animal. *Methods in Ecology and Evolution*, *9*(3), 793–797.

Chakravarthi, A., Baird, E., Dacke, M., & Kelber, A. (2016). Spatial vision in *Bombus terrestris*. *Frontiers in Behavioral Neuroscience*, *10*:17, https://doi.org/10.3389/fnbeh.2016.00017.

Champ, C., Wallis, G., Vorobyev, M., Siebeck, U., & Marshall, J. (2014). Visual acuity in a species of coral reef fish: *Rhinecanthus aculeatus*. *Brain, Behavior and Evolution*, *83*(1), 31–42.

De Jonge, J., & Videler, J. (1989). Differences between the reproductive biologies of *Tripterygion tripteronotus* and *T. delaisi* (Pisces, Perciformes, Tripterygiidae): The adaptive significance of an alternative mating strategy and a red instead of a yellow nuptial colour. *Marine Biology*, *100*(4), 431–437.

De Valois, R. L., & De Valois, K. (1990). *Spatial vision*. Oxford, UK: Oxford University Press.

De Valois, R. L., Morgan, H., & Snodderly, D. M. (1974). Psychophysical studies of monkey Vision-III. Spatial luminance contrast sensitivity tests of macaque and human observers. *Vision Research*, *14*(1), 75–81, https://doi.org/10.1016/0042-6989(74)90118-7.

Domingues, V. S., Almada, V. C., Santos, R. S., Brito, A., & Bernardi, G. (2007). Phylogeography and evolution of the triplefin *Tripterygion delaisi* (Pisces, Blennioidei). *Marine Biology*, *150*(3), 509–519.

Douglas, R., & Djamgoz, M. (2012). *The visual system of fish*. Berlin, Germany: Springer Science+Business Media.

Fritsch, R., Collin, S. P., & Michiels, N. K. (2017). Anatomical analysis of the retinal specializations to a crypto-benthic, micro-predatory lifestyle in the Mediterranean triplefin blenny *Tripterygion delaisi*. *Frontiers in Neuroanatomy, 11*:122, https://doi.org/10.3389/fnana.2017.00122.

Fritsches, K. A., & Marshall, N. J. (2002). Independent and conjugate eye movements during optokinesis in teleost fish. *Journal of Experimental Biology*, *205*(9), 1241–1252.

Ghim, M. M., & Hodos, W. (2006). Spatial contrast sensitivity of birds. *Journal of Comparative Physiology A*, *192*(5), 523–534, https://doi.org/10.1007/s00359-005-0090-5.

Hanke, F. D., Scholtyssek, C., Hanke, W., & Dehnhardt, G. (2011). Contrast sensitivity in a harbor seal (*Phoca vitulina*). *Journal of Comparative Physiology A*, *197*(2), 203–210, https://doi.org/10.1007/s00359-010-0600-y.

Harant, U. K., Santon, M., Bitton, P. P., Wehrberger, F., Griessler, T., Meadows, M. G., ... Michiels, N. K. (2018). Do the fluorescent red eyes of the marine fish *Tripterygion delaisi* stand out? In situ and in vivo measurements at two depths. *Ecology and Evolution*, *8*(9), 4685–4694, https://doi.org/10.1002/ece3.4025.

Harmening, W. M., Nikolay, P., Orlowski, J., & Wagner, H. (2009). Spatial contrast sensitivity and grating acuity of barn owls. *Journal of Vision*, *9*(7): 13, 1–12, https://doi.org/10.1167/9.7.13. [PubMed] [Article]

Hirsch, J. (1982). Falcon visual sensitivity to grating contrast. *Nature*, *300*, 57–58, https://doi.org/10.1038/300057a0.

Hodos, W., Ghim, M. M., Potocki, A., Fields, J. N., & Storm, T. (2002). Contrast sensitivity in pigeons: A comparison of behavioral and pattern ERG methods. *Documenta Ophthalmologica*, *104*(1), 107–118, https://doi.org/10.1023/a:1014427615636.

Jacobs, G. H. (1977). Visual capacities of the owl monkey (*Aotus trivirgatus*)—I. Spectral sensitivity and color vision. *Vision Research*, *17*(7), 811–820.

Jacobs, G. H., Birch, D. G., & Blakeslee, B. (1982). Visual acuity and spatial contrast sensitivity in tree squirrels. *Behavioural Processes*, *7*(4), 367–375, https://doi.org/10.1016/0376-6357(82)90008-0.

Jacobs, G. H., Blakeslee, B., McCourt, M. E., & Tootell, R. B. H. (1980). Visual sensitivity of ground squirrels to spatial and temporal luminance variations. *Journal of Comparative Physiology*, *136*(4), 291–299, https://doi.org/10.1007/bf00657349.

Jarvis, J. R., Abeyesinghe, S. M., McMahon, C. E., & Wathes, C. M. (2009). Measuring and modelling the spatial contrast sensitivity of the chicken (*Gallus g. domesticus*). *Vision Research*, *49*(11), 1448–1454, https://doi.org/10.1016/j.visres.2009.02.019.

Kelber, A., Vorobyev, M., & Osorio, D. (2003). Animal colour vision—Behavioural tests and physiological concepts. *Biological Reviews*, *78*(1), 81–118, https://doi.org/10.1017/S1464793102005985.

Land, M. F., & Nilsson, D. E. (2012). *Animal eyes* (2nd ed.). Oxford, UK: Oxford University Press.

Langston, A., Casagrande, V. A., & Fox, R. (1986). Spatial resolution of the galago. *Vision Research*, *26*(5), 791–796, https://doi.org/10.1016/0042-6989(86)90094-5.

Lind, O., & Kelber, A. (2011). The spatial tuning of achromatic and chromatic vision in budgerigars. *Journal of Vision*, *11*(7):2, 1–9, https://doi.org/10.1167/11.7.2. [PubMed] [Article]

Lind, O., Sunesson, T., Mitkus, M., & Kelber, A. (2012). Luminance-dependence of spatial vision in budgerigars (*Melopsittacus undulatus*) and Bourke's parrots (*Neopsephotus bourkii*). *Journal of Comparative Physiology A*, *198*(1), 69–77, https://doi.org/10.1007/s00359-011-0689-7.

Merigan, W. H. (1976). The contrast sensitivity of the squirrel monkey (*Saimiri sciureus*). *Vision Research*, *16*(4), 375–379, https://doi.org/10.1016/0042-6989(76)90199-1.

Michiels, N. K., Seeburger, V. C., Kalb, N., Meadows, M. G., Anthes, N., Mailli, A. A., & Jack, C. B. (2018). Controlled iris radiance in a diurnal fish looking at prey. *Royal Society Open Science*, *5*: 170838, https://doi.org/10.1098/rsos.170838.

Nakagawa, S., & Schielzeth, H. (2010). Repeatability for Gaussian and non-Gaussian data: A practical guide for biologists. *Biological Reviews*, *85*(4), 935–956.

Nakamura, E. L. (1968). Visual acuity of two tunas, *Katsuwonus pelamis* and *Euthynnus affinis*. *Copeia*, *1*, 41–49.

Northmore, D. P. M., & Dvorak, C. A. (1979). Contrast sensitivity and acuity of the goldfish. *Vision Research*, *19*(3), 255–261, https://doi.org/10.1016/0042-6989(79)90171-8.

Northmore, D. P. M., Oh, D. J., & Celenza, M. A. (2007). Acuity and contrast sensitivity of the bluegill sunfish and how they change during optic nerve regeneration. *Visual Neuroscience*, *24*(3), 319–331, https://doi.org/10.1017/S0952523807070307.

Olsson, P., Lind, O., Kelber, A., & Simmons, L. (2017). Chromatic and achromatic vision: Parameter choice and limitations for reliable model predictions. *Behavioral Ecology*, *29*(2), 273–282.

Petry, H. M., Fox, R., & Casagrande, V. A. (1984). Spatial contrast sensitivity of the tree shrew. *Vision Research*, *24*(9), 1037–1042, https://doi.org/10.1016/0042-6989(84)90080-4.

R Core Team. (2017). R: A language and environment for statistical computing. Vienna, Austria: R Foundation for Statistical Computing, https://www.R-project.org/.

Reymond, L., & Wolfe, J. (1981). Behavioural determination of the contrast sensitivity function of the eagle *Aquila audax*. *Vision Research*, *21*(2), 263–271, https://doi.org/10.1016/0042-6989(81)90120-6.

Srinivasan, M. V., & Lehrer, M. (1988). Spatial acuity of honeybee vision and its spectral properties. *Journal of Comparative Physiology A*, *162*(2), 159–172, https://doi.org/10.1007/bf00606081.

Uhlrich, D. J., Essock, E. A., & Lehmkuhle, S. (1981). Cross-species correspondence of spatial contrast sensitivity functions. *Behavioural Brain Research*, *2*(3), 291–299, https://doi.org/10.1016/0166-4328(81)90013-9.

Wood, S. N. (2006). *Generalized additive models: An introduction with R*. Boca Raton, FL: Chapman & Hall/CRC Press.

Yamanouchi, T. (1956). The visual acuity of the coral fish *Microcanthus strigatus* (Cuvier & Valenciennes). *Publication Seto Marine Biology Laboratory*, *5*, 133–156.

Zander, C. D., & Hagemann, T. (1989). Feeding ecology of littoral gobiid and blennioid fishes of the Banyuls area (Mediterranean Sea). III. Seasonal variations. *Scientia Marina*, *53*(2), 441–449.

Zuur, A., Ieno, E. N., Walker, N., Saveliev, A. A., & Smith, G. M. (2009). *Mixed effects models and extensions in ecology with R*. New York, NY: Springer.

Supplementary material

Supplementary Movie S1. The optokinetic reflex in *Tripterygion delaisi* can be seen as tracking behavior (at least one eye or the body following the rotation direction of the pattern), often mixed with opposing saccades (sudden eye movement in the opposite direction of the pattern). The grating displayed in this video is rotating left, has a spatial frequency of 0.125 c/° and a Michelson contrast of 25%.

Appendix

ID_triplefin	stimulus_ rotation	contrast_ sensitivity	stimulus_ resolution	stimulus_ speed
1	L	19.60784314	0.125	4
1	R	125	0.375	4
1	R	125	0.625	4
1	L	125	0.875	4
1	L	19.60784314	1.125	4
1	R	8.333333333	1.375	4
1	R	1.416430595	1.625	4
1	R	4.310344828	1.875	4
1	R	1.090512541	2.125	4
2	L	125	0.125	4
2	L	125	0.375	4
2	L	125	0.625	4
2	R	64.51612903	0.875	4
2	L	10	1.125	4
2	L	4.310344828	1.375	4
2	R	1.666666667	1.625	4
2	R	1.003009027	1.875	4
3	R	19.60784314	0.125	4
3	R	125	0.375	4
3	R	64.51612903	0.625	4
3	L	19.60784314	0.875	4
3	R	10	1.125	4
3	R	6.622516556	1.375	4
3	R	1.05374078	1.625	4
4	L	64.51612903	0.125	4
4	L	125	0.375	4
4	L	125	0.625	4
4	L	125	0.875	4
4	L	19.60784314	1.125	4
4	L	11.76470588	1.375	4
4	R	10	1.625	4
4	L	3.03030303	1.875	4
4	R	1.05374078	2.125	4
5	R	29.41176471	0.125	4
5	R	125	0.375	4
5	R	125	0.625	4
5	L	64.51612903	0.875	4
5	L	125	1.125	4
5	R	4.807692308	1.375	4
5	L	1.824817518	1.625	4
5	L	1.05374078	1.875	4
5	R	1.024590164	2.125	4
6	R	19.60784314	0.125	4
6	R	125	0.375	4
6	L	64.51612903	0.625	4
6	R	125	0.875	4
6	L	19.60784314	1.125	4
6	L	4.807692308	1.375	4
6	L	1.003009027	1.625	4
7	L	10	0.125	4
7	R	64.51612903	0.375	4
7	L	19.60784314	0.625	4
7	R	11.76470588	0.875	4
7	L	7.462686567	1.125	4
7	R	1.003009027	1.375	4
8	L	29.41176471	0.125	4
8	R	64.51612903	0.375	4
8	L	19.60784314	0.625	4
8	L	19.60784314	0.875	4
8	L	10	1.125	4
8	L	8.547008547	1.375	4
8	R	11.76470588	1.625	4
8	R	1.003009027	1.875	4
9	L	64.51612903	0.125	4
9	R	64.51612903	0.375	4
9	R	19.60784314	0.625	4
9	L	19.60784314	0.875	4
9	R	5.952380952	1.125	4
9	L	6.622516556	1.375	4
9	R	1.168224299	1.625	4
10	R	19.60784314	0.125	4
10	L	125	0.375	4
10	R	19.60784314	0.625	4
10	R	14.70588235	0.875	4
10	L	11.76470588	1.125	4
10	L	3.90625	1.375	4

Table A1. Experimental data. contrast_sensitivity, indicates the weakest contrast (expressed as the reciprocal of the Michelson contrast) still eliciting a response in a triplefin (ID_triplefin) for a specific stimulus spatial resolution (stimulus_resolution) and angular speed (stimulus_speed); stimulus_rotation, indicates the rotation of the striped pattern used for each session shown in this table.

Table A1. Continued.

SCIENTIFIC REPORTS

OPEN

Daytime eyeshine contributes to pupil camouflage in a cryptobenthic marine fish

Received: 29 August 2017
Accepted: 24 April 2018
Published online: 09 May 2018

Matteo Santon, Pierre-Paul Bitton, Ulrike K. Harant & Nico K. Michiels

Ocular reflectors enhance eye sensitivity in dim light, but can produce reflected eyeshine when illuminated. Some fish can occlude their reflectors during the day. The opposite is observed in cryptic sit-and-wait predators such as scorpionfish and toadfish, where reflectors are occluded at night and exposed during the day. This results in daytime eyeshine, proposed to enhance pupil camouflage by reducing the contrast between the otherwise dark pupil and the surrounding tissue. In this study, we test this hypothesis in the scorpionfish *Scorpaena porcus* and show that eyeshine is the result of two mechanisms: the previously described *Stratum Argenteum Reflected* (SAR) eyeshine, and *Pigment Epithelium Transmitted* (PET) eyeshine, a newly described mechanism for this species. We confirm that the ocular reflector is exposed only when the eye is light-adapted, and present field measurements to show that eyeshine reduces pupil contrast against the iris. We then estimate the relative contribution of SAR and PET eyeshine to pupil brightness. Visual models for different light scenarios in the field show that daytime eyeshine enhances pupil camouflage from the perspective of a prey fish. We propose that the reversed occlusion mechanism of some cryptobenthic predators has evolved as a compromise between camouflage and vision.

An ocular reflector behind the retina is a common feature of vertebrate eyes. Their presence and diversity across taxa is linked with increased visual sensitivity under dim light[1]. This is achieved by reflecting light not captured by the retina during its first pass back through the photoreceptors, allowing for an increased photon catch[2–4]. However, ocular reflectors come with two disadvantages. First, visual acuity in bright environments might be reduced by backscatter[5–7]. Second, an animal may become more conspicuous because of eyeshine caused by reflection of light out of the pupil[7]. In some elasmobranchs, teleost fish and a few reptiles, these side effects are minimized by occlusion mechanisms that cover the reflector in the light-adapted eye with black melanin pigmentation[1,8]. Hence, strong eyeshine can only be induced when the eye is dark-adapted; it is weak or absent when the eye is light-adapted.

In contrast to this general pattern, a few families of highly cryptic fishes such as toadfishes (Batrachoididae) and scorpionfishes (Scorpaenidae) feature strong eyeshine when the eye is light-adapted, but not when dark-adapted[6,9,10]. In these species, the reflector is a *stratum argenteum* located in the outer part of the choroid[1,6,11], rather than the common *tapetum lucidum*. This *stratum argenteum* is a bi-laminate reflective structure with an inner layer of pentameric uric acid crystals and an outer layer of yellow birefringent granules of unknown material[10,12]. In the light-adapted state of the eye, the melanosomes of the retinal pigment epithelium enter the cell processes between the cones, clearing the way for light that passed through the receptor layer to also penetrate the translucent choroid[1,6] and reach the *stratum argenteum*. This light is reflected out of the pupil, generating a type of eyeshine termed *Stratum Argenteum Reflected* (SAR) eyeshine[13]. Another consequence of choroid translucency is that down-welling light that penetrates the dorsal part of the eye can be transmitted through the sclera, choroid and the retinal pigment epithelium and then out through the pupil. This can result in a second type of eyeshine described as *Pigment Epithelium Transmitted* (PET) eyeshine[13]. While the translucency of the sclera and choroid has been already documented for these fishes[10,14], pupil eyeshine has always been assumed to be the exclusive result of SAR eyeshine. The possibility that PET eyeshine also contributes to total eyeshine has not been considered. Both eyeshine types might explain why scorpionfishes, toadfishes and some stonefishes have bright pupils when exposed to ambient light[14]. The possible function of this counter-intuitive occlusion mechanism, however,

Animal Evolutionary Ecology, Institute for Evolution and Ecology, Department of Biology, Faculty of Science, University of Tübingen, Auf der Morgenstelle 28, Tübingen, 72076, Germany. Correspondence and requests for materials should be addressed to M.S. (email: matteo.santon@uni-tuebingen.de)

Definition	Properties	Measurement
broad-sense ***Stratum Argenteum Reflected*** **(SAR) eyeshine**		
Light enters the pupil and is reflected back out by the *stratum argenteum*, partly through retroreflection, partly through other (unspecified) forms of reflection.	Reflectance shown in Fig. 4b.	**Source**: side-welling light. **Measures**: 1. Pupil of shaded fish. 2. Shaded diffuse white standard at same location, facing spectroradiometer. **Calculation**: 1/2
narrow-sense ***Stratum Argenteum Reflected*** **(SAR) eyeshine**		
Same as previous, but limited to the retroreflective component only.	Reflectance shown in Fig. 4a.	**Source**: light coaxial to measurement axis in dark room, light-adapted fish (light off for measurements only). **Measures**: 1. Pupil. 2. Diffuse white standard at same location, facing spectroradiometer. **Calculation**: 1/2
Pigment Epithelium Transmitted **(PET) eyeshine**		
Light is transmitted through the dorsal side of the eyes and the pigment epithelium and then leaves the eye though the pupil.	Transmittance shown in Fig. 4b.	**Source**: down-welling light. **Measures**: 1. Pupil when fish exposed. 2. Pupil when fish shaded (= broad-sense SAR eyeshine). 3. Exposed diffuse white standard at same location, parallel to the water surface. **Calculation**: (1–2)/3

Table 1. Definitions. Eyeshine in the scorpionfish *Scorpaena porcus* is a combination of two different mechanisms, SAR and PET eyeshine: SAR eyeshine is strongly affected by a retroreflective component ('narrow-sense SAR'), which was quantified independently. This overview table defines and summarizes the properties of these mechanisms. 'Calculation' numbers refer to indexed 'Measures'. See Fritsch *et al.* (2017) for an overview of eyeshine types[13].

is yet unclear. Here, we investigate the hypothesis that it conceals the pupil by allowing daytime eyeshine, thus reducing contrast with the surrounding tissue[10] (video S1).

The well-defined, often circular, dark pupil that stands out against the body in most animals makes the vertebrate eye difficult to hide[15]. Eyes are indeed considered key features for face recognition of predators, prey or conspecifics[16–22]. Consequently, mechanisms for pupil camouflage are widespread. Pupillary closure (e.g. elasmobranchs) reduces pupil size and shape in response to fluctuations in ambient light, but also minimizes pupil conspicuousness[15]. Lidless species, such as fishes and snakes, often feature an eye mask (e.g. vertical stripes in lionfishes) that embeds the pupil in a dark skin pattern[15]. For example, vertical dark stripes have been shown to effectively decrease the visibility of an eyelike pattern[23]. In some fish species, iridescent corneal reflectors have been proposed to reduce an eye's detectability[24]. Skin flaps (e.g. flatheads), where the pupil is partly covered by an irregular extension of the cryptic iris, are another adaptation to reduce pupil conspicuousness[15]. Some fishes simply have very small pupils for their body size (e.g. frogfishes), which may be a strategy to minimize eye detection at the cost of visual acuity. Thus far, the use of eyeshine for enhancing daytime eye camouflage has only been proposed for invertebrates: pelagic stomatopod larvae reduce the conspicuousness of their dark retinas by eyeshine that matches the light field of the background[25]. Scorpionfishes, toadfishes and stonefishes are sit-and-wait predators that strongly rely on crypsis. Since featuring a dark pupil could disrupt their camouflage, diurnal pupil eyeshine might help to hide their eyes.

Methods

After introducing our model species, the methods follow a specific logic: first, in the laboratory we confirm a reversed occlusion mechanism in the black scorpionfish. Second, we assess in the field if a bright pupil enhances eye concealment by reducing contrast with the surrounding iris. Third, we characterise the components of daytime eyeshine quantitatively in the laboratory (Table 1 for definitions) and test their validity by reconstructing known pupil radiance measurements from the field. Finally, we developed a visual model to compare the natural pupil and an artificial model pupil contrast against the iris and skin from the perspective of a prey fish under three light scenarios. This allowed us to assess to what extent daytime eyeshine could enhance pupil camouflage.

Model species. The black scorpionfish *Scorpaena porcus* is common in coastal marine hard-substrate and seagrass habitats, occurring from fully exposed to heavily shaded light environments, in the eastern Atlantic Ocean and Mediterranean Sea[26]. It is a generalist sit-and-wait predator that relies on crypsis to catch naïve prey, ambushing them only when close to its mouth over distances of few centimetres. Like most scorpionfish, it features prominent eyes with a partially translucent retinal pigment epithelium resulting in daytime eyeshine (Fig. 1)[6,13]. We caught 15 individuals in Calvi (Corsica, France) between 5 and 20 m depth under the general permit of STARESO (Station de Recherches Sous Marines et Océanographiques). At STARESO, fish were kept in two 300 L tanks with a continuous fresh seawater flow. For field measurements, three individuals were used and subsequently set free. The remaining twelve were transported to the University of Tübingen (Germany) in individual plastic canisters filled with 1.5 L seawater and oxygen enriched air. In Tübingen, fish were held individually in 160 L tanks (20 °C, salinity 35 ppt, pH 8.2, 12 h light/dark cycle, fed once every two days). Animal husbandry was carried out in accordance with German animal welfare legislation. Because the individuals were not experimentally manipulated, a formal permit was not required for this study (confirmed by the Animal Care Officer at the Biology Department of the University of Tübingen).

Spectroradiometry. *Occlusion of the stratum argenteum during dark-adaptation (laboratory).* To confirm that the *stratum argenteum* is occluding while the eye is dark-adapting, an individual was placed in a 12 L tank

Figure 1. Daytime pupil eyeshine in *Scorpaena porcus* in the field. Under natural light conditions, the pupil of *S. porcus* appears lit, unlike most fishes which possess dark pupils. Photo credit: N.K. Michiels.

(L × W × H: 30 × 20 × 20 cm^3) positioned on a cooling plate and equipped with an aeration stone. Before measuring, we light-adapted the fish for 2 h using a sun-simulating Plasma-i AS1300 Light Engine (Plasma International, Mühlheim am Main, Germany) pointed upwards to a diffuse reflector (#273 soft silver reflector, LEE Filters, Andover, England) attached to the ceiling to illuminate the whole room. Three polytetrafluoroethylene (PTFE) white reflectance standards (Lake Photonics, Uhldingen-Mühlhofe, Germany) were positioned in the tank for ambient light measurements. We then measured the change in reflectance of the pupil in relation to time spent in darkness, on a total of three individuals.

The radiance of the left eye pupil was measured at normal incidence (90° angle from surface) through the glass of the tank using a calibrated SpectraScan PR 740 spectroradiometer (Photo Research, NY, USA). This device uses Pritchard optics and measures the absolute spectral radiance of an area with known solid angle. The glass tank was tilted at an angle of 5° to reduce external reflection. We used a cold light source KL2500 LCD (Schott, Mainz, Germany) equipped with a blue filter (insert filter 258302, Schott, Mainz, Germany) to coaxially illuminate the pupil of the fish. The light was led through liquid light guides (LLG 380, Lumatec, Deisenhofen, Germany) to a mechanical shutter and then on to a 90° elbow-shaped glass-fibre light guide (Heine Optotechnik, Herrsching, Germany) with an exit diameter of 3 mm. The light exit was aligned coaxially with the spectroradiometer's optical axis, 15 cm in front of the lens. The distance between the lens and the fish was fixed at ∼50 cm. Slight distance adjustments were necessary to assure complete coverage of the pupil with the cross-section of the measuring area. Since scorpionfish tend to sit passively on the substrate, there was no need for the use of anaesthesia, which is known to affect fish pigmentation[27].

Measurements started immediately after turning off the plasma light source. The room was kept completely dark except for brief moments (< 10 s) during which the shutter of the coaxial source was opened for measuring, approximately once every 10 min for 2 h. The radiance of the PTFE white standard best aligned with the fish's pupil was measured orthogonal to its surface at the beginning and the end of the experiment. SAR eyeshine reflectance was calculated as the photon radiance of the pupil normalized (i.e. divided) by the average radiance of the PTFE white standard. Because it was exclusively generated by a coaxial light source in an otherwise dark environment, a condition that would be uncommon in the field and that was explicitly staged to strictly describe the reflective properties of the *stratum argenteum*, we subsequently refer to this measurement as "narrow-sense" SAR eyeshine.

We analysed the data using a Generalized Linear Model (gamma distribution, link = log) with total reflectance (reflectance integrated over the wavelength range from 380 to 700 nm) as response variable, and dark adaptation time, individual ID and their interaction as predictors using R v3.2.0[28]. Model assumptions were verified by plotting residuals against fitted values and against each covariate in the model. Significance of predictors was tested by using the 95% Credible Interval (CrI), a Bayesian analogue of the confidence interval[29]. For the response variable time, the factor individual ID, and their interaction, we computed the model estimates from the back-transformed effect sizes. The associated 95% CrI were then obtained from 10000 simulations of the mean and variance of each estimate, using the *sim* function of the R package *arm*, with non-informative priors[30]. If the CrI of one individual did not overlap with the mean of another, we concluded that their intercepts were significantly different. We considered time and its interaction with ID to be significant if the CrI values of the regression coefficient did not include zero.

Contrast of natural and model pupil against iris (field). To confirm that *S. porcus* produces enough daytime eyeshine to reduce pupil contrast against the iris in the field if compared to a dark model pupil, we measured pupil and iris radiance of three fish *in situ* in STARESO under shaded and exposed conditions. Each fish was measured in a transparent plastic terrarium (L × W × H: 20 × 15 × 15 cm^3) placed underwater on a bright sandy substrate. The side of the container through which measurements were taken consisted of Evotron optically neutral

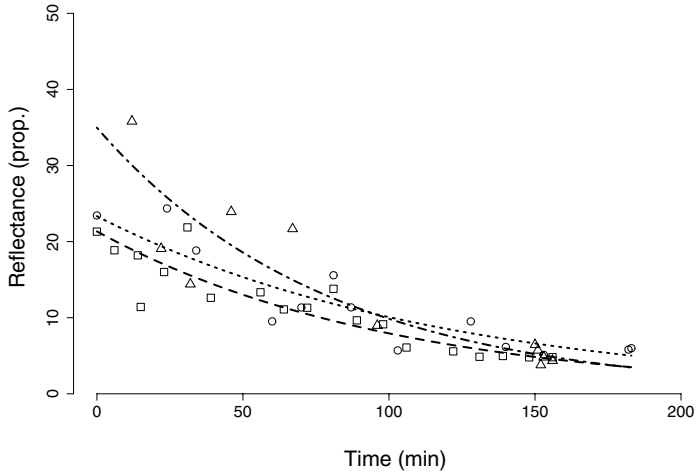

Figure 2. Reduction in narrow-sense SAR eyeshine with increased dark-adaptation in *Scorpaena porcus*. Narrow-sense SAR eyeshine total reflectance (pupil radiance normalized by white standard radiance) under coaxial illumination in the dark as function of time. At t = 0 the fish was light-adapted and the light was switched off resulting in total darkness. The small, coaxial source used to induce eyeshine was only switched on for a brief moment for each measurement. Radiance is integrated over 380–700 nm. Line styles and symbols indicate three different individuals.

Plexiglas® (Evonik Performance Materials, Essen, Germany). A black PVC sheet was added behind the fish to encourage the scorpionfish to face the spectroradiometer. The other three lateral sides of the container were transparent, exposing the scorpionfish to natural light. Such configuration should minimise possible skin colour adaptations caused by the black PVC sheet placed in the back of the container. Holes in the sides ensured water circulation. To cast an optional shade over the entire fish, we used a black plastic slate. All measurements were taken using a SpectraScan PR 740 in a custom-built underwater housing (BS Kinetics, Achern, Germany) with the spectroradiometer facing south and the fish north, at noon on clear, sunny days. The focal distance of the instrument was fixed at 80 cm. The external dimensions of the underwater housing are $35 \times 25 \times 25\,cm^3$ (L × W × H), excluding the length of the port (10 cm). The port is located at the upper edge of the housing. It is hard to evaluate the influence of the housing on the light field, but even if a partial obstruction would occur this would hardly influence our estimates since every radiance measurement was obtained under comparable geometries.

We measured pupil and iris radiance (top, bottom, left and right) at normal incidence (90° from surface) in the same three fish at 7 m and 15 m depth. Under shaded conditions, pupil radiance involves SAR reflected eyeshine only, as PET transmitted eyeshine is prevented. Under exposed conditions, both mechanisms contribute to eyeshine. We also estimated the radiance of the skin patches surrounding the iris (top, bottom, right and left of the eye) and the ambient light field for visual modelling (see below). To estimate the ambient light fields, we measured three PTFE white standards, one parallel to the water surface measured from a 45° angle as a proxy for down-welling light, and two perpendicular to the water surface, one of them exposed and the other shaded, measured at normal incidence (90° from standard surface) as a proxy for side-welling light. Finally, we also measured a model pupil (Fig. S1). The latter consisted of a black, hollowed-out PVC block (L × W × H: $6 \times 3 \times 3\,cm^3$) with a pupil-like opening at the front, and internally filled with black cloth to absorb as much light as possible. The resultant pupil is practically black, mimicking a pupil with no eyeshine. We cycled through all measurements two times, both under shaded and exposed conditions. White standards were also measured twice to control for light fluctuations between measurements.

To compare the contrast of the natural and dark model pupil against the iris, we calculated the average photon radiance of all three structures for each wavelength and exposure. We then calculated the Michelson contrasts Cm as follows:

$$C_m = \frac{L_{x1} - L_{x2}}{L_{x1} + L_{x2}} \quad (1)$$

where L_{x1} is the radiance of the pupil, L_{x2} the radiance of the iris. There is no contrast when $C_m = 0$. When $C_m > 0$, the pupil is brighter than the iris, and vice versa for $C_m < 0$.

Measurement of SAR and PET eyeshine in light-adapted fish (laboratory). To describe the relative contributions of reflected (SAR) and transmitted (PET) eyeshine to pupil radiance in light-adapted scorpionfish (Table 1 for a summary), we measured individuals in a similar setup to the one used to confirm occlusion during dark-adaptation. We used a down-welling tungsten source (650+ ARRI, Munich, Germany) attached to the ceiling pointing downward at the glass tank where the scorpionfish was placed. The light reflected by the diffuse grey metal walls of the room generated the side-welling light. To estimate the exclusive contribution of narrow-sense SAR eyeshine, induced only by the coaxial light entering through the pupil, we measured the pupil radiance of 10 individuals using the coaxial illumination system described earlier while only briefly turning off the main source

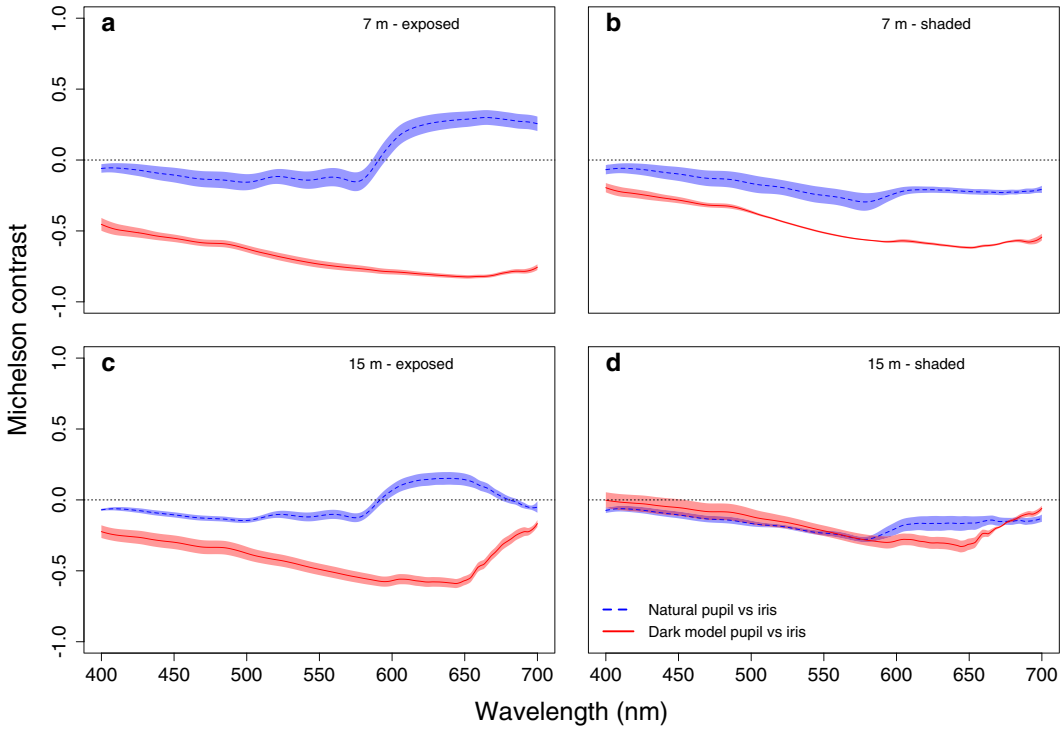

Figure 3. Michelson contrast at each wavelength between natural pupil or dark model pupil against the iris in the field. Measurements are from exposed and shaded *Scorpaena porcus* (n = 3 ind.) at 7 and 15 m depth. Positive values indicate that pupils are brighter than the irides. Shaded areas represent the standard error of the mean. **(a)** Exposed and **(b)** shaded fish at 7 m. **(c)** Exposed and **(d)** shaded fish at 15 m.

(ARRI) for the duration of the measurement to keep fish light-adapted. Narrow-sense SAR eyeshine reflectance was calculated as the coaxially induced pupil radiance divided by the radiance of a coaxially illuminated PTFE white standard normal to the coaxial source. Since the *stratum argenteum* behind the eye lens acts as a retroreflector, and reflectance is expressed relative to a diffuse reflecting surface, reflectance values readily exceed 1 under this coaxial geometry, but are much lower than 1 when looking at the eye from a non-coaxial direction. In the field, purely coaxial light conditions as used to characterise narrow-sense SAR eyeshine are very rare. Hence, to properly reconstruct the contribution of SAR eyeshine assessed in the field, we also estimated "broad-sense" SAR eyeshine by measuring the pupil of nine fish and the radiance of a PTFE white standard in the shade (to suppress PET eyeshine), under a general side-welling light field in the absence of a coaxial light source. Broad-sense SAR eyeshine reflectance was calculated as pupil radiance of the shaded fish normalized by the radiance of a shaded PTFE white standard. We assessed the exclusive contribution of PET eyeshine by measuring the pupil radiance of 10 individuals under exposed and shaded conditions. By subtracting the second measurement, which represents the contribution of SAR eyeshine only, from the first, which consists of the contributions of PET plus SAR eyeshine, we obtained the contribution of PET eyeshine only. This value was subsequently expressed as PET eyeshine transmittance dividing by the radiance of an exposed PTFE white standard positioned parallel to the water surface and measured from an angle of 45°. For visual modelling, we also measured the reflectance of the iris and the dark model pupil under exposed conditions.

Reconstructing field values using laboratory estimates. To determine if our laboratory estimates of broad-sense SAR, PET eyeshine, and iris reflectance could be used to reliably predict field observations, we used these measurements to 'reverse engineer' the pupil and iris radiance for three fish for which complete field data were available: one at 7 m and two at 15 m. We used down- and side-welling light measurements from the field as the illuminants. By combining them with the broad-sense SAR, PET eyeshine and iris relative radiances estimated in the laboratory, we then predicted pupil and iris radiance under exposed or shaded conditions for each of the three fish. We then assessed the match between the two curves by calculating the mean of the ratio between the logarithm on base 10 of the predicted and real radiances at each wavelength for iris and pupil of each fish under both exposures. Finally, we computed the averaged ratio for all three fish.

Visual models to assess pupil camouflage as perceived by prey fish. To test if PET and SAR eyeshine enhance pupil camouflage in the black scorpionfish, we determined how well the pupil matches the appearance of the iris as perceived by one of its prey species, the triplefin *Tripterygion delaisi*[31] under three light scenarios where this prey-predator interaction is likely to occur in the field. These scenarios are based on a specific geometry commonly found in the field and that was also used for all our measurements (in the lab and in the field). It assumes orthogonal view of the eye, with the scorpionfish sitting on a horizontal substrate. We

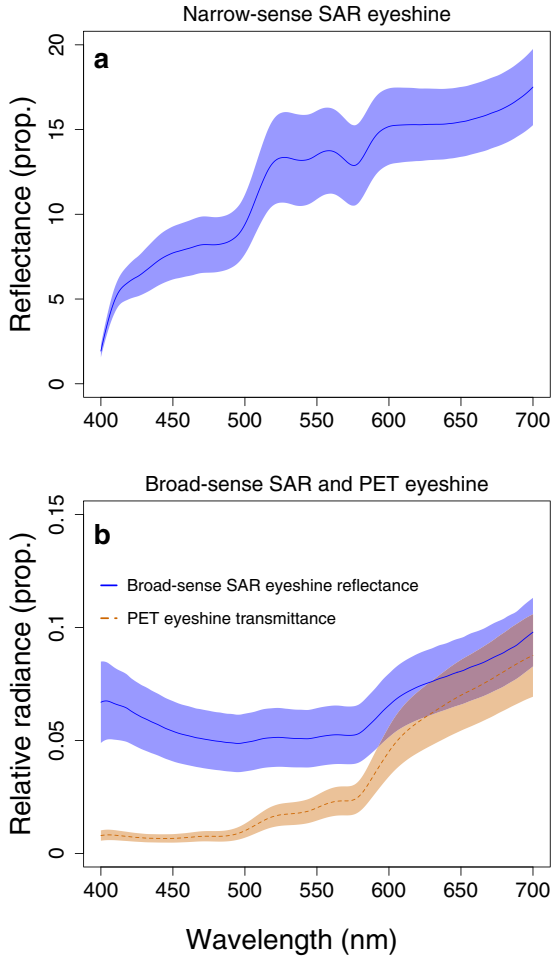

Figure 4. Wavelength dependent contribution of eyeshine types in *Scorpaena porcus*. (**a**) Narrow-sense SAR eyeshine reflectance. **(b)** Broad-sense SAR eyeshine reflectance and PET eyeshine transmittance. Y-values are expressed as proportions of the pupil photon radiance normalized by the radiance of the associated PTFE white standard. Shaded areas represent the standard error of the mean.

calculated the chromatic contrasts between the pupil and the iris using the receptor-noise model[32]. We informed the model using species-specific visual system parameters including the visual sensitivity of the photoreceptors (SWS: 468 nm, MWS: 517 nm, LWS: 530 nm), the relative photoreceptor densities in the fovea of 1:4:4 (SWS: MWS: LWS), the ocular media transmittance, and setting the Weber fraction at 0.05[31–33]. The achromatic contrasts were calculated as the absolute Michelson contrast between the luminance photon catches (sum input of the two members of the double-cone) perceived by the prey species. Using the light field measurements at 7 and 15 m depth, we reconstructed three scenarios in which scorpionfish and triplefin were likely to interact: (1) the scorpionfish and triplefin in the open against bright backgrounds where both PET and SAR eyeshine are present, (2) the scorpionfish in the open and the triplefin in the shade or against a dark background where only PET eyeshine is present (SAR eyeshine is weak or absent because of reduced side-welling illumination), and (3) the scorpionfish in the shade and the triplefin against a bright background in the open where only SAR eyeshine is induced (see Table S1 for details). The calculations generate values of chromatic contrast in just-noticeable-differences (JNDs), where values greater than one indicate discernible differences[32], and values of achromatic contrasts as absolute Michelson contrasts (ranging from 0 to 1). To enhance camouflage, the contrast between the pupil and the iris should not only be reduced, but should also be comparable to the contrast of the overall patterning of the fish's body. To assess the contrast between different skin patches on the body, we used the reflectance of four skin patches around the iris (calculated as the photon radiance of the skin normalized by the respective PTFE white standard facing the spectroradiometer) measured in the field on the three scorpionfish. We calculated the absolute Michelson achromatic contrasts as perceived by the prey species (chromatic contrasts between the two pupils and the iris were not showing substantial differences) for all pairwise comparisons of the skin patches under the three scenarios at both depths. We then compared the achromatic contrasts between the irides and the natural and model pupils with the distribution of the skin patches achromatic contrasts. Visual models were implemented using the R package 'pavo' 1.0[34].

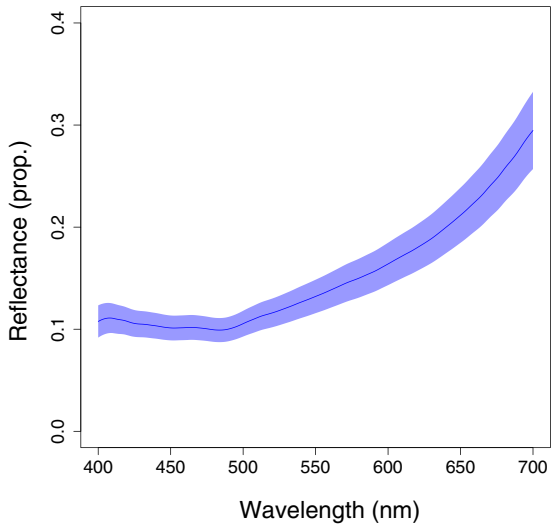

Figure 5. Iris reflectance. Reflectance values are expressed as proportions of the iris photon radiance normalized by the radiance of the associated PTFE white standard. Shaded area represents the standard error of the mean.

Units, statistics and data availability. Reflectance and transmittance are expressed in relation to the radiance of PTFE white standards, as proportions, not percentages. Means are shown ± standard deviation unless specified otherwise. All data are available in the Dryad repository (https://doi.org/10.5061/dryad.dp4kt5t), and R scripts are available upon request.

Results

Occlusion of the *stratum argenteum* during dark-adaptation (laboratory). Model validation did not show any violation of the model assumptions. The reflectance of the light-adapted pupil of *Scorpaena porcus* was on average up to 30 times as strong as a white standard (27.3 ± 7.4). This value fell significantly during dark-adaptation to 4.6 ± 0.7 (Fig. 2) with a regression coefficient of 0.0099 (95% Credible Interval (CrI): from 0.0078 to 0.0120). This implies that pupil reflectance decreased by 1% per minute. At the beginning of the experiment, one fish showed significantly higher reflectance, up to 35 times as strong as a white standard (95% CrI: from 0.1800 to 0.8089). The overall model fit was very high, $R^2 = 0.86$.

Contrast of natural and model pupil against iris (field). The natural pupil showed reduced contrast against the iris relative to the model pupil, which was always considerably darker than the iris. At 7 m depth, this was true for both shaded and exposed conditions (Fig. 3). At 15 m depth, the difference between the contrasts of the two pupils against the iris was strong only when exposed. Under shaded conditions both the natural and model pupil showed low contrast.

Measurement of SAR and PET eyeshine in light-adapted fish (laboratory). Narrow-sense reflected (SAR) eyeshine (n = 10 ind.) was stronger than a PTFE white standard, showing an average reflectance of 12.01 ± 3.82 (Fig. 4a). Broad-sense SAR eyeshine (n = 9 ind.) yielded an average reflectance of 0.06 ± 0.01 (Fig. 4b). Transmitted (PET) eyeshine (n = 10 ind.) had an average transmittance of 0.033 ± 0.028 (Fig. 4b) with a shift towards the long wavelength part of the spectrum. The iris (n = 9 ind.) showed an average reflectance of 0.15 ± 0.05 (Fig. 5) and the model pupil an average reflectance of the negligible value of 0.0008 ± 0.0001 (not shown in the figure).

Reconstructing field values using laboratory estimates. Using the laboratory estimates, we predicted the pupil and iris radiance under natural light conditions and compared them to the actual field measurements (Fig. 6). Overall, in fish exposed to ambient light, the averaged ratio between the measured and reconstructed values was 1.004 ± 0.007 for the pupil and 1.012 ± 0.012 for the iris, where a value of 1 represents the perfect match. When the fish was shaded, pupil and iris radiances were predicted with a ratio of 1.024 ± 0.009 and 1.008 ± 0.008.

Visual models to assess pupil camouflage as perceived by prey fish. A natural pupil with PET and/or SAR eyeshine showed a similar chromatic contrast against the iris if compared to a model pupil in all scenarios, except for a slight increase when only PET eyeshine was present (triplefin shaded, scorpionfish exposed) (Table 2). However, achromatic contrast was substantially reduced (Table 2). Whereas the model pupil without eyeshine against the iris showed absolute achromatic contrasts around 1, the contribution of one or both eyeshine mechanisms reduced this contrast to less than 0.4. This value is well within the range (from 0 to 0.6) of the achromatic contrasts between skin patches found near the irides (Fig. 7).

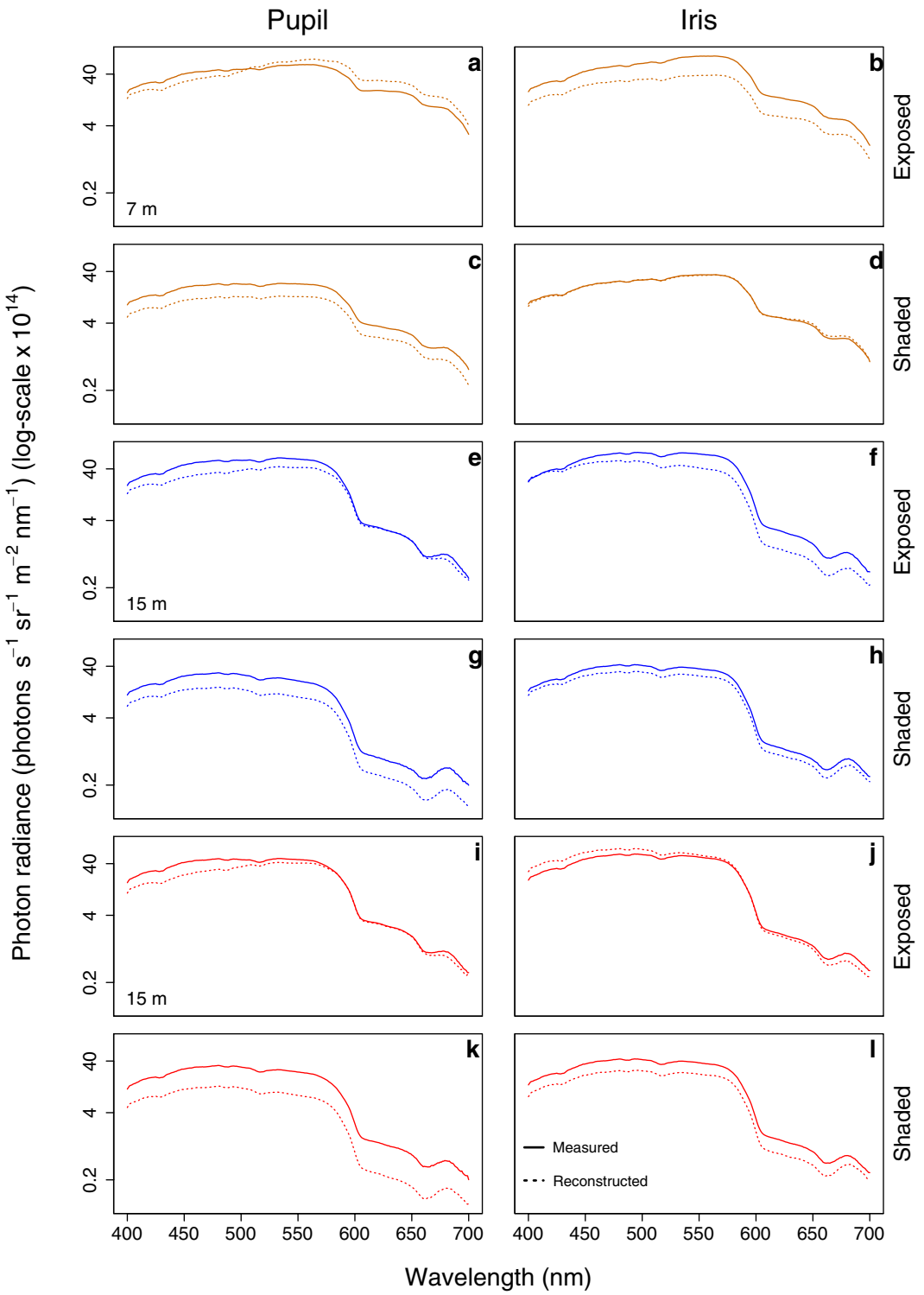

Figure 6. Reconstruction of known field pupil and iris radiance. Photon radiance of pupil (**a**, **e**, **i**) and iris (**b**, **f**, **j**) in exposed *Scorpaena porcus* individuals. Panels (**c**, **g**, **k**) and (**d**, **h**, **l**) show the same for shaded individuals. Solid lines show radiance measured in the field. Dotted lines show radiance reconstructed using the ambient light measurements for each fish combined with the eyeshine and iris relative radiances estimated in the laboratory. Photon radiance values are expressed on a log-scale. Each colour indicates a different individual, placed at 7 or 15 m depth.

Discussion

Only few families of cryptobenthic fish occlude their ocular reflector in the dark and expose it during the day, which is opposite to what is known from fish featuring an occlusible ocular reflector. Reversed occlusion can make a pupil bright during the day, but keeps it dark at night, even when illuminated. We confirmed the presence

	Model			Chromatic contrast (JNDs)		Absolute Michelson contrast	
	Conditions	Transmitted PET eyeshine	Reflected SAR eyeshine	Natural pupil against iris	Dark model against iris	Natural pupil against iris	Dark model against iris
7 m	Scorpionfish: exposed - Triplefin: exposed	+	+	1.93	1.83	0.30	0.99
	Scorpionfish: exposed - Triplefin: shaded	+	–	2.96	1.83	0.19	0.99
	Scorpionfish: shaded - Triplefin: exposed	–	+	1.42	1.84	0.39	0.99
15 m	Scorpionfish: exposed - Triplefin: exposed	+	+	2.36	1.44	0.10	0.99
	Scorpionfish: exposed - Triplefin: shaded	+	–	3.88	1.44	0.28	0.99
	Scorpionfish: shaded - Triplefin: exposed	–	+	1.19	0.72	0.38	0.99

Table 2. Estimated chromatic and achromatic contrast in the eye of a scorpionfish. Chromatic contrast values in just-noticeable-differences (JNDs) are calculated between the natural pupil (with eyeshine), the model pupil (without eyeshine) and the iris for three light scenarios (described by rows 1–3) at two depths. Achromatic contrast values are expressed as absolute Michelson contrasts between the same three structures. All contrasts are calculated from the perspective of the triplefin *Tripterygion delaisi*, a common prey species. SAR eyeshine refers to "broad-sense" SAR eyeshine. See Material and Methods and Table S1 for details.

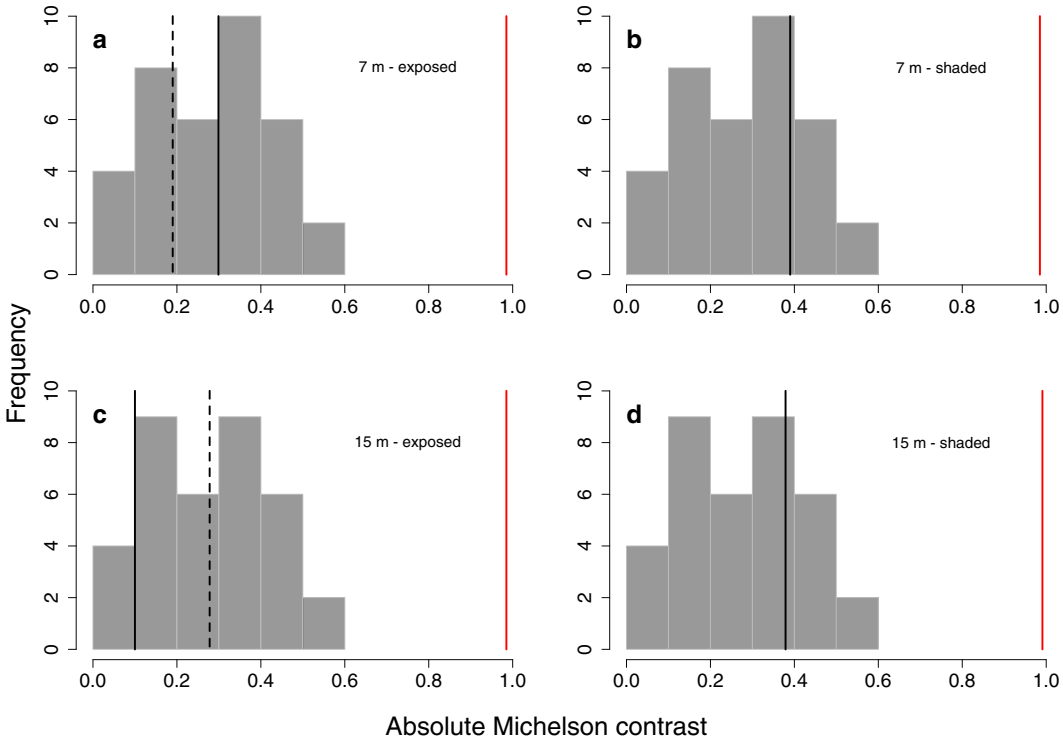

Figure 7. Predicted absolute achromatic contrast of the pupil with and without eyeshine against the iris of *Scorpaena porcus* compared to the contrast among body patches as perceived by a prey species. The achromatic contrast between a natural pupil with eyeshine and its iris (black lines) was small and fell within the distribution of the achromatic contrasts between skin patches (all combinations of four patches in each of the three fish measured; histogram bars). This was not the case when eyeshine was prevented, as in the dark model pupil (red lines). Black lines indicate contrast values between the natural pupil and the iris when *Tripterygion delaisi* is shaded (dashed) or exposed (solid) for four *S. porcus* scenarios: (**a**) exposed and (**b**) shaded at 7 m depth, (**c**) exposed and (**d**) shaded at 15 m depth. Red lines indicate contrast values between the dark model pupil and the iris when *T. delaisi* is shaded (dashed) or exposed (solid) for the same four *S. porcus* scenarios (note that in scenario (a) and (c) two lines overlap).

of reversed occlusion in the scorpionfish *Scorpaena porcus* and show that two different eyeshine types contribute to daytime pupil radiance: *Stratum Argenteum Reflected* (SAR) and *Pigment Epithelium Transmitted* (PET) eyeshine. Spectroradiometry in the field shows that daytime eyeshine reduces the contrast between pupil and iris,

which may help to conceal an otherwise dark pupil during the day. Visual modelling confirmed this observation: daytime eyeshine reduces pupil contrast against the surrounding tissue, decreasing the detectability of *S. porcus* pupil from the perspective of a prey species under three light scenarios where SAR and PET eyeshine differ in their contribution to pupil radiance.

The presence of an occluded *stratum argenteum* in the dark-adapted eye was first observed in *S. porcus* during night dives (pers. obs.). The occlusion mechanism responsible for this phenomenon may be similar to the one described for other species of toadfishes and scorpionfishes[6,10]. Why these fishes suppress eyeshine when dark-adapted remains unclear. Using the *stratum argenteum* as a reflector in dim light conditions would allow for an increased quantal catch and thus increased visual acuity[10]. Covering it with pigmentation, however, forgoes this option. Enhanced pupil camouflage by reversed occlusion may come at the expense of reduced visual acuity due to a possible increase in internal scatter in the light-adapted eye and a reduced photon catch in the dark-adapted eye. However, pupil concealment by means of daytime eyeshine may explain why scorpionfish possess unobstructed, large pupils. Most other cryptobenthic predators feature fringes, skin flaps, or have small pupils to reduce eye conspicuousness.

Daytime eyeshine due to the absence of melanocytes in the choroid has been already described for toadfishes and scorpionfishes[6,10,14]. Until now, however, the focus was exclusively on reflected (SAR) eyeshine[6,10,14]. Our measurements in the laboratory show that eyeshine in *S. porcus* has a second component in the form of transmitted (PET) eyeshine. These two eyeshines could be mechanistically linked because they both rely on the translucent choroid and the exposed *stratum argenteum*. Since the combination of PET and SAR eyeshine could enhance pupil camouflage, the bright pupils of this fish should not be seen just as a side-effect of eye anatomy, but rather as a possible adaptive trait.

For a sit-and-wait predator, successful prey capture strongly depends on its crypsis[35]. In this study, we show that daytime eyeshine enhances the camouflage of the pupil in a cryptobenthic predator. Eyeshine does not perfectly camouflage the eye, but it likely reduces the probability of detection compared to a situation in which the pupil is dark. The contribution of SAR eyeshine to pupil brightness had already been summarily described[6], but we also showed that transmitted PET eyeshine is an additional component that makes a significant contribution, regardless of its low transmittance, particularly because it is induced by the relatively strong down-welling light rather than the relatively weak side-welling light. A similar concealing process has been described for pelagic stomatopod crustacean larvae that use a photonic structure external to the optical pathway of the eye to hide their dark retinas[25]. Since in *S. porcus* the *stratum argenteum* is located in the optical pathway, this ocular reflector may also improve visual sensitivity in dim light environments[10]. However, reversed occlusion of the *stratum argenteum* strongly suggests that this function is secondary to camouflage. Future behavioural studies could be implemented to strengthen these findings.

As alternative explanation, bright pupils could be rather used as a lure for attracting potential prey, a mechanism that is similar to the one proposed for the bright lures of some deep-sea organisms[36]. However, since this type of eyeshine is diurnal, it is unlikely that the pupil could become bright enough to stand out against the surroundings, especially considering the amount of bright structures and surfaces already present in the field.

We did not inform our visual models with the true physical properties of (narrow-sense) SAR eyeshine. This parameter showed extremely high reflectance values (Fig. 4), as expected in the presence of a retroreflector, and it would only have to be considered if the observer possesses a light source close to its eyes, or if sunlight is shining parallel to the observer's visual axis in an otherwise dark environment, e.g. a narrow crevice. Under these conditions, the target pupil would appear so bright that it may stand out against the iris, potentially decreasing eye camouflage. Our visual models instead focused on the broad-sense SAR eyeshine reflectance, which represents the more general situation in which the complete side-welling light field is considered.

This is the first study showing that a vertebrate features daytime eyeshine by means of two complementary mechanisms to reduce the conspicuousness of its large pupils to the perspective of one of its prey species. We propose that the unusual reversed occlusion of the ocular reflector has evolved in response to selection to optimize the trade-off between camouflage and vision.

References

1. Ollivier, F. *et al*. Comparative morphology of the tapetum lucidum (among selected species). *Vet. Ophthalmology* **7**, 11–22 (2004).
2. Greene, N. R. & Filko, B. J. Animal-eyeball vs. road-sign retroreflectors. *Ophthalmic Physiol. Opt.* **30**, 76–84 (2010).
3. Land, M. F. & Nilsson, D.-E. *Animal eyes* (Oxford University Press, 2012).
4. Schwab, I. R., Yuen, C. K., Buyukmihci, N. C., Blankenship, T. N. & Fitzgerald, P. G. Evolution of the tapetum. *Transactions Am. Ophthalmol. Soc.* **100**, 187 (2002).
5. Barton, M. & Bond, C. E. *Bond's biology of fishes* (Thomson, 2007).
6. Best, A. & Nicol, J. Eyeshine in fishes. a review of ocular reflectors. *Can. J. Zool.* **58**, 945–956 (1980).
7. Denton, E. On the organization of reflecting surfaces in some marine animals. *Phil. Trans. R. Soc. Lond. B* **258**, 285–313 (1970).
8. Denton, E. & Nicol, J. The chorioidal tapeta of some cartilaginous fishes (chondrichthyes). *J. Mar. Biol. Assoc. United Kingd.* **44**, 219–258 (1964).
9. Grover, D. A. & Zigman, S. Funduscopic morphology of the light-and dark-adapted eye of the toadfish (*Opsanus tau*) *in vivo*. *Can. J. Zool.* **69**, 2498–2500 (1991).
10. Nicol, J. Studies on the eyes of toadfishes opsanus. structure and reflectivity of the stratum argenteum. *Can. J. Zool.* **58**, 114–121 (1980).
11. Herring, P. J. Reflective systems in aquatic animals. *Comparative Biochemistry and Physiol. Part A: Physiol.* **109**, 513–546 (1994).
12. Nicol, J. Uric acid in the stratum argenteum of toadfishes opsanus. *Can. J. Zool.* **58**, 492–496 (1980).
13. Fritsch, R., Ullmann, J. F., Bitton, P.-P., Collin, S. P. & Michiels, N. K. Optic-nerve-transmitted eyeshine, a new type of light emission from fish eyes. *Front. Zool.* **14**, 14 (2017).
14. Nicol, J. A. C. & Somiya, H. *The eyes of fishes* (Oxford University Press, USA, 1989).
15. Cott, H. B. *Adaptive coloration in animals* (Methuen & Co., Ltd., 1940).
16. Gothard, K. M., Brooks, K. N. & Peterson, M. A. Multiple perceptual strategies used by macaque monkeys for face recognition. *Animal Cogn.* **12**, 155–167 (2009).

17. Jones, R. Reactions of male domestic chicks to two-dimensional eye-like shapes. *Animal Behav.* **28**, 212–218 (1980).
18. Kano, F. & Tomonaga, M. Face scanning in chimpanzees and humans: Continuity and discontinuity. *Animal Behav.* **79**, 227–235 (2010).
19. Kjernsmo, K., Grönholm, M. & Merilaita, S. Adaptive constellations of protective marks: eyespots, eye stripes and diversion of attacks by fish. *Animal Behav.* **111**, 189–195 (2016).
20. Satoh, S., Tanaka, H. & Kohda, M. Facial recognition in a discus fish (cichlidae): Experimental approach using digital models. *PloS ONE* **11**, e0154543 (2016).
21. Scaife, M. The response to eye-like shapes by birds. i. the effect of context: a predator and a strange bird. *Animal Behav.* **24**, 195–199 (1976).
22. Trnka, A., Prokop, P. & Grim, T. Uncovering dangerous cheats: how do avian hosts recognize adult brood parasites? *PLoS ONE* **7**, e37445 (2012).
23. Karplus, I. & Algom, D. Visual cues for predator face recognition by reef fishes. *Ethol.* **55**, 343–364 (1981).
24. Lythgoe, J. The structure and function of iridescent corneas in teleost fishes. *Proc. Royal Soc. Lond. B: Biol. Sci.* **188**, 437–457 (1975).
25. Feller, K. D. & Cronin, T. W. Hiding opaque eyes in transparent organisms: a potential role for larval eyeshine in stomatopod crustaceans. *J. Exp. Biol.* **217**, 3263–3273 (2014).
26. Louisy, P. & Ade, C. *Meeresfische: Westeuropa und Mittelmeer* (Ulmer, 2002).
27. Gray, S. M., Hart, F. L., Tremblay, M. E., Lisney, T. J. & Hawryshyn, C. W. The effects of handling time, ambient light, and anaesthetic method, on the standardized measurement of fish colouration. *Can. J. Fish. Aquatic Sci.* **68**, 330–342 (2011).
28. R Core Team. *R: A Language and Environment for Statistical Computing*. R Foundation for Statistical Computing, Vienna, Austria). https://www.R-project.org/ (2017).
29. Bolker, B. M. *et al*. Generalized linear mixed models: a practical guide for ecology and evolution. *Trends Ecol. & Evol.* **24**, 127–135 (2009).
30. Korner-Nievergelt, F. *et al*. *Bayesian data analysis in ecology using linear models with R, BUGS, and Stan* (Academic Press, 2015).
31. Bitton, P.-P. *et al*. Red fluorescence of the triplefin *Tripterygion delaisi* is increasingly visible against background light with increasing depth. *Royal Soc. Open Sci.* **4**, 161009 (2017).
32. Vorobyev, M. & Osorio, D. Receptor noise as a determinant of colour thresholds. *Proc. Royal Soc. Lond. B: Biol. Sci.* **265**, 351–358 (1998).
33. Douglas, R. & Djamgoz, M. *The visual system of fish* (Springer Science & Business Media, 2012).
34. Maia, R., Eliason, C. M., Bitton, P.-P., Doucet, S. M. & Shawkey, M. D. pavo: an r package for the analysis, visualization and organization of spectral data. *Methods Ecol. Evol.* **4**, 906–913 (2013).
35. Stevens, M. & Merilaita, S. Animal camouflage: current issues and new perspectives. *Philos. Transactions Royal Soc. Lond. B: Biol. Sci.* **364**, 423–427 (2009).
36. Haddock, S. H., Dunn, C. W., Pugh, P. R. & Schnitzler, C. E. Bioluminescent and red-fluorescent lures in a deep-sea siphonophore. *Sci.* **309**, 263–263 (2005).

Acknowledgements

We warmly thank the STARESO staff for hosting and supporting our research group in their field station, Oeli Oelkrug for fish maintenance at the University of Tübingen. We also thank Dr. Martin J. How and Dr. Yakir Gagnon for fruitful comments and suggestions and Dr. Nils Anthes and four anonymous reviewers for useful comments on previous drafts of the manuscript. We acknowledge support by Deutsche Forschungsgemeinschaft and Open Access Publishing Fund of University of Tübingen. The project was funded by the by the German Science Foundation Koselleck grant (Mi482/13-1) and the Volkswagen Foundation (Az. 89148 and Az. 91816) awarded to NKM. P-PB was funded by a Postdoctoral Fellowship from the Natural Science and Engineer Research Council of Canada.

Author Contributions

M.S. conceptualised the study. M.S. and N.K.M. designed the experimental setups. M.S. performed spectroradiometry in the laboratory. M.S., U.K.H. and N.K.M. performed spectroradiometry in the field. M.S. analysed the data. M.S. and P.-P.B. implemented the visual models. M.S. drafted the manuscript. M.S., N.K.M. and P.-P.B. edited the manuscript and all authors commented on the completed manuscript.

Additional Information

Supplementary information accompanies this paper at https://doi.org/10.1038/s41598-018-25599-y.

Competing Interests: The authors declare no competing interests.

Publisher's note: Springer Nature remains neutral with regard to jurisdictional claims in published maps and institutional affiliations.

Title: Active sensing with light improves predator detection in a diurnal fish

Short title: Active sensing with light in fish

Authors: Matteo Santon[1], Pierre-Paul Bitton[1,3], Jasha Dehm[1,2], Roland Fritsch[1], Ulrike K. Harant[1], Nils Anthes[1], Nico K. Michiels[1]*.

Affiliations:

[1]Animal Evolutionary Ecology, Institute of Evolution and Ecology, Department of Biology, Faculty of Science, University of Tübingen, Auf der Morgenstelle 28, 72076 Tübingen, Germany.

[2]School of Marine Studies, Faculty of Science, Technology & Environment, University of the South Pacific, Laucala Bay Rd., Suva, Fiji.

[3] Department of Psychology, Memorial University of Newfoundland, 232 Elizabeth Avenue, St. John's, NL A1B 3X9, Canada.

*Correspondence to: nico.michiels@uni-tuebingen.de

Abstract: Is active sensing with light as rare as it seems? Some diurnal fish reflect downwelling light sideways using their iris, suggesting improved visual detection through subtle, short-distance illumination. Here, we test the functionality of "diurnal active photolocation" by experimentally suppressing light redirection in triplefins, small benthic fish. When fitted with a shading hat, triplefins moved significantly closer to a cryptobenthic scorpionfish than control-treated conspecifics in three experiments. Visual modelling confirmed that light redirection by a triplefin is sufficiently strong to generate a perceptible increase in scorpionfish eyeshine over the short distances that characterize this interaction. We conclude that light redirecting by small bottom-dwelling fish improves detection of cryptic predators. This represents a new dimension in the evolution of fish eyes.

One Sentence Summary: By using their iris to reflect sunlight sideways, fish can break the camouflage of their cryptic predator by generating eyeshine in its pupils.

The only vertebrates known to use light for active sensing are nocturnal fish with a subocular chemiluminescent light organ (*1, 2*). Recent findings in the benthic triplefin *Tripterygion delaisi* showed that diurnal fish may achieve the same by controlled redirection of downwelling sunlight using their iris, generating a phenomenon called "ocular spark" (Fig. 1)(*3*). Ocular sparks arise because the lens usually protrudes from a fish's pupil, allowing downwelling light to be focused on the iris below (*3*). As a result, sunlight is reflected sideways outside the narrow range dictated by Snell's window (*4*). Here, we hypothesize that ocular sparks improve visual detection of nearby cryptic organisms, a process called "diurnal active photolocation". Because the amount of redirected light is small, detectable structures must be nearby and highly reflective. We focus on retroreflective eyes consisting of a focusing lens in front of a reflective layer (*5, 6*). This design improves dim light vision in many species (*7*), but also explains daytime eyeshine used by some cryptobenthic predatory fish to conceal their pupil (*8*) (Fig. 1). Retroreflection can only be revealed by illumination with a source next to the observer's pupil, as the reflected light is returned to the source in a narrow beam (*9, 10*). As a consequence, even weak illumination can generate perceivable eyeshine in a retroreflective eye (Fig. 1). Although this is the accepted explanation for the subocular position of light organs in chemiluminescent fishes (*1*), it remains to be demonstrated whether light redirection in triplefins works in a similar way (*3, 11*). Here, we tested whether ocular sparks improve the ability of triplefins to detect scorpionfish, cryptobenthic sit-and-wait predators with daytime retroreflective eyeshine (*8, 12*). To suppress ocular sparks, we glued opaque mini-hats on triplefins (Fig. 1). Two controls permitted unobstructed spark formation: a clear-hatted and an unhatted control.

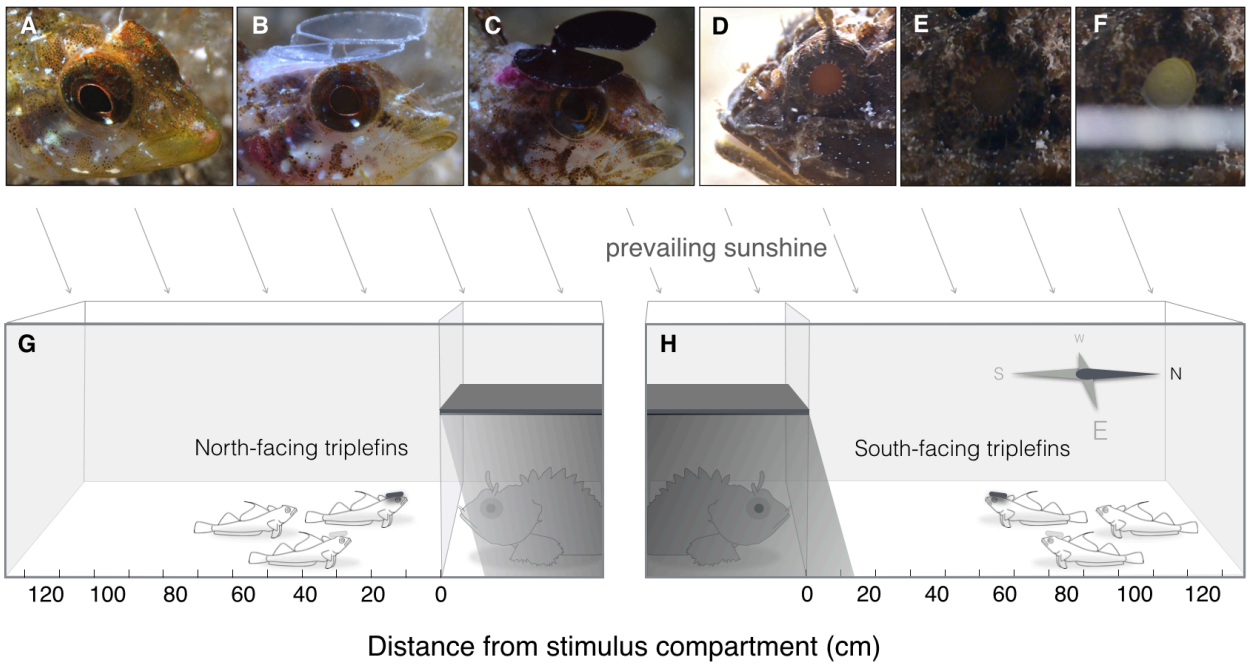

Fig. 1. Experimental design to test for diurnal active photolocation in fish. Triplefins (*Tripterygion delaisi*) were subjected to one of three treatments: **A**. Unhatted sham control, **B**. Clear-hatted control, and **c**. Shading hat treatment. While **A** and **B** can re-direct light using a blue ocular spark (bright bluish dot on the lower iris), **C** cannot. **D**. Scorpionfish (*Scorpaena porcus*) show daytime eyeshine (*8*). Coaxial "illumination" with a strip of paper reveals that the eyeshine has a distinct retroreflective component (**E** and **F**). **G**-**H**. Triplets of one triplefin per hat treatment were exposed to a shaded predator or stone (not shown) behind a windowpane. We tested two opposite orientations in the field (triplefins facing north or south). This was not required in the laboratory (not shown). The response variable was distance from the stimulus. Drawings not to scale (see Materials and Methods). Pictures by M.S. and N.K.M.

In a first experiment we released triplets consisting of one triplefin from each hat treatment in tanks with a sandy substrate. At one side, either a stone or a stone-mimicking scorpionfish was presented in the shade behind a windowpane (Fig. 1G-H). Due to their preference for hard shady substrates, triplefins were attracted to both stimuli. If active photolocation contributes to scorpionfish detection, control-hatted triplefins should keep a greater safe distance from scorpionfish than shading hatted triplefins. This experiment was carried out in the laboratory and

subsequently replicated in the field at 15 m depth, this time split by orientation (Fig. 1G-H). Following overnight (~14h) acclimatization, we recorded the distance of each triplefin to the stimulus at 3 (lab) or 5 (field) time points in the course of one day. Stimuli were swapped for the next day. Despite the environmental noise in the natural setting, the response of triplefins was similar in both experiments (Fig. 2).

All triplefins kept a longer distance from the predator than from the stone irrespective of hat treatment (all LMMs: Stimulus $p < 0.0001$) (Fig. 2, Tables S1-S2). This effect was particularly strong in triplefins from the south-facing field tanks. This indicated that triplefins can distinguish a stone from a scorpionfish independent of diurnal active photolocation. Since the response of the two control treatments was indistinguishable (LMM: Treatment $p_{lab} = 0.373$, $p_{field} = 0.844$, Tables S1A-S2A), we averaged the distances of the controls per triplet and observation in subsequent analyses. Comparing the controls with the shading hat showed that the stimulus effect depended on the hat treatment in the lab and north-facing field tanks, but not south-facing field tanks (LMM: Treatment x Stimulus $p_{lab} = 0.017$, $p_{field\text{-}north} = 0.038$, $p_{field\text{-}south} = 0.248$, Tables S1B-S2B-C). The significant interaction terms resulted from shaded individuals staying significantly closer to the scorpionfish than the controls (LMM scorpionfish: Treatment $p_{lab} < 0.0001$, $p_{field\text{-}north} = 0.011$, Tables S1C-S2B), which was not the case for the stone (LMM stone: Treatment $p_{lab} = 0.21$, $p_{field\text{-}north} = p = 0.097$, details not shown). All these results consider the effect of stimulus presentation order (Tables S1C-S2B).

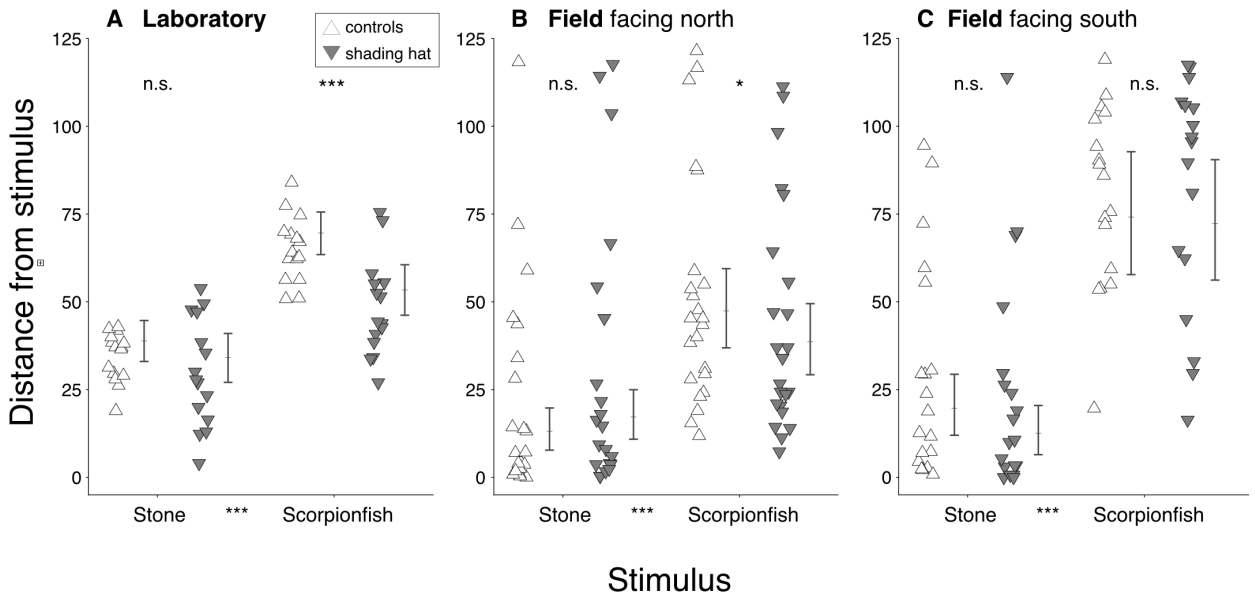

Fig. 2. Effect of hat treatment on the average distance from the stimulus as a function of stimulus type (stone or scorpionfish) in replicate experiments in the laboratory (A) and the field (B-C). **A.** Shaded individuals stayed significantly closer to a scorpionfish than the controls (n = 15 triplets). **B.** Among north-facing triplefins shaded individuals stayed closer to a scorpionfish than the controls (n = 24 triplets). **C.** Among south-facing triplefins such effect was absent, but all treatments responded more strongly to the scorpionfish (n = 19 triplets). Symbols: average per shaded individual or for both control individuals; error bars: model-predicted group means ± 95 % credible intervals; *** = $p < 0.001$, * = $p < 0.05$, n.s. = $p > 0.05$. Note: statistical comparisons rested on connected measures *within* triplets and 5 data points per stimulus, making error bars imprecise indicators of significance (details in Tables S1-S2).

The previous data had been collected after triplefins acclimated overnight, which allowed sufficient time to establish a safe distance from the scorpionfish. To understand how triplefins approach and respond to a scorpionfish immediately after release, we exposed single, shaded and clear-hatted individuals to a scorpionfish (stone stimulus omitted) in a field experiment at 10 m depth (split by north and south orientation). After release at the midpoint of the compartment (25 cm) triplefin positions were recorded 7 times within 100 min. Already after a minute, clear-hatted triplefins kept greater distances from the scorpionfish than shaded triplefins (Fig. 3):

eighteen (47%) shaded and nine (21%) clear-hatted individuals had approached the predator to within 7 cm, the average distance at which active photolocation is estimated to function (see below). Subsequently, clear-hatted fish retreated to the opposite half of the tank ~20 min earlier than shading-hatted fish (GLM: Treatment $p = 0.034$, Time $p < 0.0001$, Treatment x Time $p = 0.036$) (Table S3). Both treatments reached a similar distance after ~50 min. In contrast to the first field experiment, orientation had no effect, perhaps a consequence of the shorter distance available to triplefins to move away (50 cm *versus* 125 cm, compare Y-axis of Figs. 2 and 3).

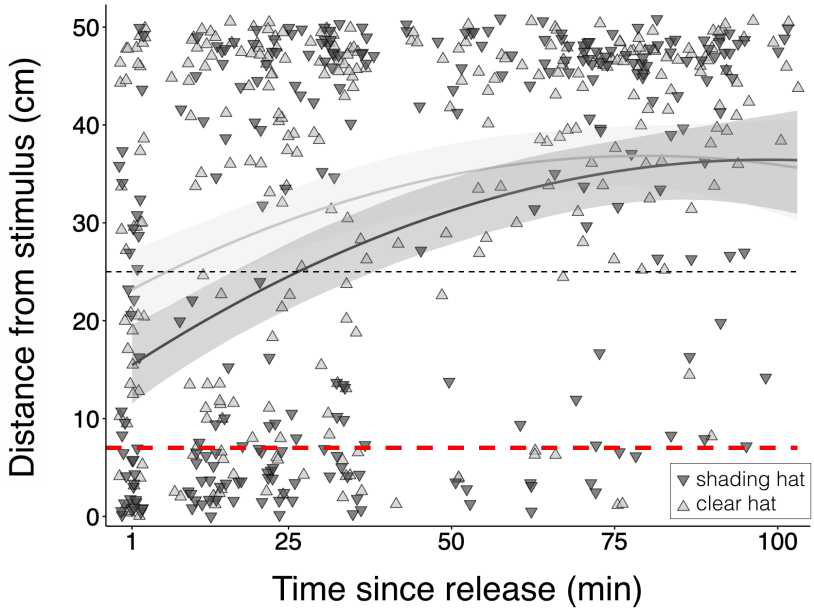

Fig. 3. Distance from a scorpionfish as a function of hat treatment and time since release in the field at 10 m depth. Measurements ($n = 7$ per ind.) started one minute after releasing a triplefin in the middle of a 50 cm long tank (n clear hat = 42, n shading hat = 38). Curves show predictions from Generalized Linear Mixed Model for shaded (dark gray) and clear-hatted (light grey) triplefins including 95% credible intervals as shades (Table S3). Short-dashed line: point of release (~25 cm). Long-dashed line: average detection distance at which diurnal active photolocation allows triplefins to induce and perceive scorpionfish eyeshine using a spark (~7 cm, Fig. 4). Symbols were slightly jittered to reveal overlapping observations.

To validate these results, we implemented visual models to compute the contrast change in the pupil of a scorpionfish as perceived by an untreated triplefin when producing an ocular spark. We informed the model using previously published parameters (*3, 8, 13-15*) supplemented by additional measurements under the conditions of the 10 m field experiment. These included the baseline brightness of a scorpionfish pupil, which is not black during the day (*8*). Here, we limit ourselves to modelling the effect of blue ocular sparks, which is the stronger of the two ocular spark types known from triplefins (*3*). Relative to a white standard, blue ocular sparks have an average proportional reflectance of 1.34 over the 400-700 nm range, with an averaged maximum of 2.15 at 472 nm. These larger-than-one values are caused by the focusing effect of the lens (*3*). We used the receptor-noise model (*16*) for estimating chromatic contrasts and Michelson contrasts using cone-catch values of the double cones for achromatic contrasts.

While ocular sparks did not generate chromatic contrast above the discriminability threshold at any distance between the triplefin and the scorpionfish, achromatic Michelson contrasts exceeded the detection thresholds across a broad range of conditions (Fig. 4). For comparison, identical calculations for spark-generated contrast changes in a scorpionfish's iris rather than its pupil showed no perceptible effect under any of the tested conditions. This confirms that subocular light emission is subtle and can only generate detectable contrasts in strong reflectors, e.g. retroreflective eyes. For north-facing triplefins, the reflections induced by an ocular spark in a scorpionfish’s pupil would be detectable up to 6 cm under average conditions, and up to 10 cm for higher values of ocular spark radiance and scorpionfish pupil retroreflectance. These distances increased by 2-3 cm for south-facing triplefins, and coincide well with the observed approach distances seen in the third experiment (Fig. 3).

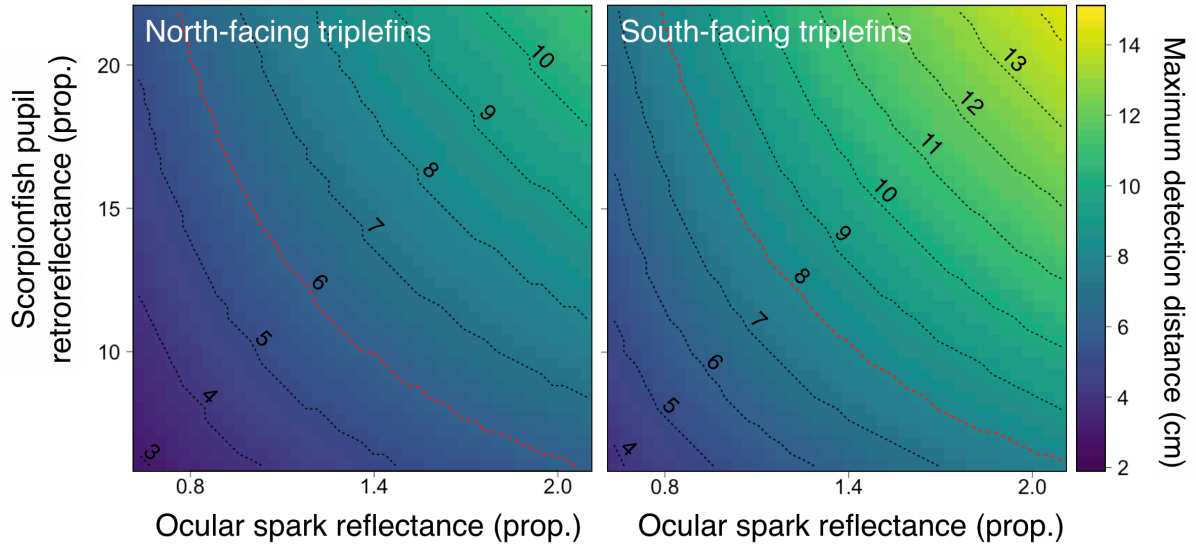

Fig. 4. Visual modelling summary showing detection distances (color) by a triplefin of reflections in a scorpionfish pupil induced by a blue ocular spark. The outcome is shown as a function of spark reflectance and scorpionfish pupil retroreflectance, and separated for north- and south-facing orientations. Red lines represent the average detection distances that were combined in the 7 cm value shown in Fig. 3. Values were obtained from calculating the Michelson contrast based on triplefin cone-catches of the double cones between 1 ad 15 cm, and identifying the distance at which the contrast reached the achromatic contrast threshold of *T. delaisi* (*15*) (Material and Methods).

Our results provide an unequivocal proof of principle for the diurnal active photolocation hypothesis. Although diurnal active photolocation is neither failproof, as shown by the limitations set by the visual modelling, neither required, as shown by the response of shaded triplefins to scorpionfish, the ability to redirect light significantly increases the range over which scorpionfish can be detected. This will increase triplefins' survival in cases where regular vision alone fails to detect a scorpionfish in time. This is confirmed by the fact that even clear-hatted triplefins approached scorpionfish within ranges that are likely to fall within the striking range of a scorpionfish (*17-19*).

In triplefins, the chromatophore patch on the lower iris is a diffuse, Lambertian reflector (*14*). This produces a light field that covers most of the hemispherical zone over a short distance, as seen by a single eye (Fig. 4). In lantern and flashlight fish, subocular light organs are also considered diffuse sources (*1, 20*). However, many other fish possess silvery irides with near-specular properties. Such reflectors are more directional, presumably allowing specific illumination of objects over greater distances. Yet, this property also increases visibility to predators. Trade-offs like this may explain variation seen among fish in types of ocular light redirection (*3, 21*). As for the target organism, highly reflective structures such as retroreflective eyes in predatory fish (*8, 12*) or reflective eyecups or ommatidia in crustacean prey (*3, 14*) are also common and diverse. Since none of these have been studied in this context, it is too early to speculate which combination of observer/target reflectors and ambient conditions may allow active photolocation. Yet, it is clear that the building blocks required for this process are ubiquitous. For this reason, we propose that diurnal active photolocation may also have been an important contributing factor to the phenomenon that most marine cryptobenthic predators show eye adaptations that hamper the visual detection of their pupils. Stonefish (*Synanceia*) and frogfish (*Antennarius*) have small pupils for their body size. Other species have skin flaps that cover the pupil as in crocodile fishes (*Papilloculiceps*) and scorpionfishes (some *Scorpaenopsis*), or possess slit-like pupils as in some flatheads (*Thysanophrys*), flounders (*Bothus*) and sandperches (*Parapercis*). In lionfishes (*Pterois*) the eyes are embedded in a black vertical band. All of these traits reduce pupil size, distort its shape or mask its presence. A special feature of scorpionfish in this context is their diurnal eyeshine, resulting in a bright pupil caused by light reflection and transmission (*12, 22*). Since eyes are commonly used for face recognition (*23, 24*) it is uncontested that all these pupil modifications hamper visual detection (*25*). Diurnal active photolocation may well be a contributor to this arms race. Unfortunately, surprisingly little is known about the visual and behavioral interactions between cryptobenthic predatory fish and their fish prey, presumably because such interactions are difficult to study experimentally. As a consequence, this field is governed by theoretically plausible, yet largely untested interpretations, which may explain why diurnal active photolocation has been neglected thus far.

References and Notes:

1. H. C. Howland, C. J. Murphy, J. E. McCosker, Detection of eyeshine by flashlight fishes of the family Anomalopidae. *Vision Res* **32**, 765-769 (1992).
2. J. Hellinger *et al*., The Flashlight Fish *Anomalops katoptron* Uses Bioluminescent Light to Detect Prey in the Dark. *PLoS ONE* **12**, e0170489 (2017).
3. N. K. Michiels *et al*., Controlled iris radiance in a diurnal fish looking at prey. *R Soc open sci* **5**, 170838 (2018).
4. J. N. Lythgoe, *The Ecology of Vision*. (Clarendon Press, Oxford, 1979).
5. I. R. Schwab, C. K. Yuen, N. C. Buyukmihci, T. N. Blankenship, P. G. Fitzgerald, Evolution of the tapetum. *Trans Am Ophthalmol Soc* **100**, 187-199; discussion 199-200 (2002).
6. R. Fritsch, J. F. P. Ullmann, P. P. Bitton, S. P. Collin, N. K. Michiels, Optic-nerve-transmitted eyeshine, a new type of light emission from fish eyes. *Front Zool* **14**, 14 (2017).
7. F. J. Ollivier *et al*., Comparative morphology of the tapetum lucidum (among selected species). *Vet Ophthalmol* **7**, 11-22 (2004).
8. M. Santon, P. P. Bitton, U. K. Harant, N. K. Michiels, Daytime eyeshine contributes to pupil camouflage in a cryptobenthic marine fish. *Sci Rep* **8**, 7368 (2018).
9. H. Von Helmholtz, *Handbuch der physiologischen Optik*. (Voss, 1867), vol. 9.
10. N. R. Greene, B. J. Filko, Animal-eyeball vs. road-sign retroreflectors. *Ophthalmic and Physiological Optics* **30**, 76-84 (2010).
11. C. B. Jack. (2014).
12. A. C. G. Best, J. A. C. Nicol, Eyeshine in fishes. A review of ocular reflectors. *Can J Zool* **58**, 945-956 (1980).
13. R. Fritsch, S. P. Collin, N. K. Michiels, Anatomical analysis of the retinal specializations to a crypto-benthic, micro-predatory lifestyle in the mediterranean triplefin blenny *Tripterygion delaisi*. *Front Neuroanat* **11**, 122 (2017).
14. P.-P. Bitton, S. A. Y. Christmann, M. Santon, U. K. Harant, N. K. Michiels, Visual modelling validates prey detection by means of diurnal active photolocation in a small cryptobenthic fish. *bioRxiv*, 338640 (2018).
15. M. Santon, T. A. Münch, N. K. Michiels, The contrast sensitivity function of a small cryptobenthic marine fish. *Journal of Vision*, *in press* (2019).
16. M. Vorobyev, D. Osorio, Receptor noise as a determinant of colour thresholds. *Proc R Soc B Biol Sci* **265**, 351-358 (1998).
17. J. C. Montgomery, A. R. Hamilton, Sensory contributions to nocturnal prey capture in the dwarf scorpion fish (*Scorpaena papillosus*). *Mar. Fresh. Behav. Physiol.* **30**, 209-223 (1997).
18. M. La Mesa, G. Scarcella, F. Grati, G. Fabi, Age and growth of the black scorpionfish, *Scorpaena porcus* (Pisces: Scorpaenidae) from artificial structures and natural reefs in the Adriatic Sea. *Sci Mar* **74**, 677-685 (2010).
19. M. Harmelin-Vivien, R. Kaim-Malka, M. Ledoyer, S. Jacob-Abraham, Food partitioning among scorpaenid fishes in Mediterranean seagrass beds. *J Fish Biol* **34**, 715-734 (1989).

20. J. A. C. Nicol, Studies on luminescence. On the subocular light-organs of stomiatoid fishes. *J Mar Biol Assoc U K* **39**, 529-548 (1960).
21. N. Anthes, J. Theobald, T. Gerlach, M. G. Meadows, N. K. Michiels, Diversity and ecological correlates of red fluorescence in marine fishes. *Front Ecol Evol* **4**, (2016).
22. M. Santon *et al*., Diurnal active photolocation enhances predator detection in a marine fish. *bioRxiv*, 324202 (2018).
23. K. M. Gothard, K. N. Brooks, M. A. Peterson, Multiple perceptual strategies used by macaque monkeys for face recognition. *Anim Cogn* **12**, 155-167 (2009).
24. R. Jones, Reactions of male domestic chicks to two-dimensional eye-like shapes. *Anim Behav* **28**, 212-218 (1980).
25. H. B. Cott, *Adaptive coloration in animals*. (Methuen, London, 1940).
26. P. Wirtz, The Behaviour of the Mediterranean *Tripterygion* Species (Pisces, Blennioidei). *Zeitschrift für Tierpsychologie* **48**, 142-174 (1978).
27. S. J. Brandl, C. H. Goatley, D. R. Bellwood, L. Tornabene, The hidden half: ecology and evolution of cryptobenthic fishes on coral reefs. *Biol Rev*, (2018).
28. P. Louisy, *Europe and Mediterranean marine fish identification guide*. (Ulmer, 2015).
29. J. C. Compaire, P. Casademont, R. Cabrera, C. Gómez-Cama, M. C. Soriguer, Feeding of *Scorpaena porcus* (Scorpaenidae) in intertidal rock pools in the Gulf of Cadiz (NE Atlantic). *J Mar Biol Assoc U K*, 1-9 (2017).
30. J. Dehm, University of Kiel, Kiel (2015).
31. M. A. Stoffel, S. Nakagawa, H. Schielzeth, rptR: repeatability estimation and variance decomposition by generalized linear mixed-effects models. *Methods Ecol Evol* **8**, 1639-1644 (2017).
32. M. E. Brooks *et al*., glmmTMB balances speed and flexibility among packages for zero-inflated generalized linear mixed modeling. *The R journal* **9**, 378-400 (2017).
33. R-Core-Team, *R: A language and environment for statistical computing*. (R Foundation for Statistical Computing, vienna, Austria, 2013).
34. S. N. Wood, *Generalized additive models: an introduction with R*. (Chapman and Hall/CRC, 2006).
35. H. Schielzeth, W. Forstmeier, Conclusions beyond support: overconfident estimates in mixed models. *Behav Ecol* **20**, 416-420 (2009).
36. A. F. Zuur, E. N. Ieno, N. J. Walker, A. A. Saveliev, G. M. Smith, *Mixed Effects Models and Extensions in Ecology with R*. K. Krickeberg, J. M. Samet, A. Tsiatis, W. Wong, Eds., Statistics for biology and health (Springer, New York, 2009).
37. J. S. Lefcheck, R. Freckleton, piecewiseSEM: Piecewise structural equation modelling inr for ecology, evolution, and systematics. *Methods Ecol Evol* **7**, 573-579 (2016).
38. S. Nakagawa, H. Schielzeth, Repeatability for Gaussian and non-Gaussian data: a practical guide for biologists. *Biol Rev* **85**, 935-956 (2010).
39. A. F. Zuur, E. N. Ieno, R. Freckleton, A protocol for conducting and presenting results of regression-type analyses. *Methods Ecol Evol* **7**, 636-645 (2016).
40. M. D. Abràmoff, P. J. Magalhães, S. J. Ram, Image processing with ImageJ. *Biophotonics Int* **11**, 36-42 (2004).
41. P.-P. Bitton *et al*., Red fluorescence of the triplefin *Tripterygion delaisi* is increasingly visible against background light with increasing depth. *R Soc open sci* **4**, 161009 (2017).
42. V. I. Govardovskii, N. Fyhrquist, T. Reuter, D. G. Kuzmin, K. Donner, In search of the visual pigment template. *Visual Neurosci* **17**, 509-528 (2000).

43. L. Wilkins, N. J. Marshall, S. Johnsen, D. Osorio, Modelling colour constancy in fish: implications for vision and signalling in water. *J Exp Biol* **219**, 1884-1892 (2016).
44. M. V. Matz, N. J. Marshall, M. Vorobyev, Are corals colorful? *Photochem Photobiol* **82**, 345-350 (2006).
45. R. H. Douglas, M. Djamgoz, *The visual system of fish*. (Springer Science & Business Media, 2012).
46. R. Maia, C. M. Eliason, P. P. Bitton, S. M. Doucet, M. D. Shawkey, pavo: an R package for the analysis, visualization and organization of spectral data. *Methods Ecol Evol* **4**, 906-913 (2013).
47. D. Bates, M. Mächler, B. M. Bolker, S. Walker, Fitting linear mixed-effects models using lme4. *J Stat Softw* **67**, 1-51 (2014).

Acknowledgments: We are indebted to the attendants of a workshop in November 2014 in Tübingen with Connor M. Champ, João Coimbra, Colin B. Jack, Sönke Johnsen, Almut Kelber, Melissa G. Meadows, Daniel Osorio, Shelby Temple and Annette Werner. Thanks to Martin J. How for useful suggestions on an earlier draft. Jonas Dornbach, Thomas Griessler, Katharina Hiemer, Michael Karcz, Valentina Richter, Peter Tung, Sabine Urban, Laura Warmuth and Florian Wehrberger supported data collection in the field. Gregor Schulte provided creative and technical support. Thanks to Pierre Lejeune, director of STARESO and his staff for providing excellent working conditions.

Funding: N.K.M. was supported by Koselleck Grant Mi 482/13-1 from the Deutsche Forschungsgemeinschaft and Experiment! grant Az. 89148 and Az. 91816 from the Volkswagen Foundation. P-P.B. was funded by a Postdoctoral Fellowship from the Natural Sciences and Engineering Research Council of Canada.

Author contributions: N.K.M., R.F., M.S., P-P.B. and U.K.H. conceived the study. R.F. developed the hatting technique. N.K.M., J.D., M.S., U.K.H., R.F. and P-P.B. conceptualized the experiments. J.D. collected the laboratory data. M.S. and U.K.H. collected the field data, with assistance from the whole crew. M.S. and N.A. analyzed the experimental data. P-P.B. and M.S. developed and ran the visual model using spectroradiometric data collected by M.S. and U.K.H. The manuscript was written by N.K.M., M.S., P.-P.B., R.F. and J.D. All authors edited and approved the manuscript.

Competing interests: Authors declare no competing interests.

Data and materials availability: All data is available in the main text or the supplementary materials.

Supplementary Materials:

Materials and Methods

Figures S1-S2

Tables S1-S3

References (*26-47*)

Science
AAAS

Supplementary Materials for

Active sensing with light improves predator detection in a diurnal fish

Matteo Santon[1], Pierre-Paul Bitton[1,3], Jasha Dehm[1,2], Roland Fritsch[1], Ulrike K. Harant[1], Nils Anthes[1], Nico K. Michiels[1]*.

Correspondence to: nico.michiels@uni-tuebingen.de

This PDF file includes:

Other Supplementary Materials for this manuscript include the following:

Materials and Methods

Model species and location

Triplefins (Fam. Tripterygiidae) are small, cryptobenthic micropredators that favor marine hard substrates. Our model species is *Tripterygion delaisi*. With a standard length of 3–5 cm it is one of the larger members of this family. *T. delaisi* occurs in the NE-Atlantic and Mediterranean on rocky substrates between 3-50 m depth, but reaches highest densities in 5-15 m. Aside from breeding males, it is highly cryptic and regularly produces blue and red ocular sparks (*3*). Triplefins are particularly suitable for this type of research. Unlike other small benthic fish such as blennies and gobies, they do not have a hiding place or nest where they spend most of their time (*26*). Instead, they roam on the substrate looking for micro-prey. This is made possible by their cryptic coloration (*27*), their habit of moving cautiously and secretively while assessing their surroundings with independent eye movement and by their high visual acuity and contrast sensitivity (*13, 15*). This makes them a convenient system for laboratory and field experiments that include unusual treatments such as hats.

Scorpaena porcus (Fam. Scorpaenidae) is a cryptobenthic sit-and-wait predator (12–20 cm) from coastal marine hard substrates and seagrass habitats across the NE-Atlantic and Mediterranean Sea (*28*). It responds to moving prey; non-moving or dead prey is ignored. Small benthic fish, such as triplefins, are often a component of its diet (*29*). It possesses a reflective *stratum argenteum* and partially translucent retinal pigment epithelium that allows the generation of daytime eyeshine, which is considered to improve pupil camouflage (*8*).

All experiments were conducted in Calvi (Corsica, France) under the general permit of STARESO (Station de Recherches Sous Marines et Océanographiques). The hatting technique was developed at the University of Tübingen under permit ZO1-16 from the Regierungspräsidium Tübingen prior to the field experiments.

Hatting technique to block ocular sparks

We blocked ocular spark formation by means of mini-hats excised from polyester filter sheets using a laser cutter (RLS 100, AM Laserpoint Deutschland GmbH, Hamburg, Germany). A dark red filter with average transmission 1 % was used as the shading treatment (LEE #787 “Marius Red”, LEE Filters, UK). Clear filter hats (LEE #130, “Clear”) were used in the first control group, and no hat, but the same handling procedure, in the second control group. Hats were individually adjusted with clippers and folded into their final configuration with a triangular base for attachment and raised, forward-projecting wings to shade the eyes from downwelling light only. Hats formed an "umbrella" well above the eye, allowing full eye movement in all directions (Figure 1B-C). They varied from 6 to 9 mm in diameter, matching individual head size. Given that *T. delaisi* possesses a fovea that is looking forward and downward when the eye is in a typical position (*13*), it seems unlikely that shading alone may have resulted in poorer visual detection of a benthic predator in front of the fish relative to a triplefin without hat and without ocular spark. Animals in the clear-hatted and unhatted control groups regularly generated ocular sparks both in the laboratory and in the field.

Triplefins were collected using hand nets while SCUBA diving and brought to a stock aquarium in the laboratory. Individuals were anaesthetized (100 mg L^{-1} MS-222 in seawater, pH = 8.2) until all movements ceased except for breathing (3–4.5 min). Subsequently, the dorsal head surface was gently dried with paper tissue. Hats were glued to the triangular dorso-posterior head area just behind the eyes using surgical glue (Surgibond, Sutures Limited, UK or Vetbond Tissue Adhesive, 3M). After allowing the glue to polymerize for 45 s, fish were moved into recovery containers with aerated seawater. Individuals regained consciousness and mobility within 5–10 min. This non-invasive hat fixation protocol minimized impacts on the fish's natural behavior and health, as indicated by a 97.4 % survival rate. As a trade-off, however, hats detached within 0–4 days, which reduced the number of individuals that could be used for analysis (see Statistical analysis). All fish were treated and included in trials once, but kept in the laboratory for recovery. They were returned to the field after completion of the experiment. Pilot experiments confirmed that typical behaviors such as fin flicks, push-ups, active movement across the substrate, and head and eye movements did not differ between shading and control treatments (*30*). The data presented here also showed that hatting did not affect triplefin behavior, except for scorpionfish detection. Yet, it is conceivable that a shading hat reduced a triplefin's visual field, offering an alternative explanation to poorer detection of a scorpionfish. Hat design, however, anticipated this problem. Hats were folded as small "umbrellas", hovering well above the fish's eyes (Figure 1B-C). Consequently, the forward viewing angle was well above 45° from horizontal. Moreover, triplefins typically sit in an upright position propped up on their pectoral fins. Given that the visual cues were presented at the same level as the triplefins, we have therefore no doubt that both stimuli fell well within the viewing range (scorpionfish eye < 4 cm above the substrate).

Laboratory experiment

Four aquaria (L × W × D: 130 × 50 × 50 cm^3) were used for 20 experimental runs, each employing a new triplet of size-matched *T. delaisi*. In each tank, we placed a rock and a scorpionfish in two separate perforated containers (L × W × H: 24 × 14 × 16 cm^3) with a glass front. The bottom of the aquarium was barren (avoided by the fish), except for a 10 cm strip of gravel placed along the long side of the tank, providing a sub-optimal substrate. Each tank was illuminated with a 150 W cold white LED floodlight (TIROLED Hallenleuchte, 150 W, 16000 Lumen) shielded with a LEE Filters #172 Lagoon Blue filter to simulate light at depth. The area of the tank where stimuli were displayed was shaded. Both stimuli were simultaneously present in the tank, but only one was visible on a given day. On day one, all fish were treated and placed in the tank in the evening. Observations took place on days two and three. Two aquaria started with stimulus "scorpionfish", the other two with "stone", and stimuli were swapped after day two. Hence, all triplets were exposed to a stimulus for one full day. Since fish are moving regularly, we assessed the distance to the stimulus five times per day, 5 min per individual, at 0800, 1100, 1300, 1500 and 1800.

Replicate experiment in the field

We replicated the laboratory experiment in the field using ten tanks of spectrally neutral Evotron Plexiglas (L × W × D: 150 × 25 × 50 cm^3) placed at 15 m depth on a sandy patch in the seagrass

meadow in front of STARESO. We used local silica sand mixed with gravel as substrate for the compartment in which triplefins were kept (125 x 25 cm^2). It was separated from a display compartment (15 x 25 cm^2) for the shaded visual stimulus with transparent Plexiglass. Another similar-sized compartment behind the display compartment was used to keep the stimulus not currently visible to triplefins, separated by an opaque grey PVC plate. All separators were perforated to assure that a scorpionfish invisible to the triplefins could be chemically perceived even when the stone was visible. Visual contact between tanks was excluded by surrounding each enclosure with 10 cm white side covers along the bottom edge. As a response variable, we noted the distance of each individual from the stimulus compartment three times a day at 0900, 1200 and 1500 for two days following deployment in the early evening of the first day. Stimuli were always changed after the first observation day. Triplets were replaced every three days. In total, 50 triplets were tested.

Second field experiment: short-term response over time

We carried out a second field experiment with the goal of observing the temporal pattern of triplefin inspection behavior immediately after release. To this end, we only tested shading hatted and clear-hatted triplefins individually (not in pairs or triplets) and exposed them to a shaded scorpionfish only (no stone to maximize sample size). As before, we used 10 Plexiglass tanks, 5 with triplefins facing north, another 5 with triplefins facing south. Tanks were identically built (Figure 1) and equally high, but with a smaller footprint, offering 50 x 25 cm^2 substrate for the triplefins and 12 x 25 cm^2 for the scorpionfish. To improve SCUBA diving safety, tanks were positioned at a depth of 10 m and mounted on floats with 4 plastic chains attached to 1 m metal rods anchored in the ground. The substrate on which triplefins were placed was covered with darker sand than in the previous experiments, and we used black side covers to block their view to the outside, creating a slightly darker background than in the previous experiment. Scorpionfish (n = 10) were kept as a resident in the display compartment. One triplefins was added to each tank at the beginning of a dive and its position determined about 1 min after release. Once all triplefins had been released and their distance recorded for the first time, each tank was visited another 3 times during this first dive. After a ~30 min surface interval, the divers went back to collect another 3 data points, after which all triplefins were removed. Due to this procedure, time intervals between tanks and surface interval between first and second dive varied slightly. Eight cohorts of 10 triplefins were observed, 38 shaded and 42 clear-hatted triplefins. Using controlled randomization, treatments were equally distributed across cohorts, tank ID and tank orientations to prevent any systematic bias.

Statistical analysis

Repeatability analysis

In all three experiments, distance measurements were not blind for hat treatment. However, room for error was limited as we did not interpret a behavior, but merely noted the position of the head of a fish relative to a ruler placed alongside the tank. In the laboratory, fish and ruler were very close to each other and therefore easy to align to take virtually error-free measurements. In the

field, the SCUBA diver was hovering above the tank and used rulers on both long sides for alignment and to determine fish position. To test repeatability in the field, the two divers who collected the distance data in the field (MS, UKH) determined 116 distances of triplefins in the 15 m field tanks. Using the R package *rptR* (*31*), datatype *Gaussian* and 1000 permutations, the repeatability estimate was $R = 0.995$ (Likelihood Ratio Test: $p < 0.0001$).

Statistical model choice and pooling of controls

Behavioral data were analyzed using Generalized Linear Mixed Models (GLMM) with the lme4 package (*47*) and glmmTMB package (*32*) for R v3.4.3. (*33*). For the first two experiments, we first compared the two control treatments (sham and clear hat) to verify that hatting a fish did not affect behavior, and to confirm their ability to distinguish a cryptic predator from a stone. Because controls did not differ, we then averaged the data of the two control-treated fish per triplet per observation for the final models and compared them to the shaded treatment. This allowed us to also include triplets in which only the clear-hatted fish had lost its hat for the comparison with the shaded fish (such triplets had been excluded from the comparison of the controls). This explains the variation in triplet numbers in the final analyses. Distance from the display compartment was used as the response variable in all three models, implemented using a normal distribution for the first two experiments and a beta binomial distribution (link = log) for the third one.

Predictors and transformations

For the laboratory experiment (Fig. 2A, Table S1), the initial fixed model component included the main predictors *stimulus* (stone *vs* scorpionfish), *hat treatment* (no hat *vs* clear hat, or averaged controls *vs* shaded) and their interaction. We further included the fixed covariates *time of day* for each observation, *stimulus order, cohort and tank ID*.
The models for the field replicate (Fig. 2B-C, Table S2) were identical, but also included the fixed factor *orientation* (north or south) and its interactions with the main predictors. We square-root-transformed the response variable *distance* to improve residual homogeneity in the analysis of the first field experiment. The transformation of the response variable did not cause any change in the effects of the interactions between covariates. Models to compare the response of controls *vs* shaded fish were calculated separately for north *vs* south orientation because fish responded differently to the scorpionfish depending on orientation.
For the third experiment (Fig. 3, Table S3), the initial fixed model component included the main predictors *hat treatment* (clear hat or shaded), time, orientation and their three-way interaction. We also included time as a quadratic component to explain the non-linear patterns of the data, assessed using the *gam* function of the mgvc R package (*34*), and the covariate day, as data were collected on three subsequent days. The response variable was transformed as proportion ($0 < x < 1$) of distance obtained by dividing all distances by the maximum length of the tank plus one (51 cm). The transformation of the response variable did not affect the interactions between covariates, yet allowed us to implement a beta binomial distribution, thus improving residual homogeneity. We finally included a first-order autoregressive (AR1) variance structure to correct for temporal dependency in the observations of the same individuals.

Triplet as random factor and model selection

In the first two models, the initial random component contained triplet ID with random slopes over the hat treatment. This accounts for the repeated measurements of each triplet and captures variation arising from different hat-treatment responses among triplets (*35*). Random slopes were uninformative and subsequently removed. In the third model, the random component included triplefin ID, tank ID and cohort. We then performed backward model selection using the Akaike Information Criterion (AIC) to identify the best-fitting model with the smallest number of covariates (*36*). We only report the reduced final models and provide proxies for their overall goodness-of-fit (marginal and conditional R^2) using piecewiseSEM (*37*). The marginal R^2 expresses the proportion of variation explained by the model considering fixed factors only, whereas the conditional R^2 expresses the same including the random factors (*38*). We used Wald *z*-tests to assess the significance of fixed effects. To explore significant interactions between stimulus and hat treatment, we implemented new models within the two levels of the stimulus treatment. Model assumptions were validated by plotting residuals versus fitted values and each covariate present in the full, non-reduced model (*39*).

Estimating scorpionfish pupil radiance with and without ocular spark

We assumed both triplefins and scorpionfish were looking orthogonally at one another to calculate the photon flux of the scorpionfish pupil reaching the triplefin pupil. Using retinal quantum catch estimates, we calculated the chromatic contrast (*16*) between the scorpionfish pupil with and without the contribution of the blue ocular sparks. The achromatic contrast between the same two conditions was estimated by calculating the Michelson contrast using the quantum catches of the two-long-wavelength photoreceptors. For comparison, we also performed the same calculations using photon flux from the scorpionfish iris with and without the contribution of an ocular spark. We parameterized the equations using measurements of: (1) ambient light in the tanks at 10 m depth, (2) the range of ocular spark radiance under downwelling light conditions, (3) baseline scorpionfish pupil radiance in the experimental tanks, (4) sizes of triplefin pupil, ocular spark and scorpionfish pupil, and (5) scorpionfish pupil and iris reflectance (*8*). See Table S4 for symbols used.

Spectroradiometric measurements were obtained with a calibrated SpectraScan PR-740 (Photo Research, New York USA) encased in an underwater housing (BS Kinetics, Germany). This device measures spectral radiance (watts sr^{-1} m^{-2} nm^{-1}) of an area with defined solid angle. The downwelling light was estimated by measuring the radiance of a polytetrafluoroethylene (PTFE) diffuse white reflectance standard (Berghof Fluoroplastic Technology GmbH, Germany) positioned parallel to the water surface from a 45° angle. Radiance values were subsequently transformed into photon radiance (photons s^{-1} sr^{-1} m^{-2} nm^{-1}).

We determined the relationship between the radiance of the ocular spark and that of a white PTFE standard exposed to downwelling light in live triplefins. Fish mildly sedated with clove oil (n = 10) were placed in an aquarium illuminated with a Leica EL 6000 source and a liquid light guide suspended ~20 cm above the tank. Spark radiance was normalized by comparing it to a white standard at 45° from normal positioned at the same location as the fish. For each fish, three measurements were obtained from each eye. The highest value for each fish relative to the standard was used for the model. The sizes of the triplefin pupil (n = 35), the ocular spark (n =

10), and the scorpionfish pupil (n = 20) were measured in ImageJ (*40*) using scaled images. Natural baseline pupil radiance of three different scorpionfish was measured orthogonally to the pupil from the perspective of the triplefins during the field experimental trials using a Photo Research PR-740 spectroradiometer.

Solid angles of the ocular spark as perceived from the perspective of the scorpionfish, and the pupil of the scorpionfish as perceived by the triplefin were computed using simple calculations (see below).

Visual models and maximum detection distance

The receptor-noise limited model for calculation of chromatic contrast was informed using triplefin ocular media transmission values, photoreceptor sensitivity curves (*41, 42*), and the relative photoreceptor density of single to double cone of 1:4:4 as found in the triplefin fovea (*13*). We used a Weber fraction (ω) value of 0.05 as in previous studies (*43, 44*). Chromatic contrasts are measured as just-noticeable differences (JNDs), where values greater than 1 are considered to be larger than the minimum discernible difference between two objects. We calculated the Michelson achromatic contrast as

$$C = \frac{(Q_1 - Q_2)}{(Q_1 + Q_2)}$$

where Q_1 and Q_2 are the quantum catches of the two members of the double cones which are associated with the achromatic channel, under photon $flux_1$ and photon $flux_2$. $Flux_1$ is the sum of the photon flux into a triplefin's eye caused by the baseline radiance of a scorpionfish pupil and the photon flux caused by the retroreflection of an ocular spark in the scorpionfish pupil (sum of equations (2) and (6) below). $Flux_2$ is calculated from the baseline radiance of a scorpionfish pupil only (no ocular spark reflection, equation (2) below). We determined the maximum discernible distance of the ocular spark radiance reflected through a scorpionfish pupil by calculating the chromatic and achromatic contrast at each millimeter, between 1 and 15 cm, and extracting the first value at which the contrast was equal to or exceeded the threshold of 1.0 JND for chromatic contrasts and 0.008 for Michelson contrasts as measured in *T. delaisi* (*15*) and other fish species (*45*). All visual models were performed using the R package pavo (*46*).

Visual model details

Triplefin – scorpionfish interaction

The starting conditions assume that both fish look at each other at normal incidence, i.e. the full area of the pupil of the triplefin is visible to the scorpionfish and vice versa. Solid angles are computed as explained below, assuming the ocular spark is positioned at the edge of the iris (displacement from pupil center Δ = 1.09 mm) in the plane of the triplefin pupil.

Photon flux without ocular spark

The photon radiance of the scorpionfish pupil reaching the triplefin (L_d) is a function of the measured scorpionfish pupil photon radiance (L_0) attenuated by the aquatic medium over distance d such that

$$L_d = L_0 \times e^{-\kappa d} \quad (1)$$

The photon flux reaching the retina of the triplefin without the ocular spark (Φ_{ns}) (Fig. S1) is the proportion of attenuated photon radiance reaching the triplefin's pupil (L_d) multiplied by the solid angle of the scorpionfish pupil (Ω_{sp}) and the area of the triplefin pupil (πr_t^2):

$$\Phi_{ns} = L_d \times \Omega_{sp} \times \pi r_t^2 \quad (2)$$

This value was used to calculate the quantum catches Q_1 and Q_2 mentioned earlier.

Photon flux with ocular spark

The photon radiance of the ocular spark reaching the scorpionfish (L_{os}) is a function of the radiance of a PTFE white standard parallel to the water surface (L_w), the focusing power of the lens, and the reflective properties of the iridal chromatophores on which the light is focused. For now, the focusing power and reflective properties have only been measured together as blue ocular spark reflectance (S) relative to L_w:

$$L_{os} = L_w \times S \times e^{-\kappa d} \quad (3)$$

The radiance of the scorpionfish pupil (L_{sp}) defined as the proportion of the attenuated ocular spark photon radiance that reaches the scorpionfish pupil and is re-emitted towards the triplefin is estimated by multiplying the photon radiance of the ocular spark reaching the scorpionfish (L_{os}) with the solid angle of the ocular spark as seen by the scorpionfish (Ω_{os}) and the retroreflectance of the scorpionfish pupil with illumination co-axial to the receiver (R). Because the properties of the retroreflective eye are measured in relation to a diffuse white standard, the photon exitance from the scorpionfish pupil is converted to photon radiance by dividing by π steradians:

$$L_{sp} = L_{os} \times \Omega_{os} \times R \times \pi^{-1} \quad (4)$$

The scorpionfish pupil radiance (L_{sp}) travelling towards the triplefin pupil is further attenuated, and the photon flux reaching the triplefin's retina (Φ_{os}) is obtained by multiplying the attenuated radiance by the solid angle of the scorpionfish pupil, and the area of the triplefin pupil:

$$\Phi_{os} = L_{sp} \times e^{-\kappa d} \times \Omega_{sp} \times \pi r_t^2 \quad (5)$$

The photon flux generated by the ocular spark, which reaches the triplefin retina after being reflected by the scorpionfish pupil is therefore approximated by (see also Fig. S2):

$$\Phi_{os} = L_w \times S \times e^{-\kappa d} \times \Omega_{os} \times R \times \pi^{-1} \times e^{-\kappa d} \times \Omega_{sp} \times \pi r_t^2 \quad (6)$$

The total photon flux reaching the retina of the triplefin with the ocular spark is then the sum of equations (2) and (6) (Figs. S1 and S2 combined). This sum was used to calculate the quantum catches Q_1 and Q_2 from a scorpionfish eye illuminated by an ocular spark, as mentioned earlier.

Calculation of solid angles

The solid angle of the scorpionfish pupil (Ω_{sp}) as perceived by the (dimensionless) center of the triplefin's pupil at distance d was estimated using the formula

$$\Omega_{sp} = \frac{\pi\, r_{sp}^2}{d^2}$$

The solid angle of the ocular spark as seen from the perspective of a scorpionfish eye (Ω_{os}) needs to be corrected for the fact that the ocular spark is below the triplefin's pupil by a distance Δ = 0.00109 m. The radius of the ocular spark at this distance as perceived by the scorpionfish can be calculated by multiplying the original diameter r_{os} with the ratio of the original distance d divided by the hypotenuse of the right-angled triangle defined by Δ and d:

$$r'_{os} = r_{os} \frac{d}{\sqrt{\Delta^2 + d^2}}$$

The solid angle of the ocular park as perceived by the (dimensionless) center of the scorpionfish's pupil can then be calculated as

$$\Omega_{os} = \frac{\pi\, r'^2_{os}}{d^2}$$

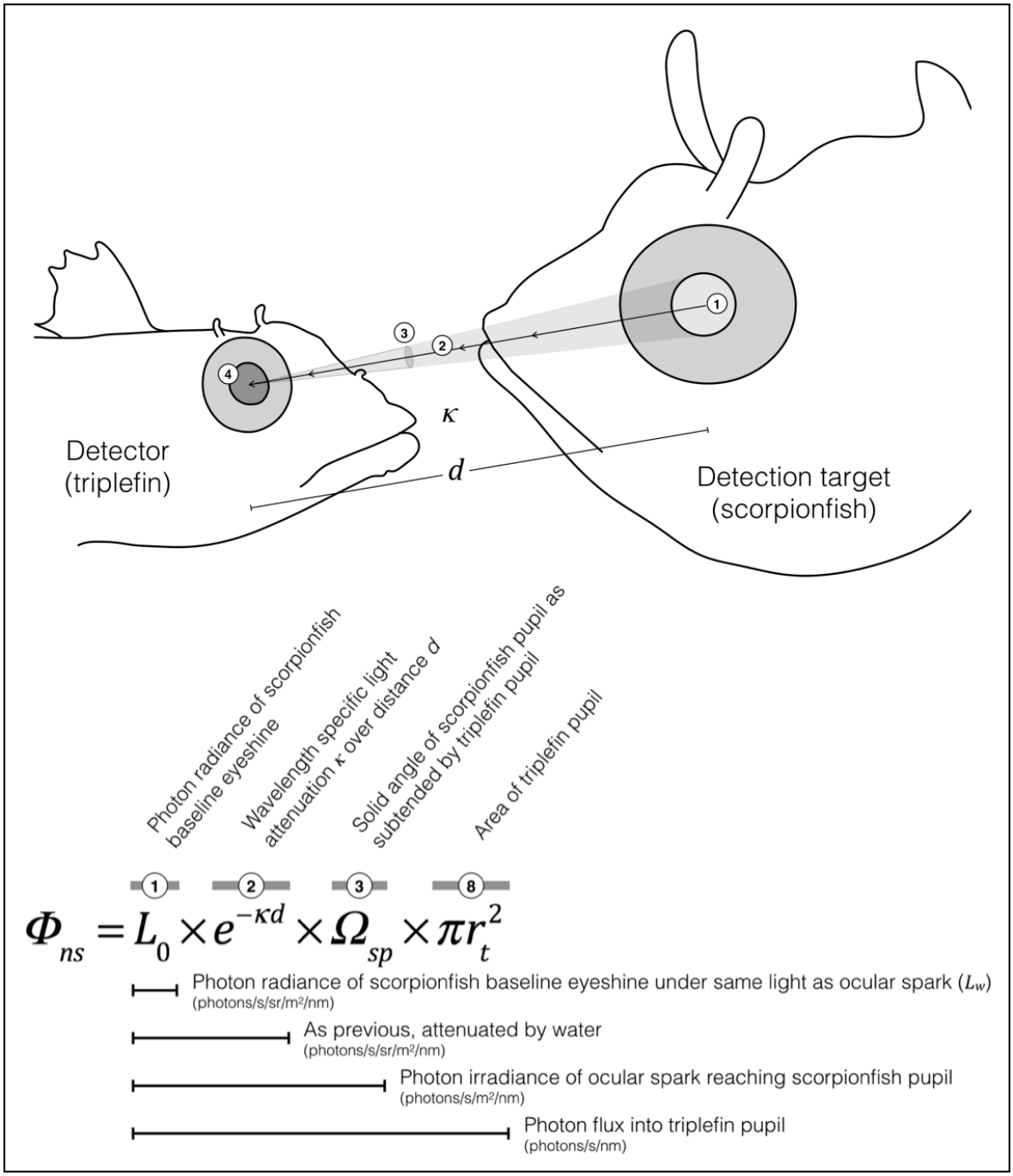

Fig. S1: Visual representation of how the photon flux Φ_{ns} originating from baseline scorpionfish eyeshine entering a triplefin's pupil is calculated. This case excludes the effect of an ocular spark, which is shown in Fig. S2. Baseline scorpionfish eyeshine was measured directly in the tanks in 10 m (second field experiment).

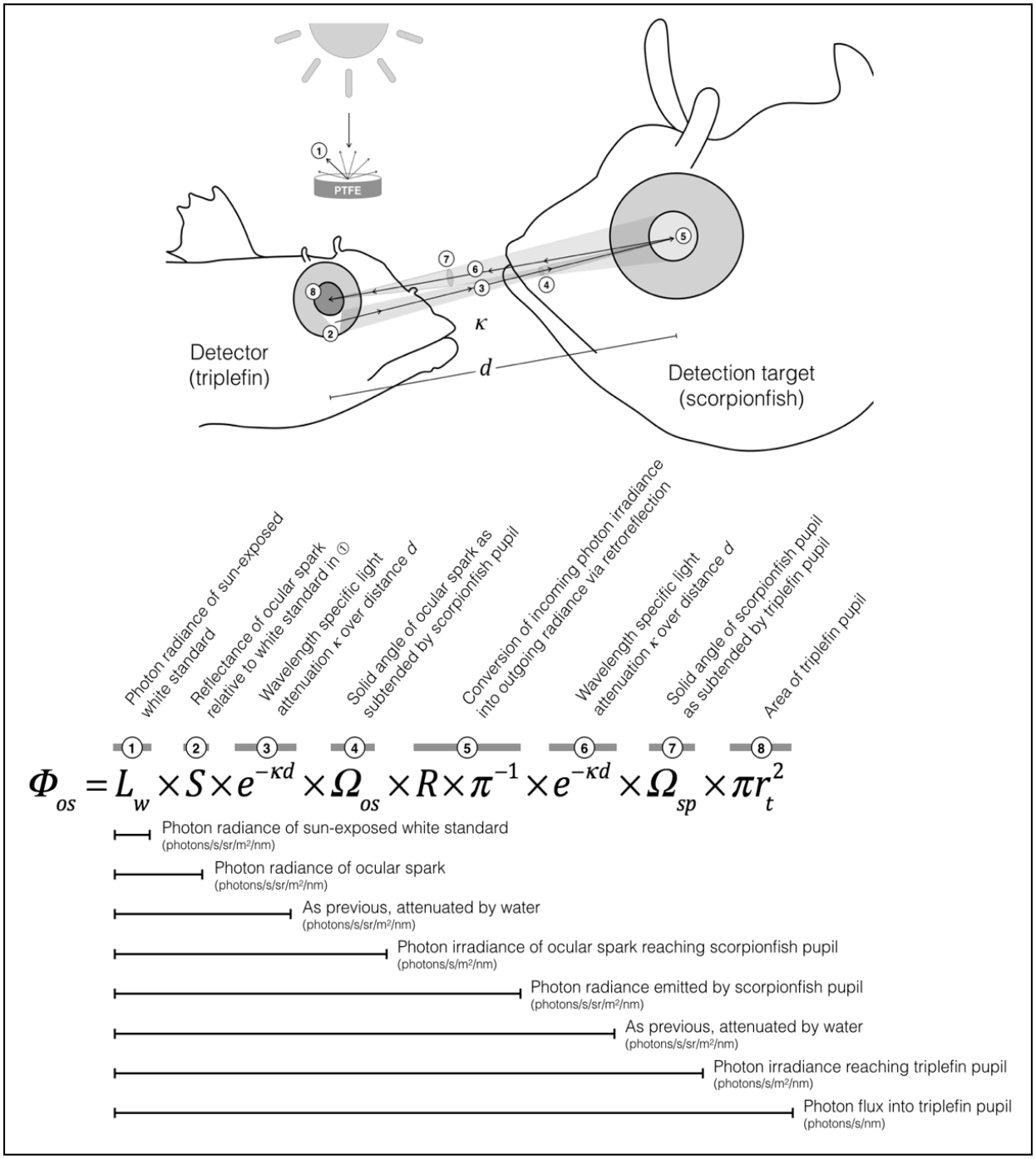

Fig. S2: Visual representation of how much of the photon flux Φ_{os} generated by a triplefin's ocular spark is reflected as scorpionfish eyeshine and ultimately reaches a triplefin's pupil. This effect needs to be added on top of baseline scorpionfish eyeshine (Fig. S1), to obtain the total photon flux from a scorpionfish eye reaching the eye of a triplefin with its ocular spark on.

Tables S1-S3

Table S1. Statistical analysis of the laboratory data presented in Fig. 2A. Linear Mixed Models with distance from the two visual stimuli (scorpionfish or stone) as the response variable. Given that the two control treatments did not differ in their response to the two stimuli (**A**), their respective measurements were averaged for the main analysis in which the response of control and shaded treatments to both stimuli was compared (**B**, Fig. 2A). The final model (**C**) tests the difference between the controls and the shaded treatment in their response to the scorpionfish only. CI = credible interval. For factorial predictors, estimates are computed using the indicated intercept levels as reference. This choice is arbitrary and does not affect overall conclusions.

	Predictors	Predicted mean	Lower 95% CI	Upper 95% CI	*P*
A. Response of unhatted and clear-hatted controls to both stimuli n = 15 triplets, R^2_{marg} = 0.30, R^2_{cond} = 0.31					
	Intercept (stone & no hat)	25.770	16.031	35.524	< 0.0001
	Treatment (clear hat)	3.416	-4.110	10.881	0.373
	Stimulus (scorpionfish)	32.917	25.385	40.419	< 0.0001
	Treatment x *Stimulus*	-4.421	-14.913	6.227	0.412
	Stimulus order	4.526	-0.791	9.886	0.100
B. Response of averaged controls and shaded individuals to both stimuli n = 15 triplets, R^2_{marg} = 0.28, R^2_{cond} = 0.28					
	Intercept (stone & controls)	31.994	27.466	36.667	< 0.0001
	Treatment (shading hat)	-4.849	-11.388	1.683	0.151
	Stimulus (scorpionfish)	30.700	25.304	35.980	< 0.0001
	Treatment x *Stimulus*	-11.390	-20.570	-2.142	0.017
	Stimulus order	4.580	0.190	8.936	0.041
C. Response of averaged controls and shaded individuals to the scorpionfish stimulus only n = 15 triplets, R^2_{marg} = 0.14, R^2_{cond} = 0.23					
	Intercept (controls)	62.918	57.127	68.660	< 0.0001
	Treatment (shading hat)	-16.220	-21.417	-11.043	< 0.0001
	Stimulus order	4.256	-4.007	12.420	0.331

Table S2. Statistical analysis of the field data presented in Fig. 2B-C. Linear Mixed Models with the distance from the two visual stimuli (scorpionfish or stone) as the response variable. Given that the two control treatments did not differ in their response to the two stimuli (A), the respective measurements were averaged for the main analysis that compared the response of control and shaded treatments to both stimuli split by the two orientations (**B-C**, Fig. 3B-C). Note that predicted means and their credible intervals (CI) are based on a square-root transformation of the response variable (see Materials and Methods). For factorial predictors, estimates are computed using the indicated intercept levels as reference. This choice is arbitrary and does not affect overall conclusions.

	Predictors	Predicted mean	Lower 95% CI	Upper 95% CI	*P*
A. Response of unhatted and clear-hatted controls to both stimuli and orientations n = 22 triplets, R^2_{marg} = 0.31, R^2_{cond} = 0.56					
	Intercept (stone & no hat & facing N)	2.323	0.773	3.864	0.004
	Treatment (clear hat)	0.085	-0.779	0.930	0.844
	Stimulus (scorpionfish)	3.068	2.082	4.061	< 0.0001
	Treatment x *Stimulus*	-0.438	-1.667	0.758	0.476
	Orientation (facing S)	-0.534	-2.358	1.298	0.556
	Stimulus x *Orientation*	2.698	1.422	3.962	< 0.0001
	Stimulus order	0.895	0.268	1.528	0.005
B. North-facing triplefins B.1. Response of averaged controls and shaded individuals to both stimuli n = 24 triplets, R^2_{marg} = 0.23, R^2_{cond} = 0.45					
	Intercept (stone & controls)	1.501	0.332	2.686	0.014
	Treatment (shading hat)	0.537	-0.282	1.351	0.201
	Stimulus (scorpionfish)	3.265	2.460	4.090	< 0.0001
	Treatment x *Stimulus*	-1.199	-2.337	-0.071	0.038
	Stimulus order	1.412	0.827	2.004	< 0.0001
B.2. Response of averaged controls and shaded individuals to the scorpionfish stimulus only n = 23 triplets, R^2_{marg} = 0.03, R^2_{cond} = 0.61					
	Intercept (controls)	6.138	3.681	8.643	< 0.0001
	Treatment (shading hat)	-0.670	-1.185	-0.165	0.011
	Stimulus order	0.492	-1.157	2.108	0.551
C. South-facing triplefins Comparison of averaged controls and shaded individuals to both stimuli n = 19 triplets, R^2_{marg} = 0.40, R^2_{cond} = 0.58					
	Intercept (stone & controls)	5.208	3.780	6.610	< 0.0001
	Treatment (shading hat)	-0.890	-1.815	0.034	0.055
	Stimulus (scorpionfish)	4.173	3.223	5.123	< 0.0001
	Treatment x *Stimulus*	0.771	-0.522	2.108	0.248
	Stimulus order	-0.513	-1.203	0.179	0.138

Table S3. Statistical analysis of the field data presented in Fig. 3. Generalized Linear Mixed Model (*n* clear hat = 42, *n* shading hat = 38, $R^2_{marg} = 0.46$) with proportional distance to the visual stimulus (scorpionfish only) as the response variable. Note that predicted means and their credible intervals (CI) are based on a beta distribution with logit link (see Materials and Methods). For factorial predictors, estimates are computed using the indicated intercept levels as reference. This choice is arbitrary and does not affect the overall conclusions. This model includes a first-order autoregressive (AR1 = 0.86) variance structure to correct for temporal dependency in the observations of the same individuals.

Predictors	Predicted mean	Lower 95% CI	Upper 95% CI	*P*
Intercept (clear hat)	0.674	0.610	0.735	< 0.0001
Treatment (shading hat)	-0.086	-0.166	-0.007	0.034
Time	0.103	0.071	0.137	< 0.0001
Time^2	-0.043	-0.071	-0.013	0.003
Treatment x Time	0.052	0.004	0.099	0.036

Table S4. Symbols and indices used in the equations to calculate the photon flux of the scorpionfish pupil reaching the triplefin, with and without the contribution of an ocular spark.

Symbol	***Definitions and units***
L	Photon radiance (photons s^{-1} sr^{-1} m^{-2})
S	Blue ocular spark reflectance (proportion in relation to PTFE white standard)
d	Distance between triplefin and scorpionfish (m)
Δ	Mean displacement of ocular spark relative to triplefin pupil center (0.00109 m)
r	Radius (m)
Ω	Solid angle (sr)
R	Reflectance of coaxially illuminated scorpionfish pupil (prop. in relation to PTFE white standard)
$\boldsymbol{\kappa}$	Diffuse attenuation coefficient (m^{-1})
Φ	Photon flux (photons s^{-1})
Indices	***Meaning and use***
0	Distance = 0, as used in L_0
w	Used for downwelling light from the water surface, used in L_w
ns	Abbreviation for "no ocular spark", used in Φ_{ns}
os	Abbreviation for ocular spark of a triplefin, used in L_{os}, r_{os} and Ω_{os}
sp	Abbreviation for scorpionfish pupil used in L_{sp}, r_{sp} and Ω_{sp}
t	Abbreviation for triplefin, used in r_t

Captions for Data S1 to S15

Data S1. (separate file)

File name: "01 Lab experiment.txt"

Caption: Data from laboratory experiment. Distance in cm. csv file.

Data S2. (separate file)

File name: "02 Field exp 1 - comparison of controls.txt"

Caption: Data from replicate (first) field experiment at 15 m depth for comparison of controls only. Distance in cm. csv file.

Data S3. (separate file)

File name: "03 Field exp 1 - shading vs controls.txt"

Caption: Data from replicate (first) field experiment for comparisons between shaded treatment and pooled controls. Distance in cm. csv file.

Data S4. (separate file)

File name: "04 Field experiment 2.csv"

Caption: Data from second field experiment at 10 m depth. Distance in cm. csv file.

Data S5. (separate file)

File name: "05 Visual model R script.R"

Caption: Complete R script to run the visual model.

Data S6a. (separate file)

File name: "06a Light field 10m north.csv"

Caption: Downwelling and sidewelling radiance (photons/s/sr/m^2/nm) of ambient light field at 10 m for north-facing triplefins. Radiance estimated measuring 3 times a diffuse white standard under two different geometries (facing upward and sideways). csv file.

Data S6b. (separate file)

File name: "06b Light field 10m south.csv"

Caption: Downwelling and sidewelling radiance (photons/s/sr/m^2/nm) of ambient light field at 10 m for south-facing triplefins. Radiance estimated measuring 3 times a diffuse

white standard for each of two different geometries (facing upward and sideways). csv file.

Data S7. (separate file)

File name: "07 Attenuation coefficient STARESO.csv"

Caption: Attenuation coefficients as determined from own measurements along a depth profile in STARESO. csv file.

Data S8. (separate file)

File name: "08 Pupil and iris radius triplefin.csv"

Caption: Pupil and iris radius in triplefins. Radius in mm. csv file.

Data S9. (separate file)

File name: "09 Ocular media transmission.csv"

Caption: Triplefin ocular media transmittance data. csv file.

Data S10. (separate file)

File name: "10 Radius pupil scorpionfish.csv"

Caption: Scorpionfish pupil radius. Radius in cm. csv file.

Data S11. (separate file)

File name: "11 Baseline radiance 3 porcus facing north.csv"

Caption: Baseline radiance (photons/s/sr/m^2/nm) in pupil of three scorpionfish in tanks with triplefins facing north at 10 m depth. csv file.

Data S12. (separate file)

File name: "12 Baseline radiance 3 porcus facing south.csv"

Caption: Baseline radiance (photons/s/sr/m^2/nm) in pupil of three scorpionfish in tanks with triplefins facing south at 10 m depth. csv file.

Data S13. (separate file)

File name: "13 Scorpionfish retroreflectance.csv"

Caption: Retroreflectance relative to diffuse white standard in scorpionfish pupil. csv file.

Data S14. (separate file)

File name: "14 Ocular spark radius.csv"

Caption: Radius of ocular spark in triplefins. Radius in mm. csv file.

Data S15. (separate file)

File name: "15 Ocular spark conversion curve.csv"

Caption: Conversion of downwelling irradiance (measured as radiance of exposed diffuse white standard) to ocular spark radiance in triplefins. csv file.

Data S16. (separate file)

File name: "16 Iris reflectance.csv"

Caption: Matrix of iris reflectance of scorpionfish on a continuous scale. Reflectance values range from the minimum to the maximum reflectance measured in scorpionfish for each wavelength between 400 and 700 nm. csv file.